STUDIES OF SOLVENT DISPLACEMENT FROM SOLVATED

METAL CARBONYL COMPLEXES OF CHROMIUM,

MOLYBDENUM, AND TUNGSTEN

DISSERTATION

Presented to the Graduate Council of the

University of North Texas in Partial

Fulfillment of the Requirements

For the Degree of

DOCTOR OF PHILOSOPHY

By

Shulin Zhang, B.S., M.S.

Denton, Texas

August, 1990

Zhang, Shulin, <u>Studies of Solvent Displacement from Solvated Metal Carbonyl Complexes of Chromium, Molybdenum, and Tungsten</u>. Doctor of Philosophy (Chemistry), August, 1990, 202 pp., 38 tables, 39 figures, reference list, 152 titles.

Flash photolysis techniques were applied to studies of solvent displacement by Lewis bases (L) from solvated metal carbonyl complexes of Cr, Mo, and W. On the basis of extensive studies of the reaction rate laws, activation parameters ($\Delta H^{\dagger}$, $\Delta S^{\dagger}$, $\Delta V^{\dagger}$), and linear-free-energy-relationships, it was concluded that the mechanisms of solvent displacement reactions depend on the electronic and steric properties of the solvents and L, as well as the identities of the metal atoms. The strengths of solvent-metal bonding interactions, varying from <u>ca.</u> 7 to 16 kcal/mol, and the bonding "modes" of solvents to metals are sensitive to the structures of the solvent molecules and the identities of the metal centers. The results indicate dissociative desolvation pathways for many arene solvents in (solvent)$Cr(CO)_5$ (solvent = benzene, fluorobenzene, toluene, <u>etc.</u>) complexes, and are consistent with competitive interchange and dissociative pathways for ($\underline{n}$-heptane)$M(CO)_5$. Different types of (arene)-$Cr(CO)_5$ interactions were suggested for chlorobenzene (CB) <u>vs.</u> fluorobenzene and other

non-halogenated arenes, i.e. via σ-halogen-Cr bond formation in the CB solvate vs. π-arene-Cr bond formation through "isolated" double bonds in solvates of the other arenes. The data also indicate the increasing importance of interchange pathways for solvent displacement from the solvates of Mo and W vs. that of Cr.

Intramolecular CB displacement from cis-(CB)(η^1-P-ol)W(CO)$_4$ (P-ol = Ph$_2$P(CH$_2$)$_n$CH=CH$_2$, n = 1-4) to form (η^3-P-ol)W(CO)$_4$ was found to take place via competitive interchange and dissociative pathways. The relative rates via the two pathways depend on the length of the -(CH$_2$)$_n$- chelate ring backbone. The reaction mechanism changes from a predominant dissociative pathway for n = 3 to a predominant interchange pathway for n = 2.

The results underscore the similarities between solvent substitution mechanisms of solvated metal carbonyl transients and ligand substitution pathways of the metal hexacarbonyls and their substitution products.

TABLE OF CONTENTS

iii

LIST OF TABLES

vi

LIST OF ILLUSTRATIONS

LIST OF ILLUSTRATIONS - Continued

CHAPTER I

GENERAL INTRODUCTION

A. The Sites of Unsaturation

Transition metal organometallic chemistry has become an extremely important area of chemistry in the past few decades, principally due to the roles of this class of compounds in catalyzing or assisting the transformation of organic substances. The bulk of studies of the organometallic compounds has dealt with transition metal carbonyl complexes and their derivatives.

It has been well known that stable, diamagnetic, mononuclear organotransition-metal complexes almost always contain 18 or fewer valence electrons, a statement known as the 18-Electron Rule and sometimes as the Effective Atomic Number Rule. A simple way to view this is to consider that a transition metal has nine valence orbitals: one ns orbital, five (n-1)d orbitals, and three np orbitals. These will hold 18 electrons in the valence orbitals to make a closed configuration: $ns^2(n-1)d^{10}np^6$. Further, looking at the molecular orbital description for such a complex indicates that the most stable bonding arrangement will be that in which the bonding and approximately nonbonding orbitals are occupied and none of the antibonding orbitals is occupied.

1

This will require 18 or fewer electrons as shown in Figure 1 for a typical octahedral hexacarbonyl complex.

The availability of a coordinatively unsaturated site on the metal for interacting with the substrate is a fundamental requirement for the activity of a catalyst.[1-3] In fact, it has been stated that "A site of coordinative unsaturation is perhaps the single most important property of a homogeneous catalyst".[4] At the same time, transition metal fragments have been considered as "the building blocks" of organometallic chemistry.[5] Understanding reactivity and selectivity of organometallic complexes relies on the examination of reaction intermediates. Theoretical organometallic chemists can predict the structure and reactivity of some transition metal fragments based on molecular orbital calculations. However, direct detection or observation of these reactive intermediates or fragments are more beneficial and important.

Among various coordinatively unsaturated species, five-coordinated "16-electron" transition metal species can be considered as a prototype since they have been found to be the intermediates in many organometallic reactions.[6-13] Furthermore, many of these "unsaturated five-coordinated species" have been believed to have structures based on a square pyramid. Figure 2 illustrates the interaction of the Lowest Unoccupied Molecular Orbital (LUMO) for a C_{4v} M(CO)$_5$ (M = Cr, Mo, W) fragment with a orbital of a σ-donor ligand.
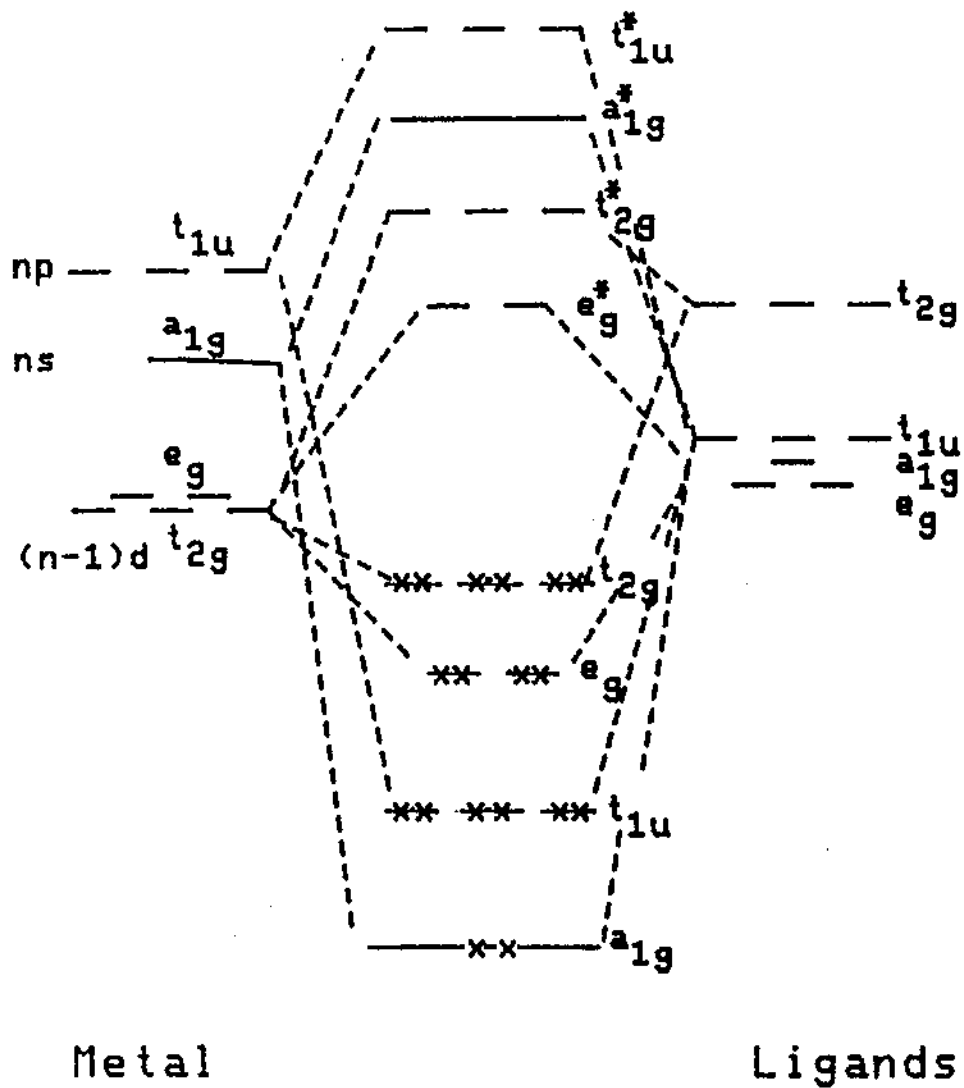
Figure 1. The 18-electron rule and molecular orbital diagram for a M(CO)$_6$ complex.
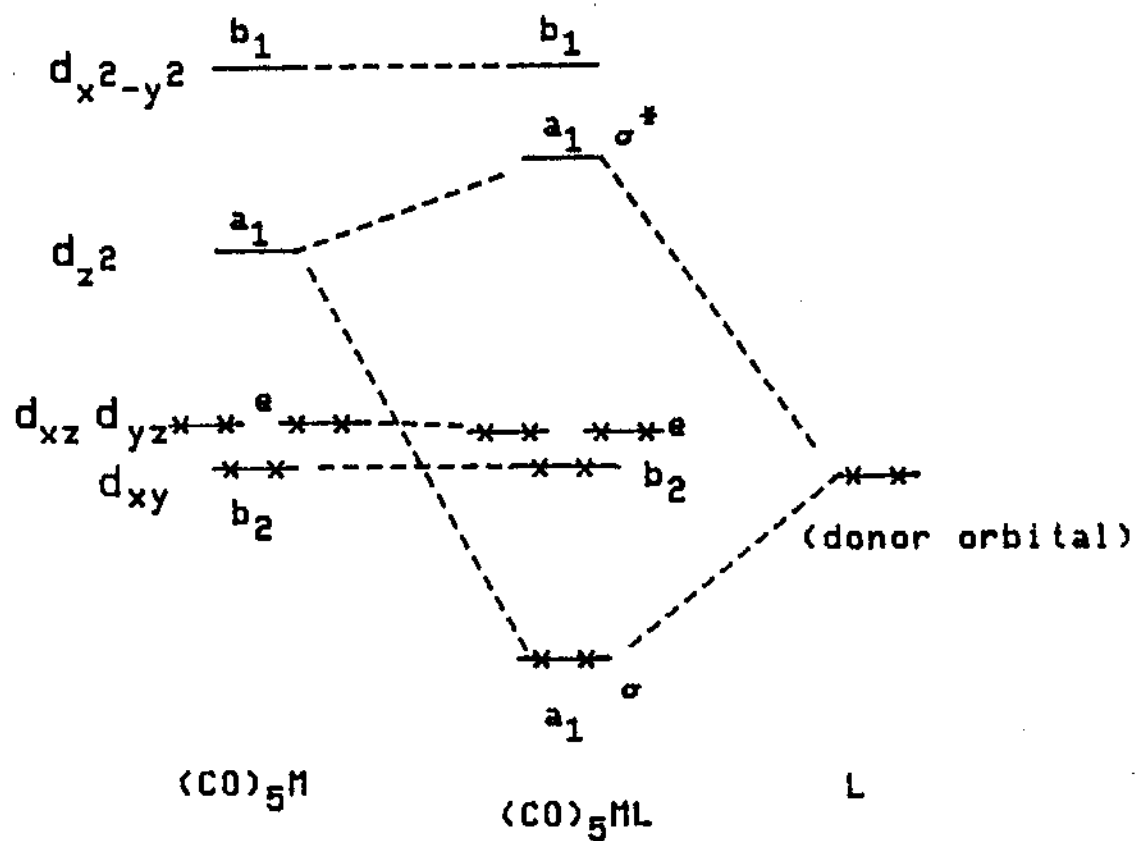
Figure 2. Molecular orbital diagram for the interaction of a C_{4v} M(CO)$_5$ fragment with a σ-donor ligand.

B. Carbon-Hydrogen Bond Activation

The activation and subsequent functionalization of a
C-H bond under normal reaction conditions have been of
interest to organometallic chemists for more than 20
years.[14-19] In the last decade, this area received a great
deal of attention because of the technological promise of
such reactions.[14-19] The interaction of hydrocarbons with
unsaturated species prior to C-H bond activation has been
described by Brookhart and Green as "agostic" bonding.[18]
Crabtree and coworkers[19] have constructed the trajectory for
the approach of C-H bond to a metal and its eventual
oxidative addition, and reaction-coordinate calculations
gave similar results[20] as shown in Figure 3.

Janowicz and Bergman reported the first direct
observation of oxidative addition of saturated hydrocarbon
C-H bond to a transition metal center in 1982;[16a,b] Hoyano and
Graham's similar results were reported shortly after.[17] They
employed systems which were precursors for [Cp*IrL] (Cp* =
pentamethylcyclopentadienyl; L = PMe_3, CO) unsaturated
intermediates. It was found that photochemical reactions of
$Cp^*Ir(PMe_3)(H_2)$ or $Cp^*Ir(CO)_2$ with cyclohexane (= C_6H_{12} = H-Cy
) afforded $Cp^*Ir(L)(H)(Cy)$.[16,17] However, the thermolysis of
$Cp^*Ir(PMe_3)(H)(Cy)$ in the presence of benzene (H-Ph)
irreversibly produced $Cp^*Ir(PMe_3)(H)(Ph)$ and C_6H_{12}.[16c,d]
Questions remain in understanding C-H bond activation by
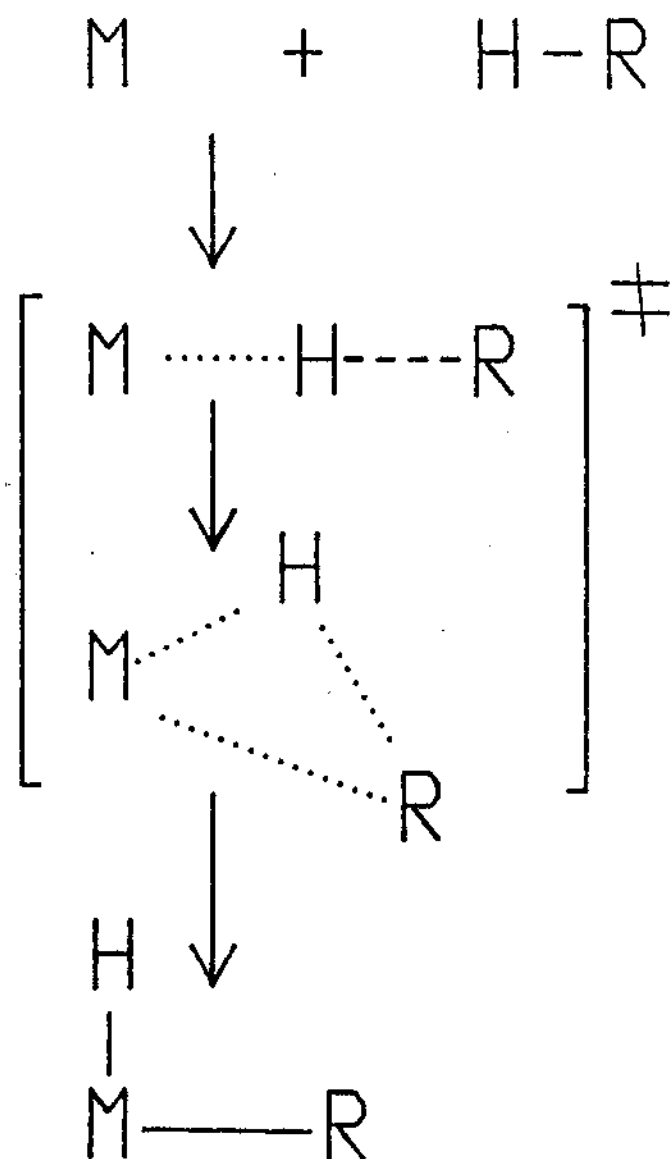
Figure 3. "Agostic" bonding, the trajectory for the
approach of C-H bond to a metal and its eventual
oxidative addition.

Cp*ML (M = Ir, Rh) which concerns the role of prior π-complexes formation by unsaturated hydrocarbons. Jones and Feher have proposed that a η^2-arene coordinated intermediate exists prior to C-H bond oxidative addition and that this initial coordination permits the activation of aromatic C-H bonds to compete with aliphatic C-H bond activation by Cp*Rh(PMe$_3$) (Figure 4a).[21-24] On the other hand, Stoutland and Bergman have conclusively demonstrated that attack by Cp*Ir(PMe$_3$) on the vinyl C-H bond in ethylene precedes π-complex formation (Figure 4b).[25,26]

The existence of η^2-arene-M bonding has been widely suggested among transition metal complexes and is supported by X-ray[27-33] and NMR studies.[34] However, the existence of the π-complex does not necessarily indicate it lies on the reaction pathway toward C-H bond activation in an arene substrate. Studies of interactions of arene and aliphatic hydrocarbons with unsaturated species may help us further understand the mechanism of C-H bond activations.

C. Mechanistic Pathways for Ligand Substitution Reactions

A substitution reaction is usually an essential first step and sometimes is the rate-determining step in catalytic and transition metal organometallic reactions.[6-13] Before the discussion on exploratory examinations of solvent substitution reactions, it is worthwhile to review the basic
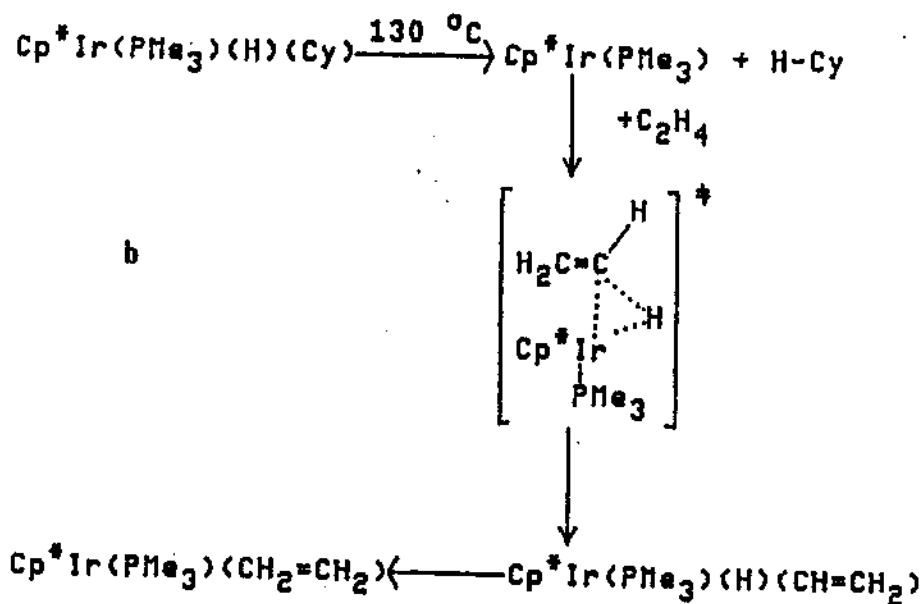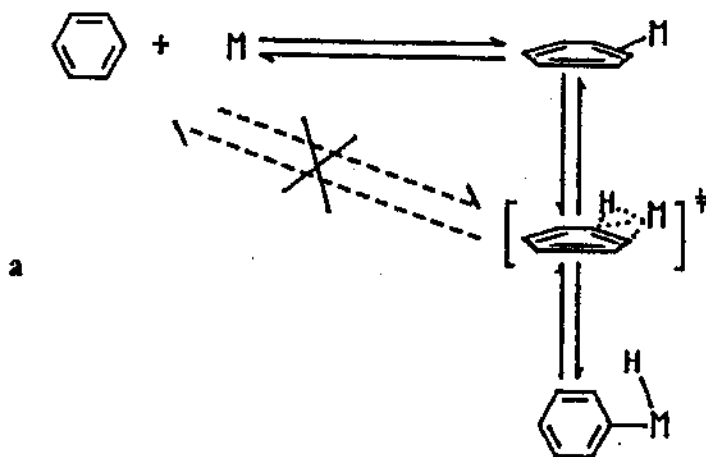
Figure 4a. η^2-arene coordinated intermediate exists prior to C-H bond oxidative addition to Cp*Rh(PMe$_3$) proposed by Jones and Feher.

4b. Attack by Cp*Ir(PMe$_3$) on the vinyl C-H bond in ethylene precedes π-complex formation demonstrated by Stoutland and Bergman.

mechanistic pathways for conventional ligand substitution

reactions. The characteristic of primary D, I, and A

substitution pathways[12] can be summarized as in following

for an octahedral ML_6 substrate.

(1) Dissociative (D) Mechanism

$$ML_6 \underset{k_{-1}}{\overset{k_1}{\rightleftharpoons}} ML_5 + L$$

$$ML_5 + L' \overset{k_2}{\longrightarrow} ML_5L'$$
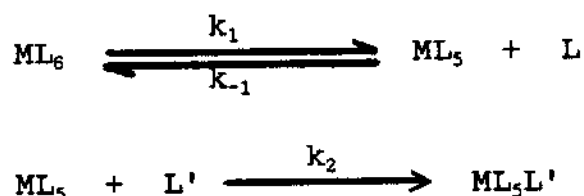
When assuming the rate determining loss of L (k_1) and

rapid reaction of the five-coordinated intermediate ML_5 with

L or L', and thus a steady state concentration of $[ML_5]$, the

rate law can be expressed as:

$$- \frac{d[ML_6]}{dt} = \frac{k_1k_2[L']}{k_{-1}[L] + k_2[L']} [ML_6]$$

(2) Dissociative Interchange (I_d) and Associative

   Interchange (I_a) Mechanisms

$$ML_6 + L' \overset{K_{diff}}{\rightleftharpoons} \left[L_5M \begin{smallmatrix} \cdots L \\ \cdots L' \end{smallmatrix} \right]^{\ddagger} \overset{k_2}{\longrightarrow} ML_5L' + L$$
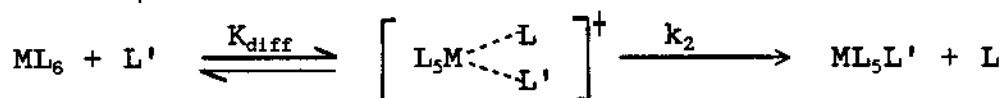
The rate law can be expressed as:

$$- \frac{d[ML_6]}{dt} = K_{diff}k_2[L'][ML_6]$$

This mechanism may be described as a diffusion-controlled

cage equilibrium prior to a transition state which positions

the new ligand L' to enter the coordination sphere on partial departure of L. In the I_d mechanism, the M-L bond experiences considerable extension, whereas in the I_a pathway, interaction between M---L' is much more advanced in the transition state.

(3) Associative (A) Mechanism

$$ML_6 + L' \xrightleftharpoons[k_{-1}(fast)]{k_1(slow)} ML_6L' \xrightarrow{k_2(fast)} ML_5L' + L$$
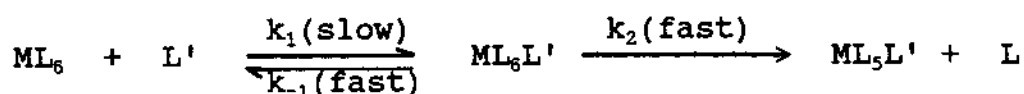
$$-\frac{d[ML_6]}{dt} = k_a[L'][ML_6]; \quad k_a = \frac{k_1 k_2}{(k_{-1}+k_2)}$$

This reaction proceeds $\underline{via}$ the formation of the seven-coordinate intermediate ML_6L' in the rate-determining step, and the rate law does not formally differ from that for a interchange mechanism.

Experimental examinations of reaction mechanisms rely on the verification of the rate law expressions and the interpretations of the activation parameters. Thus, large positive $\Delta H^{\ddagger}$, $\Delta S^{\ddagger}$ and $\Delta V^{\ddagger}$ values are highly suggestive of the dissociative pathway, whereas smaller $\Delta H^{\ddagger}$ and large negative $\Delta S^{\ddagger}$ and $\Delta V^{\ddagger}$ values usually reflect more associative pathway. Small absolute values of $\Delta S^{\ddagger}$ and $\Delta V^{\ddagger}$ often indicate the interchange mechanisms.[13,35] A schematic representation of the transition state at crucial points in the spectrum of ligand exchange mechanisms and their correlations with volumes of activation ($\Delta V^{\ddagger}$) are presented in Figure 5.[35]

$$k_p \gg k_o \qquad k_p > k_o \qquad k_p = k_o \qquad k_p < k_o \qquad k_p \ll k_o$$

$$\Delta V^{\ddagger} \ll 0 \qquad \Delta V^{\ddagger} < 0 \qquad \Delta V^{\ddagger} = 0 \qquad \Delta V^{\ddagger} > 0 \qquad \Delta V^{\ddagger} \gg 0$$

$$A \text{———} I_a \text{——} I \text{——} I_d \text{———} D$$
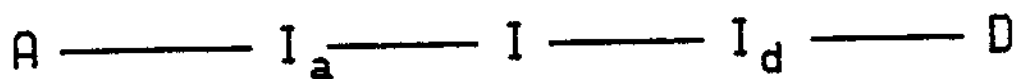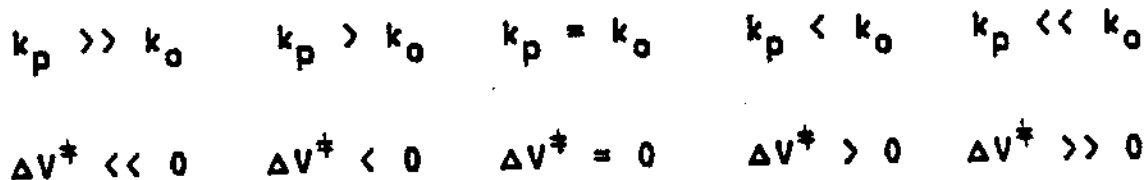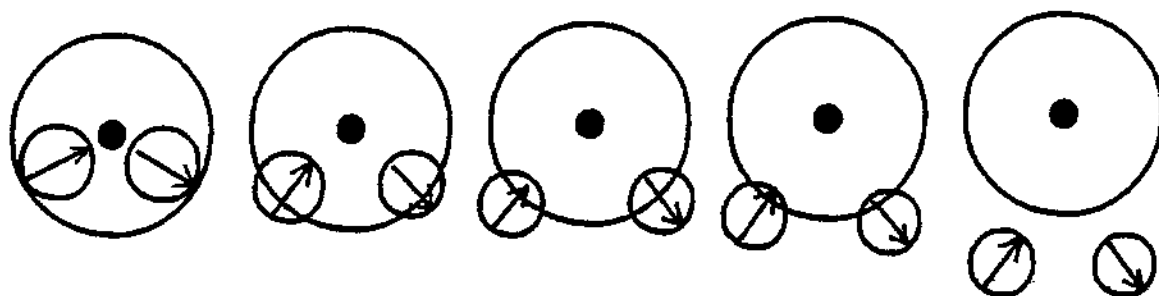
Figure 5. Schematic representation of the transition state at crucial points in the spectrum of ligand exchange mechanisms and their correlations with volumes of activation. The big circles represent the "coordination sphere"; the small circles represent the incoming ligands or leaving ligands. k_o and k_p are the rate constants for reactions under normal pressure and high pressures respectively.

D. Flash Photolysis

Most reaction intermediates cannot be observed directly in conventional thermal reactions because they are often formed only in very low concentrations relative to other predominant reactants and products.

Development and application of low temperature matrix isolation techniques have provided a large amount of spectroscopic and structural information about organometallic fragments,[36] but very limited information about reactivity of the fragments has been obtained.

Kinetic spectroscopy is a technique for spectroscopically detecting transient species generated after flash photolysis. The technique can provide information not only about structures of transition metal fragments, but also the reactivity and selectivity of short lived intermediates which exist as predominant reaction species on the time scales of milliseconds to femtoseconds.

The first flash photolysis apparatus, developed by Norrish and Porter,[37] works in a mode that is "dense in frequency domain but coarse in time". These experiments involved generation of transients with a UV flash light source and scanning of transients with another light source at certain time delays relative to the first flash. Relatively dense frequency information, i.e. spectrum, was

obtained but at only one time after a single flash. The

other mode of data collection usually involves flash

generation of transients and monitoring of transients at one

wavelength. The data obtained this way are continuous in

time at the given wavelength for a single flash, so called

"dense in time and coarse in frequency". However, in

principle, fine-grained frequency and fine-grained time

information can be obtained from multiple flash experiments

provided that a "fine-tunable" probing source is available.

In these time-resolved experiments, for each UV flash,

kinetic measurement is made at one probing wavelength. Other

flashes have to be made when detecting at different

wavelength for constructing "point-by-point"

spectra corresponding to any particular time delays after

the flash. Another feature of these time-resolved spectra is

that these are difference spectra which record only changes

in absorption before and after the flash.

Ultraviolet-visible (UV-VIS) spectroscopy is routinely

used for detecting intermediates generated by flash

photolysis. The advantages of UV-VIS detection are the

sensitivities and response times of UV-VIS detectors, the

high molar absorptivities of many chemical species, and the

high transparency of most solvents in the near-UV and VIS

regions. For systems in which a single primary ground-state

transient is generated by flash photolysis, application of

UV-VIS detection can provide satisfactory kinetic results with high time and wavelength resolution. However, when applied to the systems where there is ambiguity as to the identity of the photogenerated transient, UV-VIS detections have limitations which arise from the fact that UV-VIS spectra can provide little information about the structures of transition metal intermediates.[36a]

Much more structural and bonding information can be provided through vibrational spectroscopy,[38-39] such as time-resolved Raman spectroscopy,[40] time-resolved resonance Raman spectroscopy,[41-46] and time resolved IR spectroscopy.[47-68] Even though these detection systems are not as high in sensitivity and time resolution as in UV-VIS detection, it is clear that more applications of these techniques in the organometallic area will appear in the future.

Taking advantage of the well understood photochemistry for related metal carbonyl complexes,[2,69,70] flash photolysis with UV-VIS detection experiments can be employed to study the kinetics and mechanism of substitution reactions of solvent (= solv) in $(solv)M(CO)_4L$ (M = Cr, Mo, W; L = CO, phosphines, phosphites) which is the predominant reaction species after flash photolysis. When M = W, L = phosphine or phosphite, two isomers, cis-$(solv)W(CO)_4L$ and trans-$(solv)W(CO)_4L$, have been identified through time resolved IR spectroscopy.[60]

E. Roles of the solvents

It has been indicated by $Cr(CO)_6$ flash photolysis studies in solutions that the unsaturated species $Cr(CO)_5$ is deactivated and solvated in less than 200ps to produce [$(solv)Cr(CO)_5$] in which the solvent molecule occupies a position in the inner coordination sphere.[62,63,71-75] It is likely that the same is true for the Mo and W analogues. Such solvated intermediates appear to be widespread. Solvent effects widely exist in homogeneous catalysis and organometallic reactions may be interpreted in terms of such coordinating interactions of solvent with unsaturated species. As a matter of fact, when an "unsaturated" species is presumedly involved in a reaction mechanism in many cases, it may actually be a "coordinatively solvated" intermediate. For example, it has been indicated that the reactive "14-electron intermediate $RhCl(PPh_3)_2$" for "Wilkinson's hydrogenation catalyst" is in fact $RhCl(PPh_3)_2(\eta^2\text{-benzene})$ in benzene solutions (Figure 6).[76]

While solvent effects in most reactions have been interpreted in terms of polarities of the solvents, some so-called "donor solvents" like ethers, ketones, alcohols, and other solvents bearing electron-pair-donor atoms (N, O, S, etc.) have been recognized as coordinating solvents for many years. The roles of hydrocarbons as coordinating solvents did not draw much attention until recently when Dobson and

Wilkinson's Catalyst: $RhCl(PPh_3)_3$

$$RhCl(CO)(PPh_3)_2 \xrightarrow{h\nu} [RhCl(PPh_3)_2(PhH)] + CO$$

k_1 | k_{-1}, PPh_3

k_2, H_2

k_3, CO
$-H_2$

$Rh(H)_2Cl(PPh_3)_2$
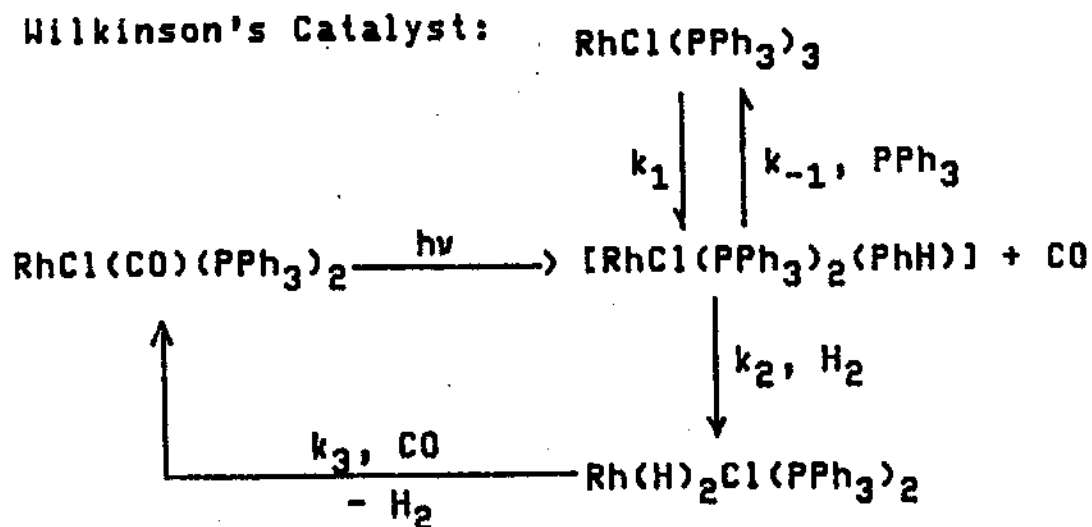
Figure 6. The benzene solvated intermediate in Wilkinson's Catalyst.

coworkers indicated that these solvents should be considered as "token ligands" in their interaction with unsaturated carbonyl species.[60] However, the mechanisms of solvent substitution reactions have not been investigated in detail.[77-83]

Since the rates of reactions of solvent molecules with photogenerated $[M(CO)_4L]$ (M = Cr, Mo, W; L = CO, phosphines) approach the diffusion-controlled rate in solution (vide supra),[62,63,71-75] there is little solv-M bond-making in

attaining the transition state. Thus, if the desolvation mechanism is dissociative, the activation enthalpy for desolvation, the microscopic reverse of the solvation process, would closely approximate the solv-M bond strength. Therefore, studies of the energetics (i.e. activation enthalpies) of desolvation reactions of hydrocarbon solvents may be correlated to the measurement of the hydrocarbon-metal bond strength, in particular of C-H-M "agostic" bonding, the step prior to C-H bond activation. However, the key to the use of activation enthalpies as possible measures of the strengths of "agostic" C-H-M bonds employing kinetics means is the development of a detailed understanding of the mechanism(s) of displacement for coordinated solvent molecules.

In summary, systematic investigations of kinetics and mechanisms of substitution reactions of various solvents in $(solv)M(CO)_4L$ by flash photolysis can provide information about the role of solvents in three respects:

(i) Their relevance to the reactivities and selectivities of organometallic and catalytic reactions.

(ii) The correlation of desolvation processes to C-H bond activation reactions through initial "agostic" interactions.

(iii) The nature of the solvent-metal interactions and their analogies to those in "normal" coordinating ligands.

The present studies will employ several techniques to probe the possible mechanistic pathways of solvent

displacement reactions:

(a) Through dilution of solvents with yet more "inert" solvents.

(b) Through the use of mixtures of ligand and solvent over wide ranges of concentrations.

(c) Through the determination of volumes of activation.

(d) Through the use of bidentate and potentially chelating ligands to take advantage of the "high effective concentration"[84] of the uncoordinated end of the ligand and the chelating effects.

CHAPTER II

EXPERIMENTAL SECTION

A. Materials

1. Metal Carbonyl Complexes

$Cr(CO)_6$, $W(CO)_6$ (Pressure Chemical Co.) and $Mo(CO)_6$ (Climax Molybdenum) were vacuum sublimed before use.

Tungsten carbonyl complexes shown in Table I (where pip = piperidine) were prepared by C.B. Dobson and I-H. Wang. The detailed procedures and their characterizations by IR and NMR have been previously described.[85-87]

2. Ligands

All the ligands employed in the studies were dried, distilled and stored under nitrogen before use. Table II summarizes the sources and purification procedures of these chemical reagents.

3. Solvents

Table III lists the sources and drying procedures for all the solvents which then were stored under nitrogen after purification.

Table I. Substituted Tungsten Carbonyl Complexes
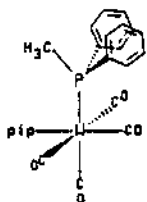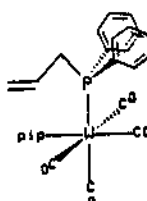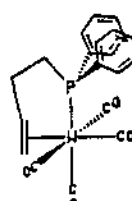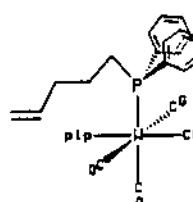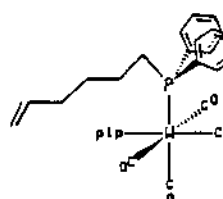
Complex	Phosphine Ligand
<u>cis</u>-(pip)(Ph$_2$PMe)W(CO)$_4$	methyldiphenylphosphine
	Ph$_2$P-CH$_3$
	(Ph$_2$PMe)

<u>cis</u>-(pip)(η^1-PRDPP)W(CO)$_4$ 2-propenyldiphenylphosphine

Ph$_2$P-CH$_2$-CH=CH$_2$

(PRDPP)

<u>cis</u>-(η^3-BDPP)W(CO)$_4$ 3-butenyldiphenylphosphine

Ph$_2$P-CH$_2$-CH$_2$-CH=CH$_2$

(BDPP)

<u>cis</u>-(pip)(η^1-PDPP)W(CO)$_4$ 4-pentenyldiphenylphosphine

Ph$_2$P-CH$_2$-CH$_2$-CH$_2$-CH=CH$_2$

(PDPP)

<u>cis</u>-(pip)(η^1-HDPP)W(CO)$_4$ 5-hexenyldiphenylphosphine

Ph$_2$P-CH$_2$-CH$_2$-CH$_2$-CH$_2$-CH=CH$_2$

(HDPP)

Table II. Ligands

Name[a]	Source	Purification[b]
Acetonitrile	Fisher Scientific	Distilled over CaH_2
Ethylenediamine (en)	Fisher Scientific	Distilled over KOH
1-Hexene (hex)	Aldrich	Distilled over $MgSO_4$
Norbornadiene (NBD)	Aldrich	Freshly distilled
2,6-Lutidine	Lancaster Synthesis Ltd.	Distilled over KOH
1,10-Phenan-throline (phen)	Aldrich	Stored under N_2
2-Picoline (pic)	Aldrich	Distilled over KOH
Piperidine (pip)	Aldrich	Distilled over KOH
Pyridine (py)	Fisher Scientific	Distilled over KOH
Tetramethylethylene	Lancaster Synthesis Ltd.	Distilled over $MgSO_4$
Tetrahydrofuran (THF)	Baker	Distilled over Na
Tributylamine	Aldrich	Distilled over KOH

a) Abbreviation in the parentheses.

b) All distillations were carried out under a stream of N_2.

Table III. Solvents

Name[a]	Source	Purification[b]
Benzene (BZ)	Mallinckrodt	Distilled over Na
Benzene-d_6 , 99.5% D	Norell, Inc.	Sealed under N_2
Bromobenzene	Matheson Coleman & Bell	Distilled over P_2O_5
o-Bromofluorobenzene	Lancaster Synthesis Ltd.	Distilled over P_2O_5
t-Butylbenzene	Eastman	Distilled over Na
Chlorobenzene (CB)	Aldrich	Distilled over P_2O_5
Cyclohexane (CH)	Baker	Distilled over Na[c]
Cyclohexylbenzene	Aldrich	Distilled over Na
Chlorobutane	Matheson Coleman & Bell	Distilled over P_2O_5
Cumene	Aldrich	Distilled over Na
o-Dichlorobenzene	Aldrich	Distilled over P_2O_5
Ethylbenzene	Aldrich	Distilled over Na
Fluorobenzene (FB)	Aldrich	Distilled over P_2O_5
n-Heptane (HP)	Fisher Scientific	Distilled over Na[c]
Hexanes (HX)	Baker	Distilled over Na
Mesitylene	Fisher Scientific	Distilled over Na
Methylcyclohexane	Aldrich	Distilled over Na

Table III - continued

Name[a]	Source	Purification
n-Octane	Aldrich	Distilled over Na
iso-Octane	Matheson Coleman & Bell	Distilled over Na
n-Octane-d_{18}, 98% D	Aldrich	Sealed under N_2
Perfluorobenzene	Aldrich	Sealed under N_2
Perfluoro(methyl-cyclohexane)	Fairfield Chemical Co.	Stored under N_2
Toluene	Mallinckrodt	Distilled over Na
1,2,3,4-Tetramethyl-benzene	Aldrich	Distilled over Na
α,α,α-Trifluoro-toluene	Lancaster Synthesis Ltd.	Distilled over P_2O_5
m-Xylene	Aldrich	Distilled over Na
o-Xylene	Aldrich	Distilled over Na
p-Xylene	Lancaster Synthesis Ltd.	Distilled over P_2O_5

a) Abbreviation in parentheses

b) All distillations were carried out under a stream of N_2.

c) The solvents were shaken with concentrated H_2SO_4 (3 times) followed by washing with distilled water (3 times) and dried over anhydrous $MgSO_4$ before distilling over Na to remove possible alkene impurities.

B. Flash Photolysis Studies

As discussed before, a kinetic spectrophotometer requires a UV flash photolyzing source. During the course of the present studies, several different photolyzing sources and flash photolysis systems have been employed.

1. Flash Photolysis with Flash Lamps

Flash photolysis studies with flash lamps (pulse width = 150 μs; rate constant = 10--10^4 s^{-1}) were carried out at the University of North Texas (UNT). This apparatus employed a Xenon-Corp. Model 720 flash photolysis system, which incorporated two high-pressure Xe lamps. The photolyzing light was focused by a collection of lenses and perpendicularly intersects with the analyzing light on an 1.0-cm jacketed cell. A 100-W Quartz Halogen lamp (Oriel Model 66172) powered by Harrison 6274A DC power supply was employed as the analyzing source. Two shutters (Uniblitz Electronics) placed between the analyzing light and the reaction cell were controlled by a sequence generator (Kinetics Instruments), which also contained an I_0 backoff module, which compensated for the detector voltage produced by the analyzing light. The slower shutter is designed to protect the faster shutter, which is not triggered until 180 μs before the flash to minimize photolysis of the reaction sample by the analyzing light. The light emerging from the

photolysis cell was focussed onto a Bausch and Lomb 33-86-20 monochromator and was detected by employing a Hamamatsu R928 photomultiplier tube operated by a Bertan PMT-2.0A-PA power supply. The spectrophotometer's output was digitized by a Nicolet 2090 IIa digital oscilloscope (fastest time resolution: 50ns per point) whose output was analyzed by employing a self-developed ASYST-based computer program[88] utilizing a standard 286 microcomputer to which it is interfaced.

2. Pulsed Laser Flash Photolysis at UNT

In this apparatus, the photolyzing source was a Lumonics TE-430 Excimer laser (351 nm, 10 ns FWHM, 25 mJ maximum energy) or a Tachisto Laser Systems Inc., Model 800 Excimer laser (351 nm, 20 ns FWHM, 200 mJ maximum energy) employing $Xe/F_2/He$ gas mixtures. The normal detection range for rate constants is $10 - 2 \times 10^5$ s^{-1}. A diagram for the flash photolysis systems built at UNT is shown in Figure 7.

3. Pulsed Laser Flash Photolysis at CFKR

Some relatively fast flash photolysis experiments (rate constant = $1 \times 10^4 - 6 \times 10^6$ s^{-1}) were performed at the Center for Fast Kinetics Research (CFKR), University of Texas at Austin, employing a Quantel Q-switched Nd.YAG laser (third harmonic, 355 nm, 11 ns FWHM, 100 mJ maximum energy output) as the photolysis source and a Xe lamp (150 W,

LASER FLASH

PHOTOLYSIS APPARATUS
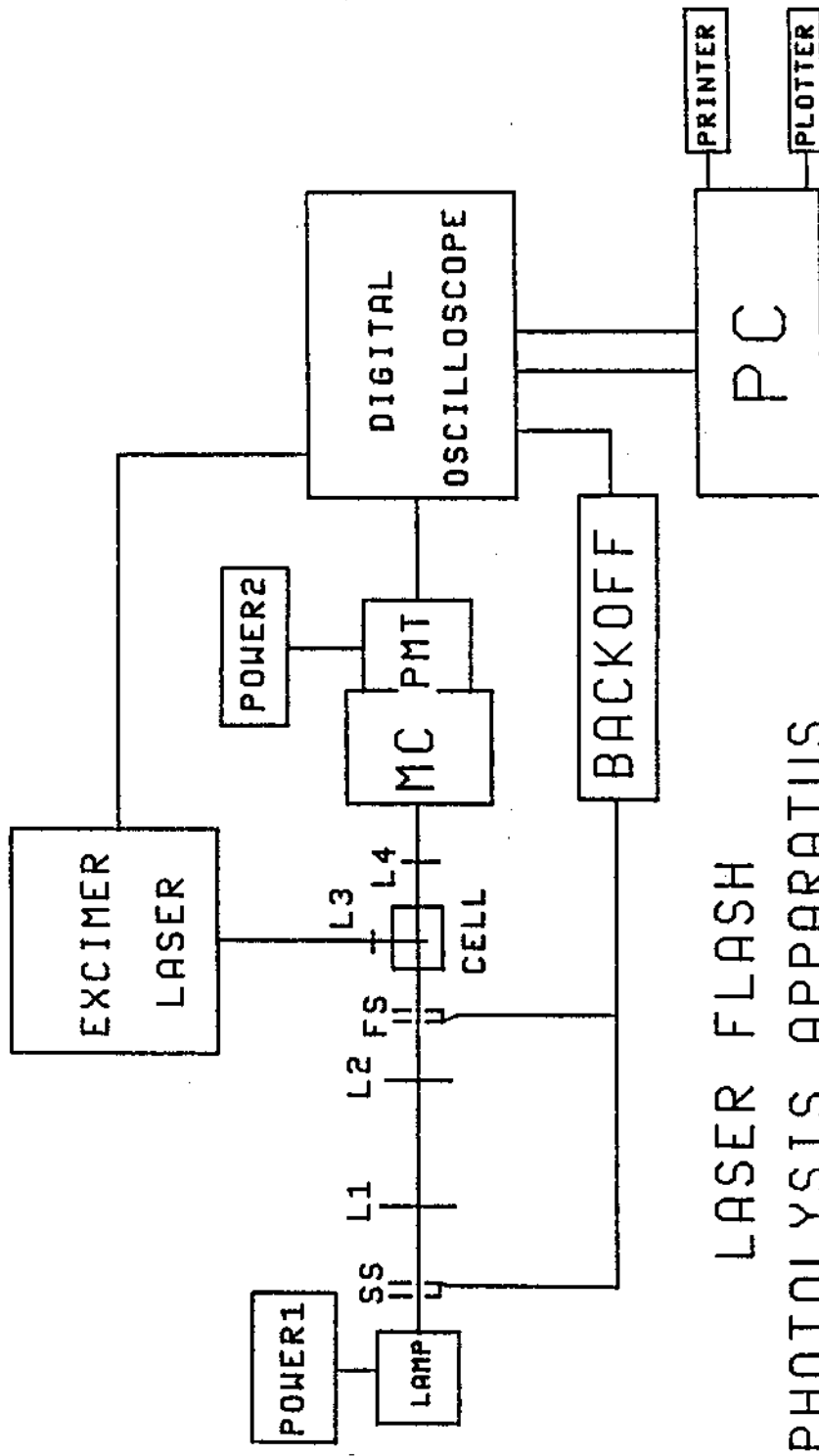
Figure 7. Laser flash photolysis apparatus at UNT.
SS: slow shutter; FS: fast shutter; L1-4: lenses;
MC: monochromator; PMT: photomultiplier tube.

Oriel) as the analyzing source. This apparatus has been described in detail in the literature.[89]

4. Flash Photolysis Studies under High Pressures

The flash photolysis under high pressure (1--2500 atm) was performed at both CFKR and UNT employing a pulsed laser as the photolyzing source. The laser beam was focussed upon a thermostated high pressure autoclave, which contained a "pill-box" optical cell. These experiments were carried out in collaboration with Prof. Rudi van Eldik, Dr. Hari C. Bajaj, and Volker Zang of the University of Witten/Herdecke, Federal Republic of Germany. The high pressure instrumentation has been previously described in detail.[90,91] A diagram of the compact and transportable high-pressure unit which was employed in these experiments is shown in Figure 8.[90b]

5. The Kinetics Conditions and the Reaction Products

The kinetics results obtained have been found to be totally reproducible independent of the different apparatus employed.[92] Thus the data will be discussed in the following text indistinguishably among the flash photolysis instruments.

The temperatures within the jacket reaction cell were regulated by employing a Forma-Temp Jr. Model 2095 J circulating bath and monitored ($\pm$ 0.1 °C) within the cell
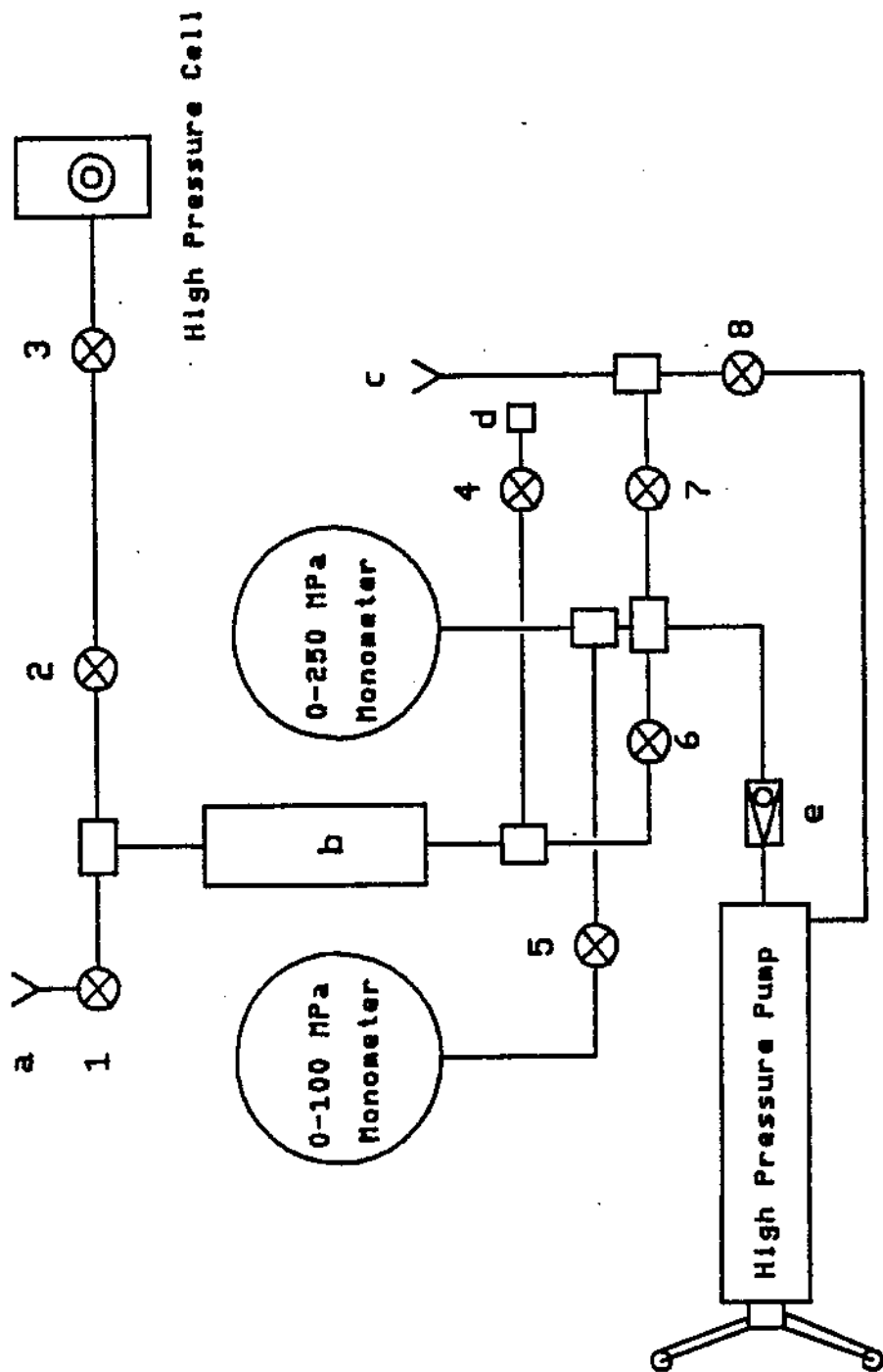
Figure 8. Schematic diagram of the high-pressure unit. (a) Water (pressure medium) reservoir, (b) separator unit, (c) oil reservoir, (d) to vacuum line, (e) one-way valve. 1-8: High-pressure valves.

with a Keithley 872 digital thermometer (FeCuNi thermocouple).

The monitoring wavelengths for the transient reactions were chosen according to the individual reactions studied to give the best signal-to-noise ratio in the range of 350 nm to 600 nm.

A single product for a studied reaction within the kinetics time window is usually produced as is evident from the single isosbestic point observed in the UV-VIS time-resolved spectra after flash photolysis (vide infra). The stable product, for example, $(pip)Cr(CO)_5$, has been identified through comparison of the UV-VIS spectra at long reaction times to that observed for an authentic sample. Reaction products for cis-$(pip)(L)W(CO)_4$ (L = phosphines) have been previously identified through IR spectroscopy.[87]

For a typical reaction, a solution about 3.5×10^{-3} M in metal carbonyl complex and containing much excess of "trapping reagent" (i.e. ligands: piperidine, 1-hexene and pyridine) was employed to ensure that pseudo-first-order reaction conditions were attained. It was determined that there were no significant differences between the traces obtained from the first flash and after many flashes. The pseudo-first-order rate constants, k_{obsd}, obtained from average of 1 to 10 traces, will be presented together with error limits in parentheses as the uncertainty of the last digit(s) of cited value to one standard deviation.

CHAPTER III

KINETICS AND MECHANISMS OF SOLVENT DISPLACEMENT
FROM PHOTOGENERATED [(SOLVENT)Cr(CO)$_5$]
(SOLVENT = CHLOROBENZENE, BENZENE)[93]

Chlorobenzene and benzene are among common solvents employed in many organometallic reactions. Some reactive intermediates exist in homogeneous catalysis have been found to be specifically solvated by these solvent molecules.[76] There are several possible "bonding sites" for these solvent-metal interactions, for example, Cl-M, η^2-coordination through an "isolated" double bond, and "agostic" C-H-M interactions. Meanwhile, Cr(CO)$_6$ has served as a model for studies of solvation in coordinatively-unsaturated intermediates. It has been found that upon Cr-CO bond photodissociation in Cr(CO)$_6$, the [Cr(CO)$_5$] produced reacts very rapidly with the solvent to afford [(solvent)Cr(CO)$_5$] species,[62,63,71-75] in which the solvent molecule specifically interacts with the metal center.

Examination of the nature of these solvent-metal interactions through studies of the mechanism of desolvation are of much interest for understanding the reactivities of reaction intermediates, especially since η^2- as well as "agostic" interactions have been implicated in the reaction pathways to C-H bond activation by transition metals.[14-26]

30

Cr(CO)$_6$ has also been implicated as the precursor to photochemically-generated catalysis involved in olefin isomerization, hydrogenation and hydrosilylation reactions.[2] Thus there are compelling reasons to study the mechanism of solvent displacement reaction of [(solv)Cr(CO)$_5$] transients by Lewis bases (L), such as piperidine, pyridine, and olefins, common reactants in catalysis, to afford LCr(CO)$_5$ products.

A. Identification of Reaction Intermediates and Products

The time-resolved spectra obtained after flash photolysis of Cr(CO)$_6$ in pip/BZ ([pip] = 2.531 M) solutions are shown in Figure 9. The inset shows the resolution by the best Gaussian/Lorentzian fit of the experimental data,[88] for one of these traces, recorded 5 μs after the flash. It is resolved into spectra for the species generated initially (λ_{max} = 458(10) nm) whose absorbance gradually decreases and the species whose absorbance increases during the reaction (λ_{max} = 410(1) nm). The first maximum is attributable to formation of [(BZ)Cr(CO)$_5$], which has been observed in solution with λ_{max} at 460 nm[94a] and 465 nm[94b] after flash photolysis. The band observed at 410 nm has likewise been attributed to (pip)Cr(CO)$_5$ (LF, $^1A_1 \rightarrow {}^1E$),[95a] the reaction product. The time-resolved spectra obtained after flash photolysis of Cr(CO)$_6$ in a pip/CB solution afforded
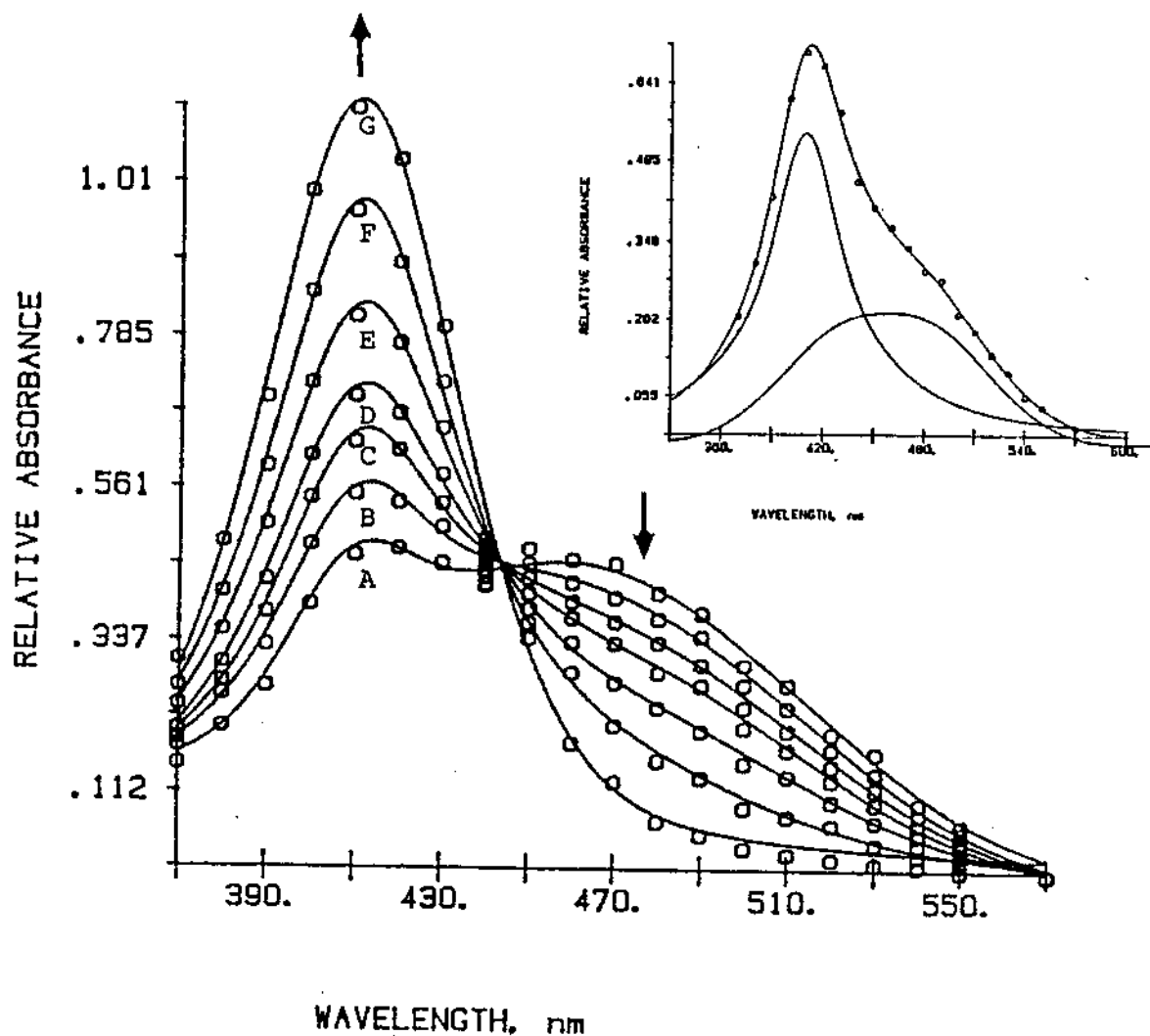
Figure 9. Time-resolved spectra obtained after flash photolysis of $Cr(CO)_6$ in pip/BZ solutions ([pip] = 2.531 M) at 25.0 °C. Time after the flash: (a) 0.5 μs; (b) 2.0 μs; (c) 3.5 μs; (d) 5.0 μs; (e) 8.5 μs; (f) 16 μs; (g) 67 μs. Inset: plot of relative absorbance vs wavelength for spectrum (d) showing resolution of the plot into spectra for [η^2-BZ)$Cr(CO)_5$] (λ_{max} = 458(10) nm) and (pip)$Cr(CO)_5$ (λ_{max} = 410(1) nm).

$\lambda_{max} \approx 480$ nm for $(CB)Cr(CO)_5$ and $\lambda_{max} \approx 420$ nm for

$(pip)Cr(CO)_5$ in CB solvent. The lower energy absorptions for

BZ and CB solvated species than that of $(pip)Cr(CO)_5$ are

consistent with a weaker interaction between BZ or CB with

Cr than between pip and Cr.[85b,c] (cf Figure 2). Figure 10

shows analogous spectra obtained after flash photolysis of

$Cr(CO)_6$/hex/BZ ([hex] = 2.366 M) solution. Resolution

(inset) affords a relatively more accurate λ_{max} for

$(BZ)Cr(CO)_5$ at 468(2) nm due to the amplified scale for the

absorbance. Another λ_{max} at 344(6) nm, obtained by

extrapolation, is attributed to $(\eta^2-hex)Cr(CO)_5$, the

reaction product. The higher energy absorption wavelength

for $(\eta^2-hex)Cr(CO)_5$ is attributable to the metal to olefin

π-back-bonding.[69] It is noted in Figure 9 and 10 that the

time-resolved spectra exhibit isosbestic points, indicating

conversion of $(BZ)Cr(CO)_5$ to single products. Thus the

reaction stoichiometry accompanying flash photolysis of

$Cr(CO)_6$ is that shown in Eq. 1:

$$Cr(CO)_6 \xrightarrow[+solv]{h\nu} [(solv)Cr(CO)_5] \xrightarrow[+L]{k_{obsd}} LCr(CO)_5 \qquad (1)$$
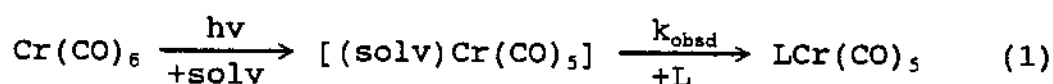
A typical plot of absorbance vs time after flash

photolysis of $Cr(CO)_6$/pip/BZ solution ([pip] = 2.085 M),

monitoring at 490 nm, is shown in Figure 11. The trace was

fitted as an exponential decay and the inset shows the

34
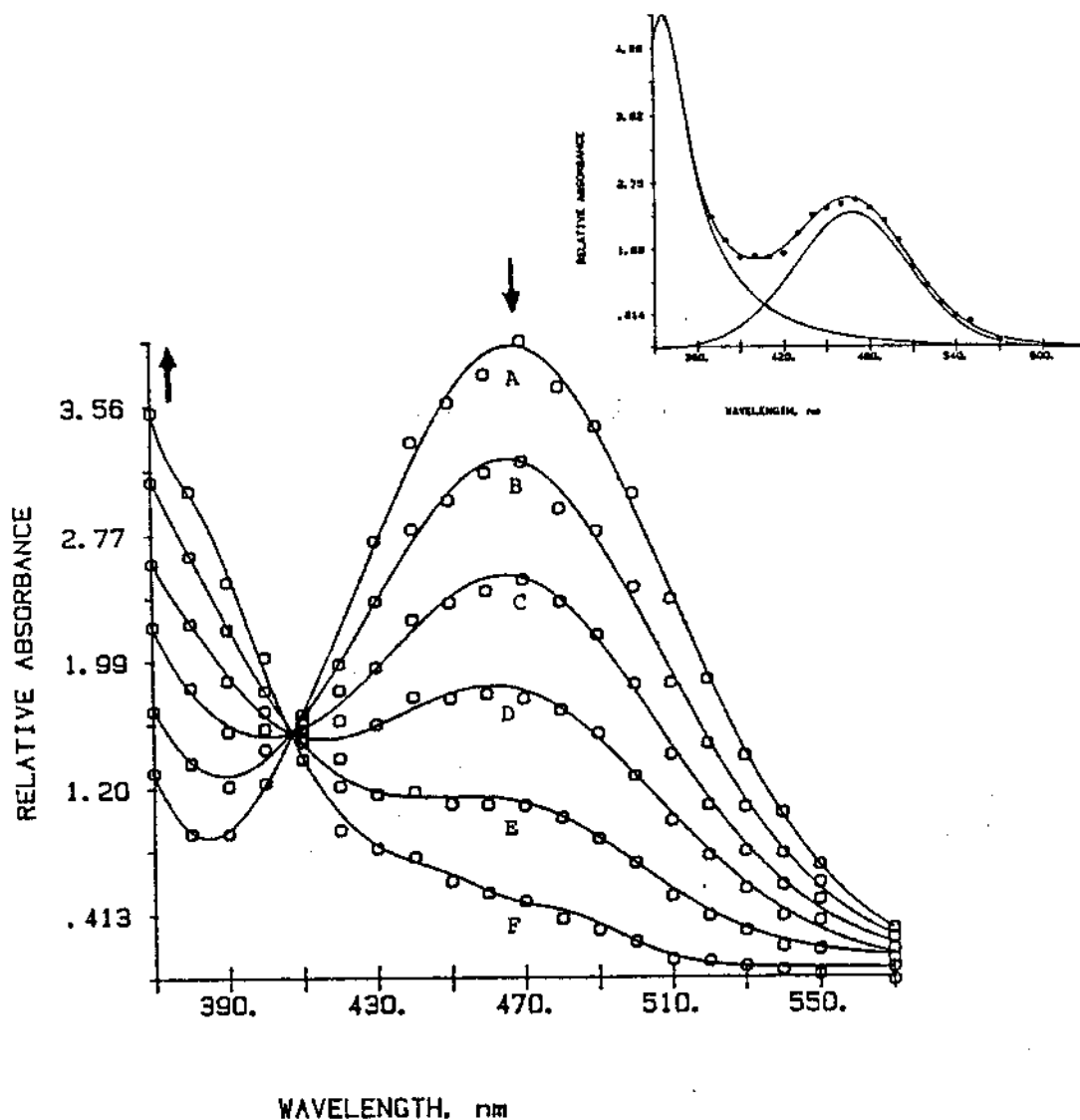
Figure 10. Time-resolved spectra obtained after flash
photolysis of $Cr(CO)_6$ in hex/BZ solutions ([hex] = 2.366
M) at 25.0 °C. Time after the flash: (a) 1.0 μs; (b) 10.0
μs; (c) 22.0 μs; (d) 37.0 μs; (e) 64.5 μs; (f) 134.5 μs.
Inset: plot of relative absorbance vs wavelength for
spectrum (c) showing resolution of the plot into spectra
for [η^2-BZ)Cr(CO)$_5$] (λ_{max} = 468(2) nm) and (hex)Cr(CO)$_5$
(λ_{max} = 344(6) nm).
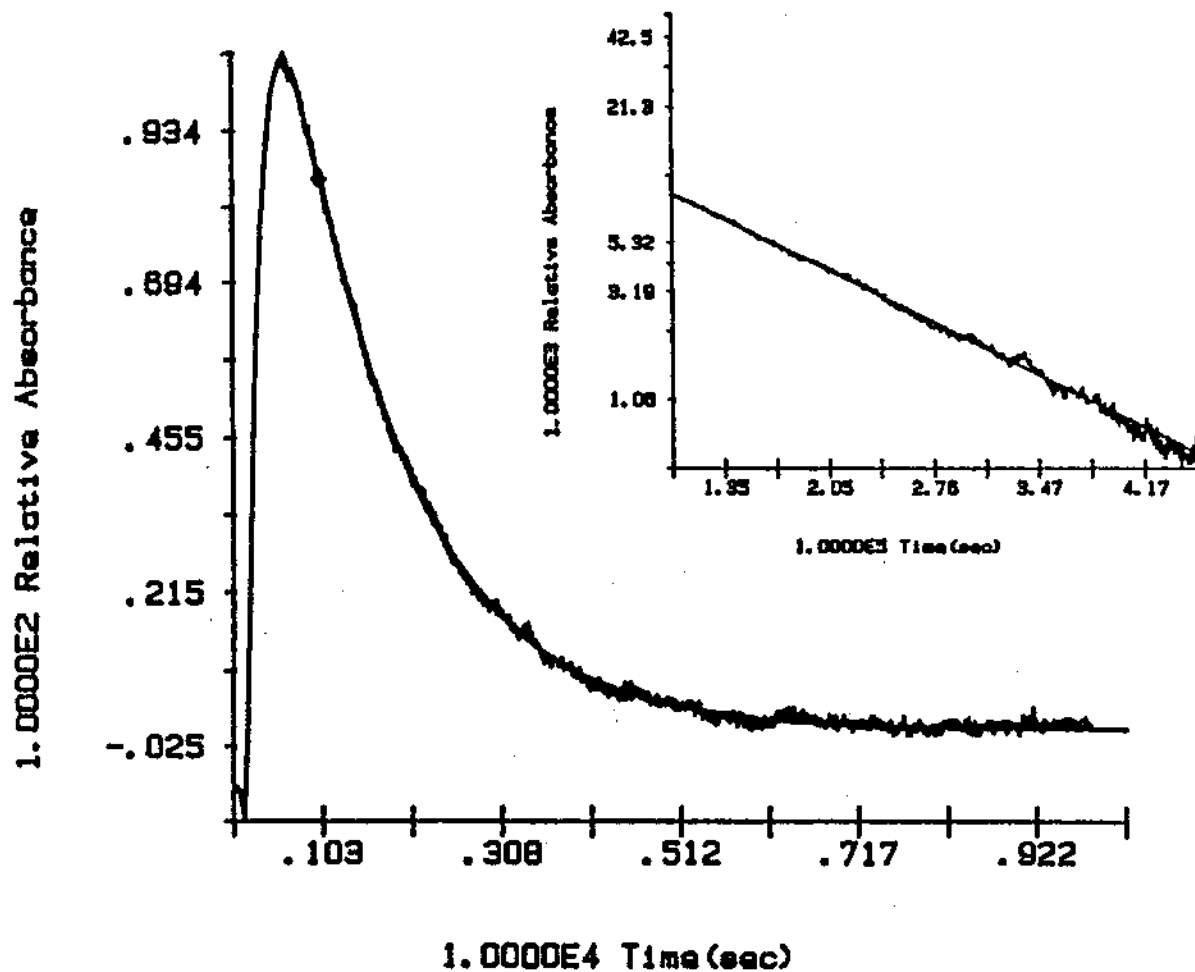
Figure 11. Plot of absorbance vs time monitoring 490 nm for reaction taking place after flash photolysis of $Cr(CO)_6$ in pip/BZ solution ([pip] = 2.085 M) at 25.0 °C. The inset shows the data plotted as ln $(A_t - A_\infty)$ vs time.

corresponding linear plot of $\ln(A_t - A_\infty)$ vs time, where A_t and A_∞ are absorbances at time t and at "infinite" time respectively. Similar plots were obtained for reactions in other solvents and with other Lewis bases. These plots indicate that the disappearance of the photogenerated transient, $(solv)Cr(CO)_5$, obeys pseudo-first-order kinetics.

B. Kinetics of the Displacement of Chlorobenzene

Previous studies for reactions of $(CB)Cr(CO)_5$ produced after flash photolysis of $Cr(CO)_6$ were carried out in CB solutions containing various concentrations of pip.[92] The plot of the pseudo-first-order rate constants, k_{obsd}, vs [pip], taken at 31.1 °C afforded a straight line going through the origin, which is consistent with Eq.2,

$$k_{obsd} = k[pip] \qquad (2)$$

To obtain further mechanistic information, studies in which the concentrations of CB could be varied widely were also carried out. Such studies are possible in pip/CB/HX (HX = hexanes) solutions. In these solutions, $(HX)Cr(CO)_5$ intermediates will be present in steady-state concentrations on the time scale of reaction of $(CB)Cr(CO)_5$ since the observed rate constants for displacement of alkanes from $(alkane)Cr(CO)_5$ intermediates are more than three orders of

magnitude greater than is that for displacement of CB from (CB)Cr(CO)$_5$ (vide infra; see Chapter IV).[60] The values of k_{obsd} obtained from rate studies of reactions of (CB)Cr(CO)$_5$ in pip/CB/HX solutions at three temperatures are given in Table IV.

Figure 12 illustrates plots of the pseudo first-order rate constants, k_{obsd}, vs [pip]/[CB] which obey the rate law,

$$kobsd = \frac{k'[pip]}{[CB] + k''[pip]} \qquad (3)$$

Eq. 3 can be rearranged to Eq. 4,

$$1/k_{obsd} = k''/k' + [CB]/(k'[pip]) \qquad (4)$$

for which plots of $1/k_{obsd}$ vs [CB]/[pip] are expected to be linear. These plots are shown in Figure 13. Values for the rate constants k' and k", as well as for k'/k" (vide infra), obtained from plots of $1/k_{obsd}$ vs [CB]/[pip], together with activation parameters derived from the data at three temperatures, are given in Table V.

The rate behavior observed for the reaction of (CB)Cr(CO)$_5$ in CB (Eq. 2) can reasonably be attributed to either of two mechanisms. The first of these involves the displacement of CB by pip via a seven-coordinated activated complex, i.e., through an interchange reaction pathway. The

Table IV. Pseudo First-order Rate Constants for Reactions
Taking Place After Flash Photolysis of $Cr(CO)_6$ in
pip/CB/hexanes Solutions at Various Temperatures

[pip] (M)	[CB] (M)	[CB]/[pip]	Temp. (°C)	$10^{-4}k_{obsd}$ (s^{-1})
0.1032	0.5026	4.870	13.8	0.919(1)
0.1291	0.4961	3.843		1.12(3)
0.1654	0.5159	3.119		1.29(1)
0.2669	0.5192	1.945		1.84(1)
0.5082	0.5132	1.010		2.58(18)
0.4927	0.3044	0.6178		2.96(5)
0.4956	0.2141	0.4320		3.19(2)
1.000	8.820	8.820	24.5	2.22(2) (in neat CB)
0.1032	0.5026	4.870		1.95(5)
0.1291	0.4961	3.843		2.47(6)
0.1654	0.5159	3.119		2.84(2)
0.2669	0.5192	1.945		3.66(5)
0.5082	0.5132	1.010		5.21(6)
0.4927	0.3044	0.6178		5.90(9)
0.4956	0.2141	0.4320		6.52(26)
0.1116	0.7871	7.053	35.4	2.52(6)
0.1032	0.5026	4.870		3.48(15)
0.1291	0.4961	3.843		4.06(15)
0.1654	0.5159	3.119		4.60(2)
0.2669	0.5192	1.945		6.46(8)
0.5082	0.5132	1.010		9.4(4)
0.4927	0.3044	0.6178		10.9(1)
0.4956	0.2141	0.4320		11.65(7)
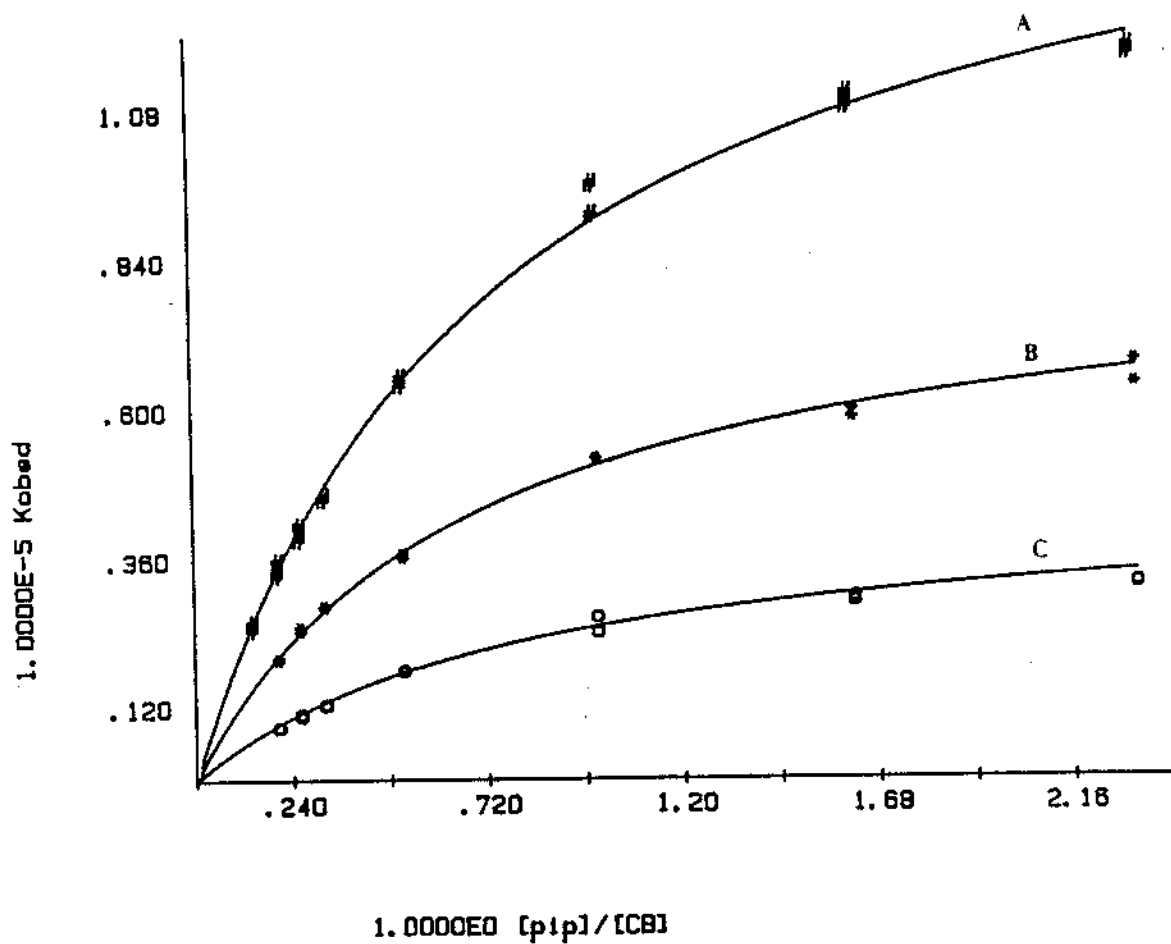
Figure 12. Plots of k_{obsd} vs [pip]/[CB] for the reaction taking place after flash photolysis of $Cr(CO)_6$ in pip/CB/HX solutions at (A) 35.4, (B) 24.5, (C) 13.8 °C.
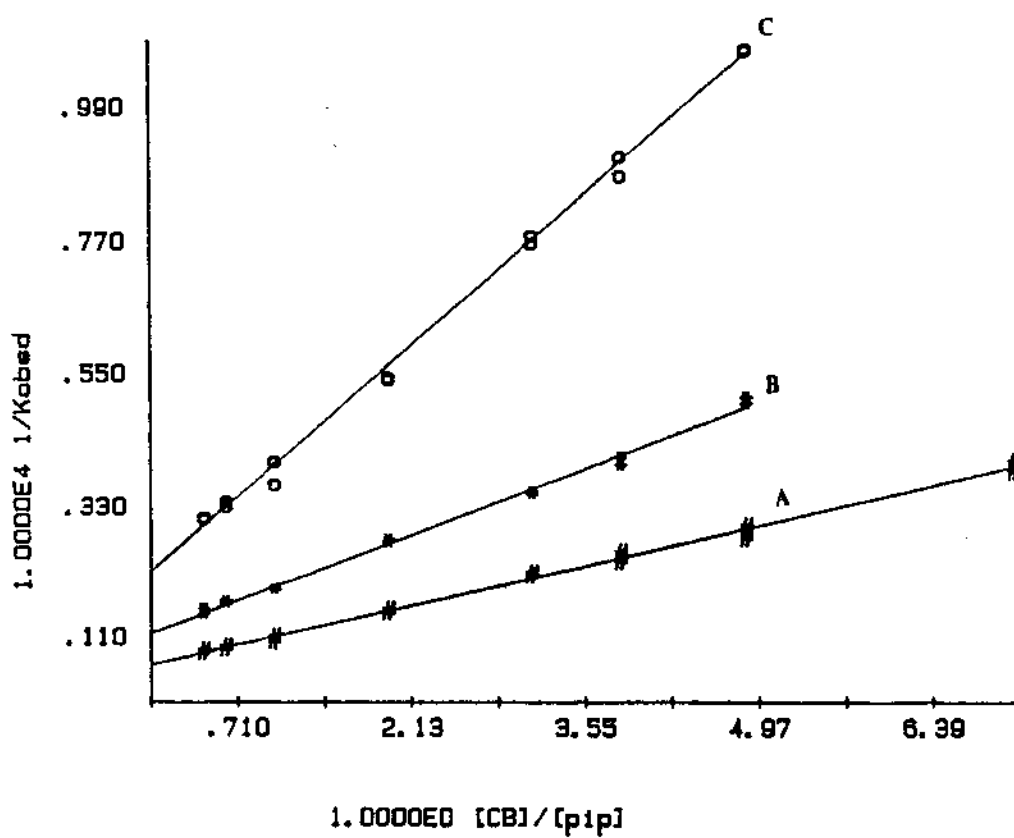
Figure 13. Plots of $1/k_{obsd}$ vs [CB]/[pip] for the reaction
taking place after flash photolysis of $Cr(CO)_6$ in
pip/CB/HX solutions at (A) 35.4, (B) 24.5, (C) 13.8 °C.

Table V. Rate Constants and Activation Parameters for the

Reaction Taking Place After Flash Photolysis of

$Cr(CO)_6$ in pip/CB/HX Solutions at Various Temperatures

Temp. (°C)	$10^{-4}k_1k_2/k_{-1}$ $(= 10^{-4}k')$ (s^{-1})	$10^{-4}k_1$ $(= 10^{-4}k'/k'')$ (s^{-1})	k_2/k_{-1} $(= k'')$
13.8	5.65(13)	4.41(19)	1.28(9)
24.5	12.6(3)	8.6(4)	1.47(9)
35.4	21.2(3)	15.8(6)	1.35(7)

$\Delta H^{\ddagger}_1 + \Delta H^{\ddagger}_2 - \Delta H^{\ddagger}_{-1} = 10.2(8)$ kcal/mol;

$\Delta S^{\ddagger}_1 + \Delta S^{\ddagger}_2 - \Delta S^{\ddagger}_{-1} = 0.0(20)$ cal/(deg mol).

$\Delta H^{\ddagger}_1 = 9.8(1)$ kcal/mol; $\Delta S^{\ddagger}_1 = -2.9(4)$ cal/(deg mol).

$\Delta H^{\ddagger}_2 - \Delta H^{\ddagger}_{-1} = 0.4(9)$ kcal/mol;

$\Delta S^{\ddagger}_2 - \Delta S^{\ddagger}_{-1} = 2.4(24)$ cal/(deg mol).

second envisions a dissociative process involving a rapid
equilibrium between $(CB)Cr(CO)_5$ and the five-coordinated
$[Cr(CO)_5]$, followed by attack by pip at the latter. The two
pathways are described in Scheme I, where solv = CB, L =
pip. Assuming a steady-state concentration of $[Cr(CO)_5]$, the
rate law corresponding to the dissociative pathway obeys
Eq. 5,

Scheme I
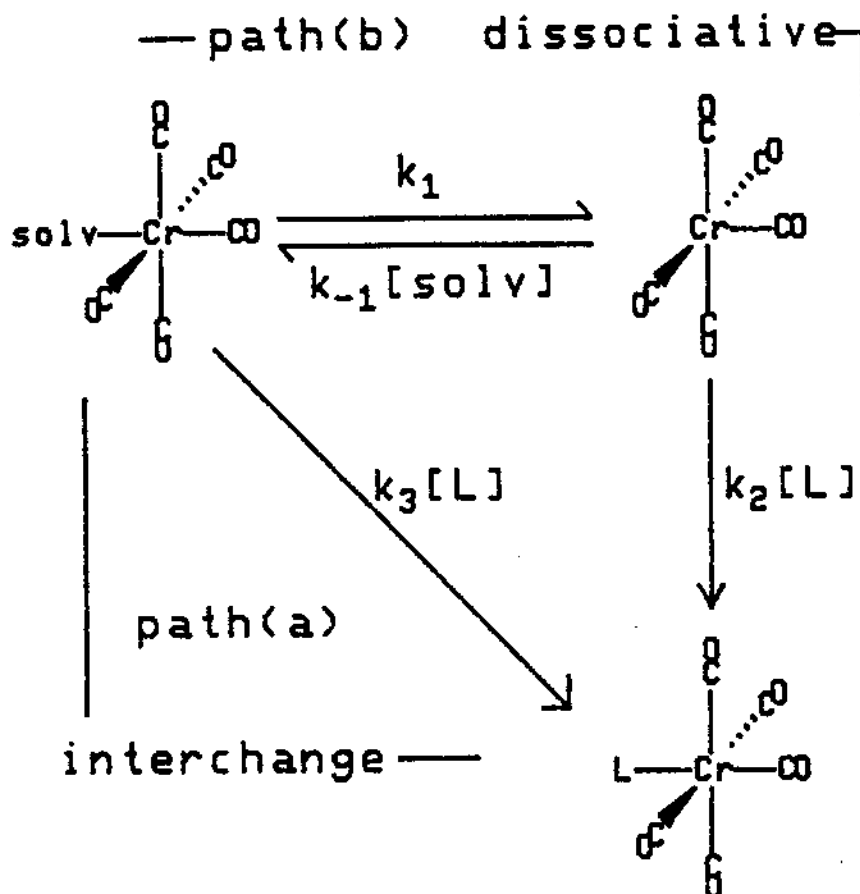
$$- \frac{d[(solv)Cr(CO)_5]}{dt} = \frac{k_1 k_2[L]}{k_{-1}[solv] + k_2[L]} [(solv)Cr(CO)_5]$$

$$(5)$$

for which the pseudo-first-order rate constants, k_{obsd}, obey the relationship,

$$k_{obsd} = \frac{k_1 k_2[L]}{k_{-1}[solv] + k_2[L]} \qquad (6)$$

or, upon rearrangement,

$$1/k_{obsd} = 1 /k_1 + (k_{-1}/k_1 k_2)([solv]/[L]) \qquad (7)$$

For present reaction solv = CB, L = pip, since [CB] >> [pip], it is not unreasonable to presume that $k_{-1}[CB]$ >> $k_2[pip]$, whereupon Eq. 6 becomes,

$$k_{obsd} = \{k_1 k_2/(k_{-1}[solv])\}[L] \qquad (8)$$

where $k_1 k_2/(k_{-1}[solv])$ is almost constant when [solv] >> [L]; thus Eq. 8 is consistent the observed rate expression Eq. 2.

The rate behavior in pip/CB/HX solutions (Eq. 3, 4), however, is consistent the dissociative pathway (Eq. 7). A dissociative mechanism is also consistent with the mechanism observed for displacement of CB from cis-(CB)(L)W(CO)$_4$ (L = P(O-i-Pr)$_3$) by pip.[80]

However the use of HX as an "inert" solvent for these studies, where [CB]/[pip] values were widely varied, raises yet another mechanistic possibility, that (CB)Cr(CO)$_5$ and (pip)Cr(CO)$_5$ are formed via interchange processes from [(HX)Cr(CO)$_5$]; this possibility, illustrated in Scheme II,

Scheme II

$$\text{(CB)Cr(CO)}_5 \underset{k'_{-1}[CB]}{\overset{k'_1[HX]}{\rightleftharpoons}} \text{(HX)Cr(CO)}_5 \overset{k'_2[pip]}{\longrightarrow} \text{(pip)Cr(CO)}_5$$
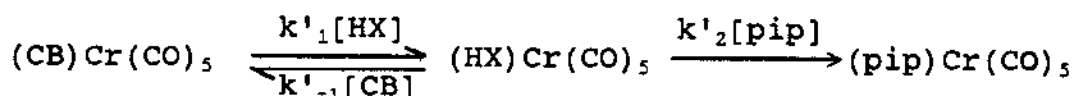
affords a rate law,

$$K_{obsd} = \frac{k'_1 k'_2 [pip]}{k'_{-1}[CB] + k'_2[pip]} [HX] \qquad (9)$$

of the same form as Eq. 6. This mechanism, which envisions

significant HX-Cr interaction in the transition state <u>via</u>

"agostic" bonding, is that proposed by Yang, Vaida and

Peters,[83] for displacement of <u>n</u>-heptane (HP) from   .

$(HP)Cr(CO)_5$ by various Lewis bases. The interchange

transition state differs from that for the dissociative

pathway only in its relationship to the reactants and

products: the dissociative pathway envisions a "late"

transition state, while the interchange pathway involves an

earlier one in which both HP-Cr bond-breaking and pip-Cr

bond-making take place.

The observed kinetics behavior in pip/CB/HX solutions

(Eq. 3) supports either the dissociative pathway in Scheme I

(Eq. 6), <u>via</u> the $[Cr(CO)_5]$ intermediate, or the mechanistic

pathway in Scheme II (Eq. 9), <u>via</u> the $(HX)Cr(CO)_5$

intermediates, since under the conditions employed for the

reactions, $[HX] \gg ([pip] + [CB])$ and thus $[HX]$ is

essentially constant.

We will presume for the moment that the applicable

mechanism is the dissociative pathway in Scheme I. If this

is the case, from Eq. 4 and Eq. 7, $k' = k_1 k_2/k_{-1}$, $k'' =$

k_2/k_{-1}, the "competition ratios" of the rate constants for

attack at $[Cr(CO)_5]$ by pip and CB, respectively, and $k'/k'' =$

k_1, the rate constant for dissociation of CB from

(CB)Cr(CO)$_5$. These rate constants, together with the corresponding activation parameters, are given in Table V. As is shown in the table, the "competition ratios" are independent of temperature. Thus, $\Delta H^\ddagger_2 - \Delta H^\ddagger_{-1}$ is zero within experimental error (0.4 (9) kcal/mol). This value may be compared to the corresponding difference in $\Delta H^\ddagger$'s for the reverse processes, for dissociation of pip from (pip)Cr(CO)$_5$, 25.7(6) kcal/mol,[96] and for dissociation of CB from (CB)Cr(CO)$_5$, governed by k_1 Scheme I, 9.8(1) kcal/mol (Table V). Thus, the strengths of pip-Cr and CB-Cr bonds differ very significantly, while the rates of attack by these ligands at the intermediate, whatever its identity, are virtually the same.

However, several points remain uncertain after these studies on CB displacement from (CB)Cr(CO)$_5$ by pip. (i) What is the intermediate(s), [Cr(CO)$_5$] or (HX)Cr(CO)$_5$, or both in CB/HX solutions? (ii) What is the bonding mode of CB with Cr, through Cl, "C=C" or C-H "agostic" interaction? (iii) The entropy of activation, $\Delta S^\ddagger_1 = -2.9(4)$ cal/(deg mol) (Table V) is considerably more negative than might be anticipated for a dissociation process. (iv) Comparisons of the ratio of rate constants, at 24.5 °C, $k_1 k_2/k_{-1}$, (k', Eq. 4), in HX solution with the same ratio in CB solution, obtained as k_{obsd}[CB]/[pip] (Eq. 8) are 1.26(3) x 10^5 s^{-1} and 1.97(2) x 10^5 s^{-1}, respectively. The difference is greater than expected from experimental errors, which may be

attributed to "bulk solvent effects", since in one case the solvent is CB and in the other, the bulk solvent is HX. This difference may also arise from the possible accessibility of interchange pathway (Scheme I) for CB displacement from $(CB)Cr(CO)_5$ by pip in CB, while in pip/CB/HX solutions, this influence might be small due to the much lower concentrations of pip employed. Therefore, further investigations planned to probe these mechanistic possibilities will be discussed later.

C. Reactions of Benzene Displacement From $(BZ)Cr(CO)_5$

To obtain the most mechanistic information, while avoiding the complications due to the introduction of a "second solvent" (vide supra), mechanistic studies of reactions of $[(BZ)Cr(CO)_5]$ produced after flash photolysis of $Cr(CO)_6$ were carried out in "binary systems" of pip/benzene, hex/benzene, py/benzene and pip/benzene-d_6 mixtures, in which both the concentrations of ligand and benzene were widely varied:

$$1.7 \text{ M} < [pip] < 4.9 \text{ M};$$
$$1.6 \text{ M} < [hex] < 5.9 \text{ M};$$
$$1.2 \text{ M} < [py] < 6.2 \text{ M};$$
$$2.8 \text{ M} < [BZ] < 10.0 \text{ M}.$$

Values of all pseudo-first-order rate constants obtained for these systems are presented in Table VI.

Table VI. Pseudo First-order Rate Constants for Reactions
Taking Place After Flash Photolysis of $Cr(CO)_6$ in
L/Benzene (L = pip, hex, py) and pip/Benzene-d_6
Solutions at Various Temperatures and Pressures

[solv] (M)	[L] (M)	Temp. (°C)	Pres. (atm)	$10^{-4}k_{obsd}$ (s^{-1})
Benzene	piperidine			
5.851	4.925	35.0	1	28.0(6)
				27.8(6)
		25.0		16.04(14)
				15.99(10)
		15.0		9.20(2)
				9.30(2)
		5.0		4.98(1)
				5.01(1)
7.951	3.022	35.0		18.2(1)
				18.5(2)
		25.0		10.71(9)
				10.92(8)
		15.0		6.24(2)
				6.34(3)
		5.0		3.496(6)
				3.494(7)
8.997	2.085	35.0		13.3(2)
				13.8(2)
		25.0		7.89(3)
				7.88(2)
		15.0		4.61(1)
				4.69(1)
		5.0		2.575(8)
				2.579(8)
9.337	1.717	35.0		11.77(8)
				11.50(8)
		25.0		6.66(2)
				6.84(5)
		15.0		4.054(4)
				4.040(4)
		5.0		2.213(6)
				2.197(5)

Table VI. Continued

[solv] (M)	[L] (M)	Temp. (°C)	Pres. (atm)	$10^{-4}k_{obsd}$ (s^{-1})
	1-hexene			
3.305	5.540	25.0		9.59(16)
5.661	3.983			5.49(6)
6.702	3.168			3.88(6)
7.685	2.424			2.68(4)
8.912	1.645			1.64(2)
2.802	5.893	35.0		21.96(17)
		15.0		5.86(26)
		5.0		2.65(2)
5.302	4.175	35.0		11.37(33)
		15.0		2.82(6)
		5.0		1.287(8)
6.874	3.012	35.0		7.12(14)
		15.0		1.75(2)
		5.0		0.771(6)
8.130	2.134	35.0		4.60(4)
		15.0		1.07(2)
		5.0		0.486(4)
8.797	1.669	35.0		3.45(4)
		15.0		0.807(14)
		5.0		0.354(6)
	pyridine			
5.625	6.183	25.0		58.1(12)
6.737	4.937			49.4(4)
7.842	3.706			38.4(10)
8.973	2.472			27.0(5)
10.061	1.244			14.51(7)
Benzene-d$_6$	piperidine			
3.181	7.131	25.0		23.4(2)
				24.6(13)
				24.9(4)
		15.0		13.33(6)
				13.52(10)
				13.37(7)
		5.0		7.91(4)
				7.41(3)
				8.04(4)
5.358	5.235	35.0		26.7(4)

Table VI. Continued

[solv] (M)	[L] (M)	Temp. (°C)	Pres. (atm)	$10^{-4}k_{obsd}$ (s^{-1})
				28.6(5)
				27.1(5)
		25.0		16.98(8)
				17.82(11)
				17.42(14)
		15.0		9.93(5)
				10.21(5)
				10.42(7)
		5.0		5.93(3)
				6.60(2)
				5.95(3)
7.074	3.668	35.0		21.2(3)
				21.0(3)
				22.4(2)
		25.0		12.58(6)
				13.25(5)
				12.81(5)
		15.0		7.22(3)
				7.38(3)
				7.14(3)
		5.0		4.11(1)
				3.99(1)
				4.11(1)
8.474	2.488	35.0		14.45(9)
				14.64(9)
				13.60(20)
		25.0		8.79(3)
				8.32(2)
				8.43(3)
		15.0		4.92(2)
				5.02(2)
				5.08(2)
		5.0		2.92(1)
				2.98(1)
				2.91(1)
9.112	1.830	35.0		10.82(4)
				10.74(10)
				10.84(6)
		25.0		6.58(4)
				6.52(2)
				6.68(2)
		15.0		3.82(1)
				3.86(2)

Table VI. Continued

[solv] (M)	[L] (M)	Temp. (°C)	Pres. (atm)	$10^{-4}k_{obsd}$ (s^{-1})
				3.85(1)
		5.0		2.293(5)
				2.242(6)
				2.270(6)
Benzene	piperidine			
3.941	6.524	25.0	50	23.7(6)
			250	21.0(9)
			500	18.8(3)
			750	18.0(3)
			1000	17.5(2)
6.583	4.163		50	15.4(4)
			250	14.1(1)
			500	13.0(1)
			750	11.8(1)
			1000	11.1(1)
8.231	2.700		50	10.16(17)
			250	9.52(15)
			500	8.59(4)
			750	8.16(6)
			1000	7.78(8)
8.958	2.001		50	7.45(7)
			250	6.71(10)
			500	6.34(6)
			750	6.11(1)
			1000	5.86(14)
9.331	1.667		50	6.14(12)
			250	5.74(4)
			500	5.45(14)
			750	5.18(13)
			1000	5.02(7)
10.70	0.4010		200	2.27(7)
			400	2.18(2)
			600	2.10(6)
			800	2.05(1)

Figure 14 illustrates plots of the pseudo first-order rate constants, k_{obsd}, vs [L]/[BZ] (L = pip, hex) obtained at 25.0 °C. The observed curvatures in these plots are suggestive of mechanisms involving consecutive steps, one or more of which is reversible. Thus the most plausible mechanism for the reaction of [(BZ)Cr(CO)$_5$] involves the reversible dissociation of benzene from [(BZ)Cr(CO)$_5$], followed by the nucleophilic attack of L at the coordinatively unsaturated intermediate [Cr(CO)$_5$] as described in Scheme I, where solv = BZ. Thus, plots of $1/k_{obsd}$ vs [BZ]/[L] are expected to be linear according to Eq. 7. These plots are shown in Figure 15. For L = pip and hex, the linearity of these plots and especially the common intercept ($1/k_1$) are strong indication of the dissociative pathway (Scheme I) for reactions of (BZ)Cr(CO)$_5$ with piperidine and 1-hexene, since the value of k_1 (the rate constant for benzene dissociation from (BZ)Cr(CO)$_5$) should be independent of the identities of the incoming nucleophiles.

For L = py, the plot of $1/k_{obsd}$ vs [BZ]/[py] exhibit a slight non-linearity, with an intercept different from those observed for reactions with pip and hex. However, the subtraction of a value (k_3[py]; k_3 = 6.3 x 10^4 M^{-1}s^{-1} at 25.0 °C) from k_{obsd} so that the three intercepts are coincident affords a linear plot of $1/(k_{obsd} - k_3[py])$ vs [BZ]/[py]. This plot is also illustrated in Figure 15.
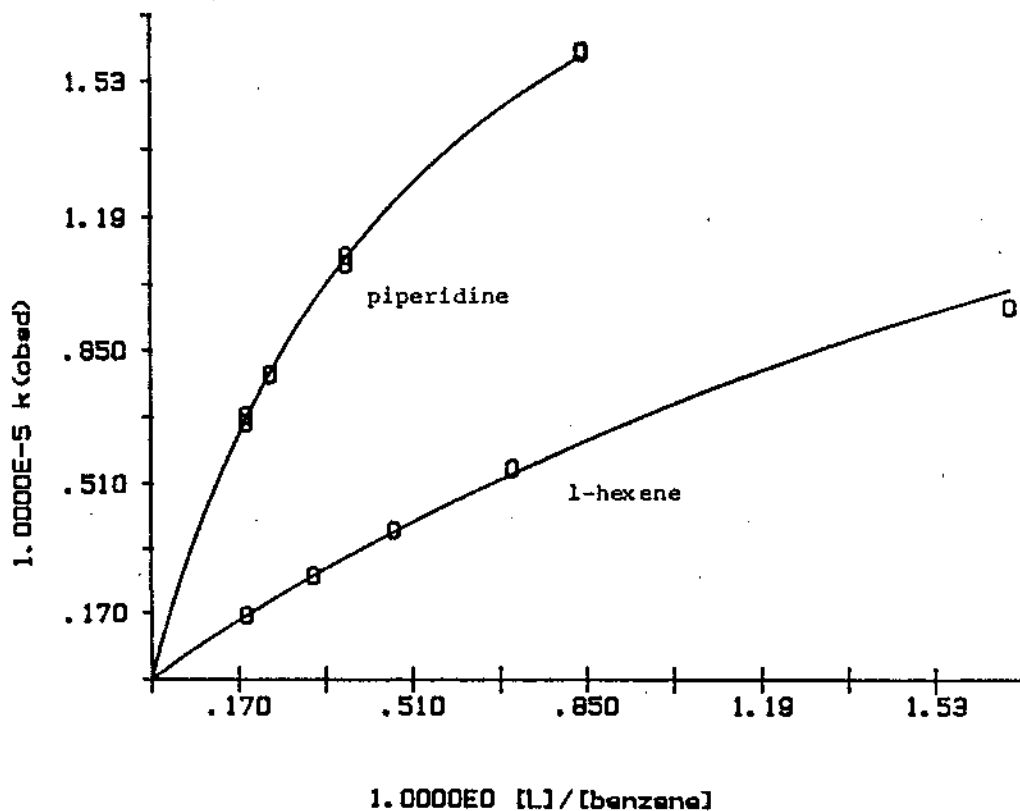
Figure 14. Plots of k_{obsd} vs [L]/[BZ] (L = pip, hex) for reactions taking place after flash photolysis of $Cr(CO)_6$ in L/BZ solutions at 25.0 °C.
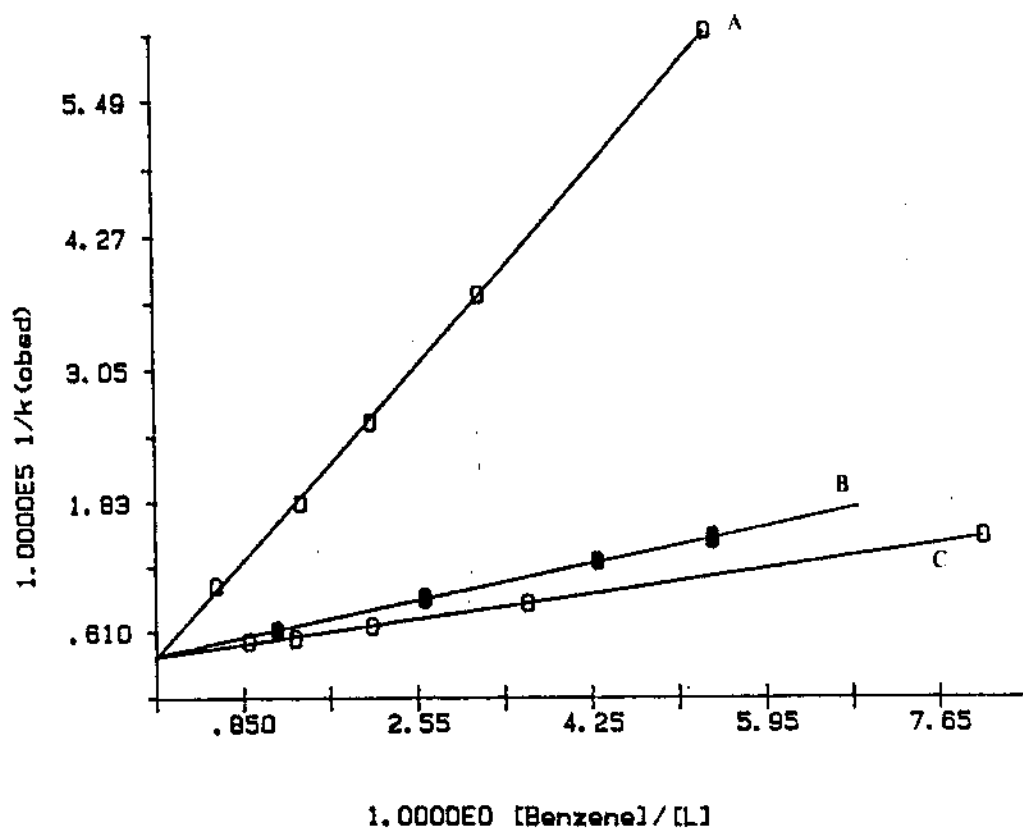
Figure 15. Plots of $1/k_{obsd}$ vs [BZ]/[L] (A = hex, B = pip) and $1/(k_{obsd} - k_3[py])$ vs [BZ]/[py] (C = py) for reactions taking place after flash photolysis of $Cr(CO)_6$ in L/BZ solutions at 25.0 °C.

These results suggest the accessibility of a competing interchange mechanism for L = py at higher [py] involving benzene displacement, a pathway not observed for pip and hex. The rate law derived from this mechanism (Scheme I, Eq. 10 and 11, where solv = BZ, L = py) is consistent with the observed kinetics.

$$k_{obsd} = k_3[L] + \frac{k_1k_2[L]}{k_{-1}[solv] + k_2[L]} \qquad (10)$$

$$1/(k_{obsd} - k_3[L]) = 1/k_1 + (k_{-1}/k_1k_2)([solv]/[L]) \qquad (11)$$

To probe the energetic information for reaction of $(BZ)Cr(CO)_5$ with L, studies were also carried out at other temperatures (5.0 to 35.0 °C). Plots of $1/k_{obsd}$ vs [BZ]/[pip] which obey Eq. 7, are illustrated in Figure 16. Rate constants obtained according to Eq. 7 and 11 for these reactions at various temperatures are given in Table VII.

The relative rates of attack by various L at $[Cr(CO)_5]$ can be determined from values of k_2/k_{-1} obtained as the ratio intercept/slope of the reciprocal plots (Eq. 12). These relative rates at 25.0 °C vary,

py (2.7(1)) > pip (1.9(1)) > BZ (1) > hex (0.35(4)),

and would appear to be unrelated to the strengths of the bond being formed, which vary $pip^{[96]} \approx py^{[96]} > hex > BZ$.

It is noteworthy that the kinetics data for L = pip,
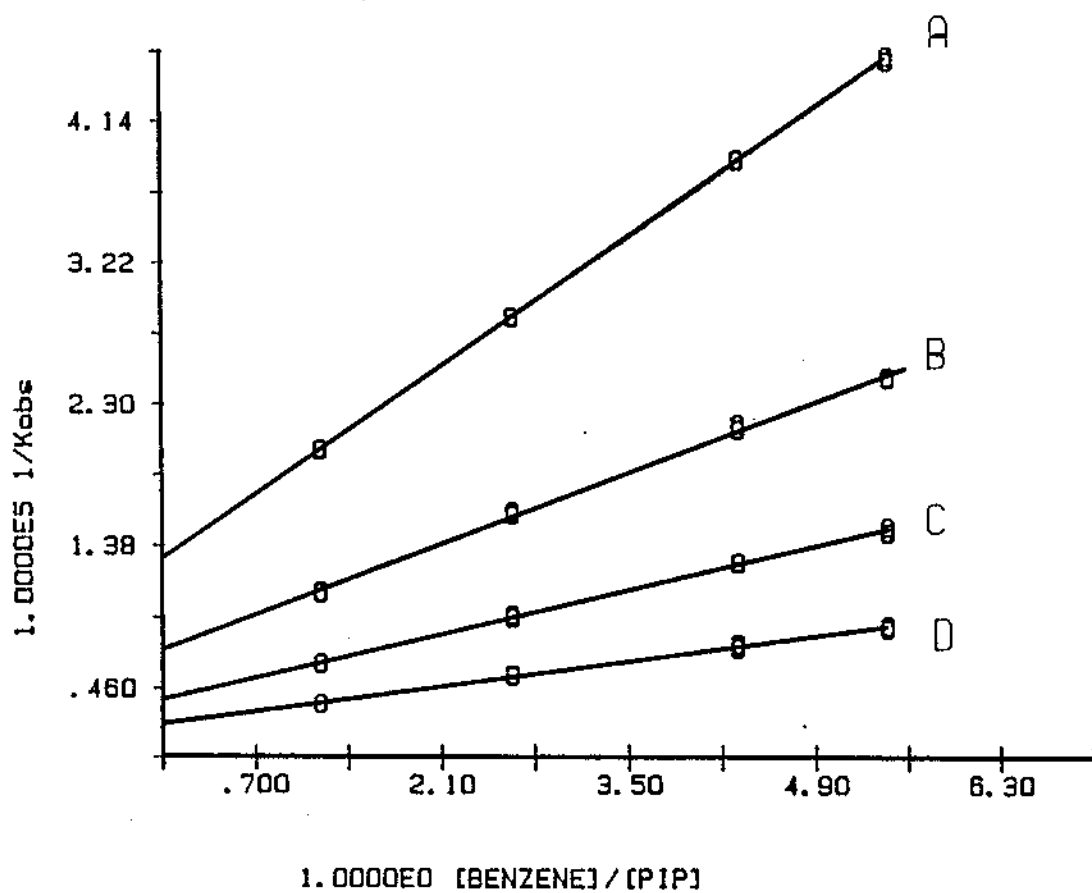
Figure 16. Plots of $1/k_{obsd}$ vs [BZ]/[pip] for reactions taking place after flash photolysis of $Cr(CO)_6$ in pip/BZ solutions at (A) 5.0, (B) 15.0, (C) 25.0, (D) 35.0 °C.

Table VII. Rate Constants for Thermal Reactions Taking Place

   After Flash Photolysis of $Cr(CO)_6$ in L/Benzene and

   pip/benzene-d_6 at various temperatures

L	Solvent	Temp. (°C)	$10^{-5}k_1$ (s^{-1})	k_2/k_{-1}
pip	C_6H_6			
		5.0	0.773(6)	2.17(3)
		15.0	1.41(5)	2.16(11)
		25.0	2.57(8)	1.93(9)
		35.0	4.4(2)	1.92(14)
	C_6D_6			
		5.0	0.98(4)	1.47(8)
		15.0	1.75(4)	1.39(4)
		25.0	3.17(11)	1.28(6)
		35.0	4.9(3)	1.41(12)
hex	C_6H_6			
		5.0	0.76(5)	0.26(2)
		15.0	1.5(2)	0.30(4)
		25.0	2.7(2)	0.35(4)
		35.0	4.4(2)	0.45(3)
py[a]	C_6H_6			
		25.0	2.7(1)	2.72(14)

a) Calculated after substraction of k_3[py]; see the text.

hex obey the rate law shown in Eq. 10 over the entire
concentration range, from solutions in which benzene is
present in predominant concentration to ones in which L
predominates. This evidently is the case because
interactions of benzene and L at the vacant coordination
site in $[Cr(CO)_5]$ are strong when compared to other possible
"bulk solvent effects".

Activation parameters for the reaction shown in Scheme
III for L = pip, and hex are presented in Table VIII. The
enthalpy of activation, $\Delta H^{\ddagger}_1$ = 9.4(1) kcal/mol for BZ
dissociation from $(BZ)Cr(CO)_5$, should represent the upper
limit of the (BZ)-Cr bond strength. In light of the very
rapid solvation reactions observed for photogenerated
$[Cr(CO)_5]$,[62,63,71-75] the difference between the enthalpy of
activation observed here and the bond-dissociation energy is
expected to be small. Note in this regard that the
comparative enthalpies of activation for BZ _vs._ pip and hex
$(\Delta H^{\ddagger}_2 - \Delta H^{\ddagger}_{-1}$; Table VIII) are -0.8(3) and +3.0(4) kcal/mol,
respectively.

D. Reactions of (BZ)Cr(CO)₅ with pip Under High Pressures

The entropy of activations for benzene dissociation
from $(BZ)Cr(CO)_5$, $\Delta S^{\ddagger}_1$ = -2.4(3) cal/(deg mol), is
considerably more negative than might be anticipated for a
dissociative process. However, this value is not too

Table VIII. Activation Parameters for Reactions Taking Place
After Flash Photolysis of $Cr(CO)_6$ in pip/Benzene,
pip/Benzene-d_6 and hex/Benzene Solutions

Activation Parameters	Ligand = Solvent =	pip C_6H_6	pip C_6D_6	hex C_6H_6
$\Delta H^{\ddagger}_1$ (kcal/mol)		9.4(1)	8.6(3)	9.4(4)
$\Delta H^{\ddagger}_2 - \Delta H^{\ddagger}_{-1}$ (kcal/mol)		-0.8(3)	-0.3(5)	+3.0(4)
$\Delta S^{\ddagger}_1$ (cal/(deg mol))		-2.4(3)	-4.5(10)	-2.2(12)
$\Delta S^{\ddagger}_2 - \Delta S^{\ddagger}_{-1}$ (cal/(deg mol))		-1.4(10)	-0.6(24)	+8.8(15)
$\Delta V^{\ddagger}_1$ (cm^3/mol)		+12.3(14)	-----	-----
$\Delta V^{\ddagger}_2 - \Delta V^{\ddagger}_{-1}$ (cm^3/mol)		-8.3(19)	-----	-----

different from those observed for related solvent-replacement reactions taking place via dissociative pathways,[80] or from displacement of CO from $Cr(CO)_6$ by pip.[96]

It has been demonstrated that the volume of activation for a ligand exchange reaction is a useful mechanistic indicator[35,97] which describes the volume change from the reactant(s) to activated complex, presumably a better measurement than entropy of activation for change of bond distance(s) along the reaction coordinate. The volume of activation, is related to the rate constant and pressure as in Eq. 12:

$$-RT(\partial \ln k/\partial P)_T = \Delta V^{\ddagger} \tag{12}$$

and where $\Delta V^{\ddagger}$ is independent of P,

$$\ln k = \text{constant} - (\Delta V^{\ddagger}/RT)P \tag{13}$$

Reactions of $(BZ)Cr(CO)_5$ under high pressures were investigated. The initial pressure studies were carried out in $Cr(CO)_6$/pip/BZ solution ([pip] = 0.401 M) at 25.0 °C, to 800 atm; studies at higher pressures were not possible because of solidification of the solution. Under these conditions $k_{-1}[BZ] \gg k_2[pip]$, Eq. 7 can be simplified as Eq. 8, where solv = BZ, L = pip. Thus the value of $\Delta V^{\ddagger}_{obsd}$ ($= \Delta V^{\ddagger}_1 + \Delta V^{\ddagger}_2 - \Delta V^{\ddagger}_{-1}$), +4.2(3) cm^3/mol, was calculated from the slope of a plot of $\ln k_{obsd}$ vs P (Figure 17).
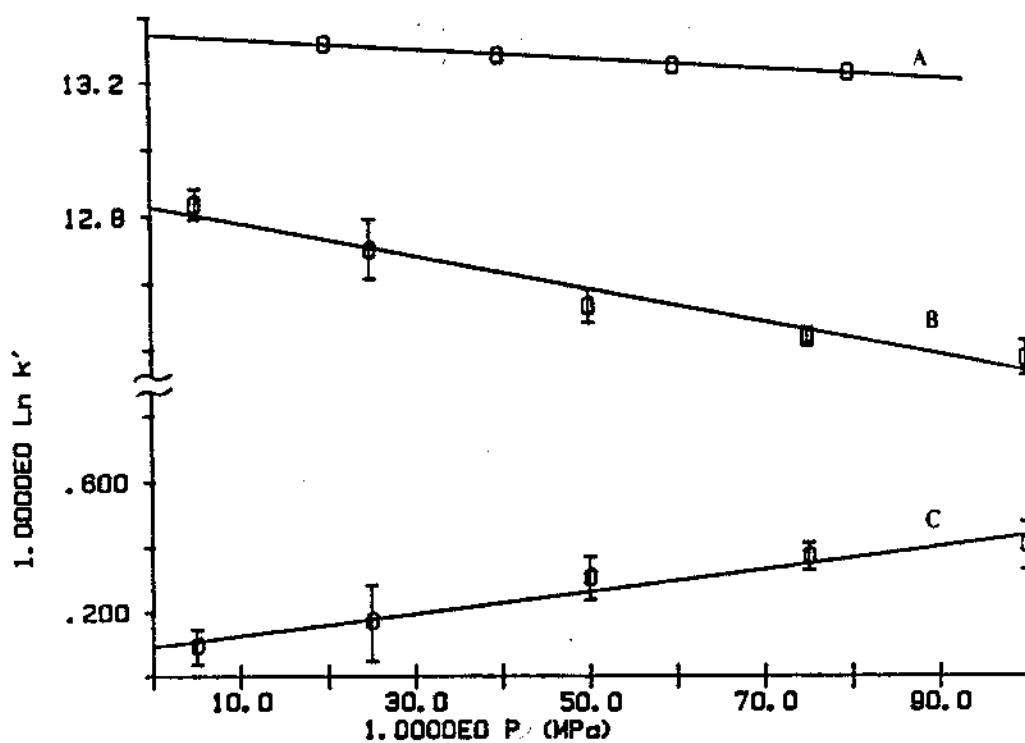
Figure 17. Plots of (A) ln (k_1k_2/k_{-1}) <u>vs</u> P; (B) ln k_1 <u>vs</u> P; and (C) ln (k_2/k_{-1}) <u>vs.</u> P for reactions at various pressures after flash photolysis of $Cr(CO)_6$ in pip/BZ solutions at 25.0 °C.

To resolve values of $\Delta V^{\ddagger}_1$ and $\Delta V^{\ddagger}_2 - \Delta V^{\ddagger}_{-1}$, further pressure studies were carried out in Cr(CO)$_6$/pip/benzene mixtures, in which [BZ] and [pip] were varied over a large range (Table VI). Values of k_1 and k_2/k_{-1} can be obtained from plots of $1/k_{obsd}$ vs [BZ]/[pip] (Eq. 7) at various pressures. Plots of ln k_1 vs P (Figure 17) afforded $\Delta V^{\ddagger}_1 = +12.3(14)$ cm^3/mol, a value consistent with a (BZ)-Cr bond fission process. A plot of ln (k_2/k_{-1}) vs P afforded $\Delta V^{\ddagger}_2 - \Delta V^{\ddagger}_{-1} = -8.3(19)$ cm^3/mol, which indicates less volume collapse upon BZ-Cr bond-making than pip-Cr bond formation. While the plots in Figure 17 appear slightly curved, this curvature does not arise from the influence of the compressibility of the solvent, which is predicted to be in the opposite direction and small compared to the observed experimental uncertainties. The close agreement between the values $\Delta V^{\ddagger}_1 + \Delta V^{\ddagger}_2 - \Delta V^{\ddagger}_{-1}$ from data obtained at low [pip], 4.2(3) cm^3/mol, and from widely varying [pip]/[BZ] ratios, 4.0(5) cm^3/mol supports this conclusion.

E. Reactions of (C$_6$D$_6$)Cr(CO)$_5$ with pip

The question about the bonding mode(s) of benzene to the metal center should naturally be raised since there exist several possible bonding sites in the benzene molecule. Stolz, Haas and Sheline[98] suggested, on the basis of carbonyl stretching data, that the bonding in

$[(C_6H_6)W(CO)_5]$ involves the whole aromatic ring, while the $\eta^2-(C_6H_6)-M$ bonding through an "edge-on isolated double bond" has been widely suggested among transition metal complexes[1,23,93,99] and supported by X-ray[27-33] and NMR studies.[34] The third mode of bonding of aromatic and aliphatic hydrocarbons to a transition metal is _via_ a three-center, two-electron "agostic" or "σ-complex" interaction (Figure 3).[17-19,100] In this context, formation of a η^2-arene complex has been envisioned by Jones and Feher[23] to precede the creation of a "σ-complex" along the reaction path to C-H bond activation on the $[(\eta^5-Cp^*)Rh(PMe_3)]$ intermediate.

The flash photolysis of $Cr(CO)_6$ in pip/benzene-d_6 mixtures were also investigated (Table VI) to probe the bonding possibilities in $(BZ)Cr(CO)_5$. Figure 18 compares plots of $1/k_{obsd}$ _vs_ $[C_6H_6]/[pip]$ and $1/k_{obsd}$ _vs_ $[C_6D_6]/[pip]$, which afford the ratios $k_{1H}/k_{1D} = 0.81(5)$ and $k_{-1H}/k_{-1D} = 0.67(6)$ at 25.0 °C (Table VII). These ratios are indicative of a weak "inverse" kinetic deuterium isotope effect for both BZ-Cr bond breaking and bond formation. The activation enthalpies (Table VIII) also indicate that there is slightly higher activation barrier in the case of C_6H_6 compared to C_6D_6: $\Delta H^{\ddagger}_{1H} - \Delta H^{\ddagger}_{1D} = +0.8(4)$ kcal/mol.

A comparison of the rates of n-octane displacement by 1-hexene from $[(C_8H_{18})Cr(CO)_5]$ and $[(C_8D_{18})Cr(CO)_5]$ species (see chapter IV), on the other hand, has afforded a normal kinetic deuterium isotope effect ($k_H/k_D = 1.4(2)$). Since
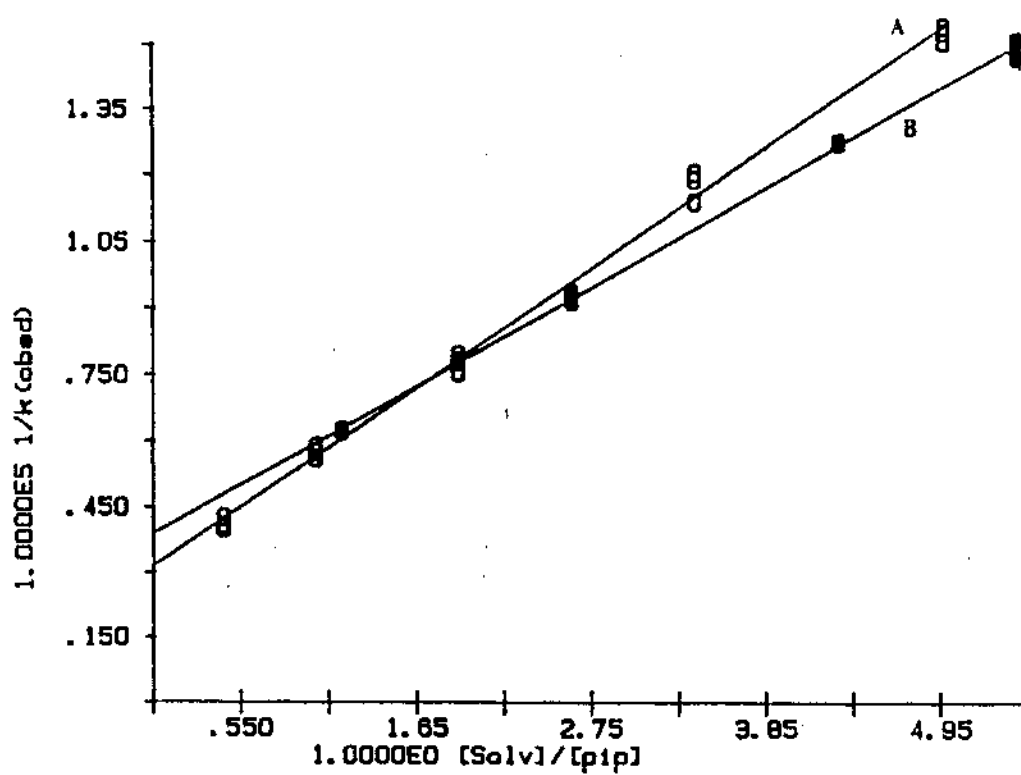
Figure 18. Plots of (A) $1/k_{obsd}$ vs [C_6D_6]/[pip] and (B)
$1/k_{obsd}$ vs [C_6H_6]/[pip] for reactions after flash
photolysis of $Cr(CO)_6$ in pip/C_6D_6 and pip/C_6H_6 solutions
respectively.

there should be stronger H-Cr ("agostic" or "σ-complex")
interaction in the ground states (octane)Cr(CO)5 than in the
transition state leading to its bond breaking, a greater
difference in zero-point energy in the ground states would
result in a normal primary kinetic deuterium isotope effect.

It has been noted, both empirically[101,102] and
theoretically,[103,104] that the kinetic deuterium isotope
effect may become inverse for an elementary reaction, even
though Parkin and Bercaw have indicated that there is no
definitive experimental evidence that a single elementary
step exhibits an inverse primary kinetic isotope effect and
that all inverse primary kinetic isotope effects may be
explained by the occurrence of a pre-equilibrium.[105] However,
the present results would appear to be indicative of more H-
Cr bonding in the transition state leading to formation of
(BZ)Cr(CO)$_5$ than in (BZ)Cr(CO)$_5$ itself. This may suggest
that the bonding in (BZ)Cr(CO)$_5$ involves an "isolated"
double bond and that in the transition state involves
"agostic" or "σ-complex" bonding. A hypothetical reaction
coordinate diagram is shown in Figure 19 to illustrate the
observed results in terms of zero-point energy differences
among the two ground states and the common transition state
of the microscopically reversible desolvation and solvation
processes. While the difference in zero-point energy for the
transition state (Δ_2) may arise from both Cr-H(D) and C-
H(D) interactions, the differences in zero-point energy for
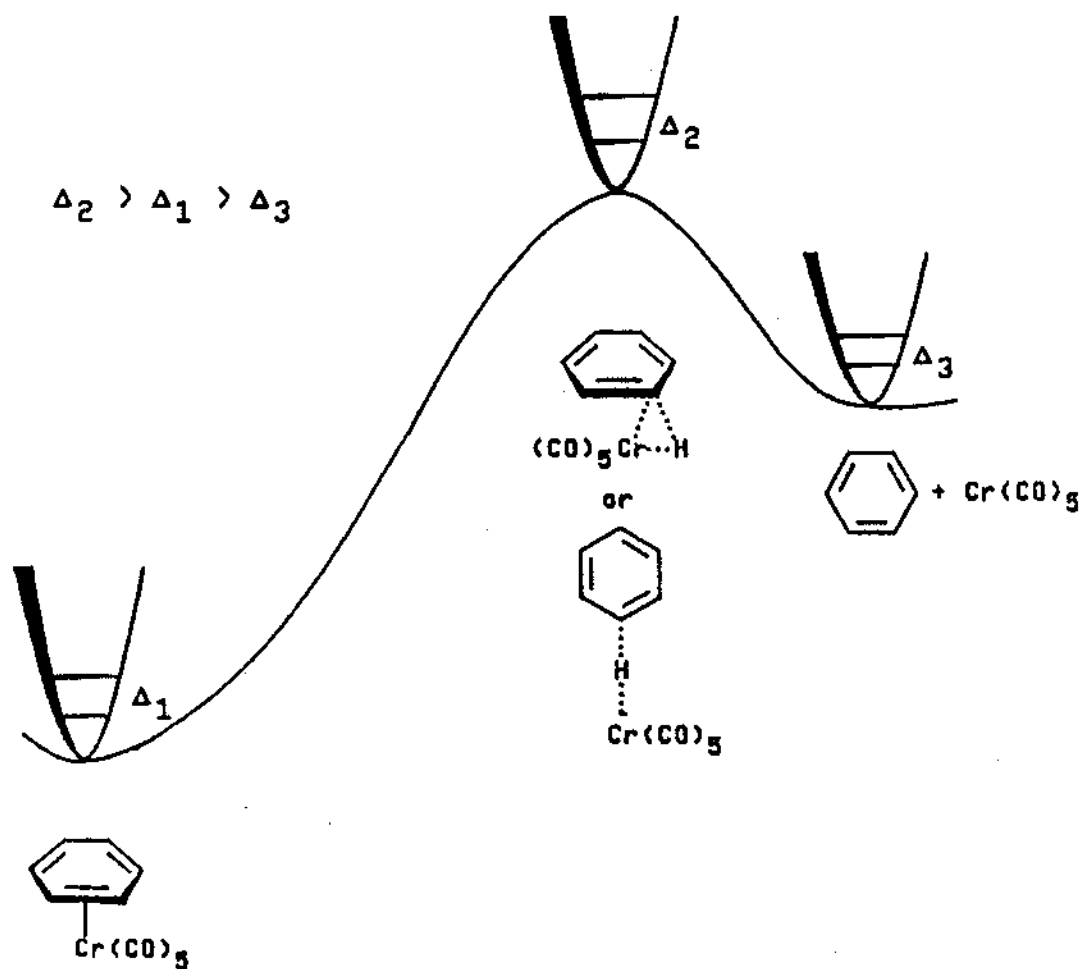
Figure 19. A hypothetical plot of potential energy vs reaction coordinate for solvation/desolvation of $(\eta^2\text{-BZ})\text{Cr(CO)}_5$.

the ground states (Δ_1, Δ_3) arise from C-H(D) interactions in η^2-coordinated benzene and free benzene molecules. To account for the observed kinetic isotope effects, it is evident that $\Delta_2 > \Delta_1 > \Delta_3$ (cf Figure 17) since $k_{1H}/k_{1D} < 1$, $k_{-1H}/k_{-1D} < 1$ and $K_H/K_D = (k_{1H}/k_{-1H})/(k_{1D}/k_{-1D}) = 1.2(2) \geq 1$. The slight difference between Δ_1 and Δ_3 might be attributed to secondary isotope effects.[106] Streitwieser et al. have proposed that such an isotope effect might arise from the change in frequencies of the out-of-plane C-H bending modes in sp^2 and sp^3 hybrid states of carbon.[107] Applying the Streitwieser concept to the interaction of Cr to an isolated double bond of benzene, which is accompanied by the sp^2 to sp^3 rehybridization of the two carbon atoms involved, one would expect a greater zero-point energy difference in η^2-coordinated benzene than in free benzene, as observed. However, since the interaction of benzene with [Cr(CO)$_5$] is relatively weak overall, secondary isotope effects might not be expected to be important in the transition state.

The highly-ordered three-centered structure in the transition state, as proposed in Figure 19, is consistent with the slightly negative entropies of activation observed for BZ-Cr bond breaking. The positive volume of activation indicates an increase in volume on the transition state accompanying η^2-BZ-Cr bond fission. It should be noted that entropy of activation and volume of activation can provide complementary information about reaction mechanisms.

The possible existence of Cr-H "agostic" or "σ-complex" interactions along the reaction pathway leading to the formation of η^2-arene complex is inconsistent with the mechanism proposed for C-H bond activation in arenes.[23] One might note that the existence of η^2-arene complex[33] does not necessarily indicate it lies on the reaction pathway toward C-H bond activation in arene substrates.

Chapter Summary

Studies of displacement of CB by pip from (CB)Cr(CO)$_5$ generated by flash photolysis in CB and in CB/HX solutions have been carried out, where HX functioned as a diluent through use of which [CB] could be varied. The studies revealed that rates of desolvation were inhibited with increasing [CB]; thus a desolvation mechanism involved CB-Cr bond breaking was indicated. However, either [Cr(CO)$_5$] or (HX)Cr(CO)$_5$ could conceivably be the reactive intermediate even though the former was favored based on the "competition ratios".

Pulsed laser flash photolysis of Cr(CO)$_6$ in L/BZ solutions (L= pip, hex, py) affords [(η^2-BZ)Cr(CO)$_5$] as the predominant reaction species which reacts with L on the μs time scale to afford LCr(CO)$_5$ products. Based upon kinetics studies over a wide range of L and BZ concentrations at various temperatures (5 - 35 °C), pressures to 1000 atm and

studies of kinetic isotope effects employing BZ-d_6, it is concluded that the displacement of BZ from (η^2-BZ)Cr(CO)$_5$] by pip and hex takes place by means of reversible dissociation via the [Cr(CO)$_5$] intermediate. The data also suggested that BZ is bonded via a "isolated" double bond in (η^2-BZ)Cr(CO)$_5$], and that there may be some "agostic" C-H-Cr or "σ-complex" interaction in the transition state for the reversible solvation/disolvation processes of the [Cr(CO)$_5$] intermediate. For displacement of BZ from (η^2-BZ)Cr(CO)$_5$] by py, an interchange mechanism may also be accessible. The observed rate laws incorporate the concentrations of all chemical species present in solution in significant concentration after flash photolysis. Thus benzene may be classified the same as any other ligands instead of a "solvent" in this time scale. The upper limit of the BZ-Cr bond strength is estimated to be 9.4(1) kcal/mol on the basis of enthalpy of activation of BZ dissociation from (BZ)Cr(CO)$_5$.

CHAPTER IV

SURVEY ACCORDING TO SOLVENTS, INCOMING NUCLEOPHILES AND

METALS FOR SOLVENT DISPLACEMENT FROM

(SOLVENT)$M(CO)_5$ (M = Cr, Mo, W)

The mechanism of solvent displacement by Lewis base (=
L) from (solv)$M(CO)_5$ transients produced after flash
photolysis has not been a simple subject. Both dissociative
and interchange mechanism have been implicated by the
kinetic results for M = Cr as shown in Scheme I (Chapter
III). Under the conditions normally employed in kinetics
studies, [solv] >> [L], these mechanisms are kinetically
indistinguishable, since for the dissociative pathway, where
k_1 and k_2 are comparable,

$$- \frac{d[(solv)Cr(CO)_5]}{dt} = \frac{k_1 k_2}{k_{-1}[solv]}[L][(solv)Cr(CO)_5] \quad (14)$$

For the interchange pathway, the anticipated rate law is,

$$- \frac{d[(solv)Cr(CO)_5]}{dt} = k_3[L][(solv)Cr(CO)_5] \quad (15)$$

and thus the pseudo-first-order rate constants is, k_{obsd} =
k[L] (Eq. 2), where k = $k_1 k_2/(k_{-1}[solv])$ and k_3 respectively.

Thus indirect means have been employed to study the

mechanisms of these solvent-displacement reactions, through the observed activation enthalpies, entropies and the solv-Cr bond strengths. Peters, Vaida and Yang, employing time-resolved photoacoustic calorimetry, have estimated the HP-Cr (HP = $\underline{n}$-heptane) bond strength in (HP)Cr(CO)$_5$ to be $\underline{ca.}$ 10 kcal/mol,[83] which is in close agreement with a later study by Morse, Parker and Burkey for several alkanes.[108] However, the enthalpy of activation for HP displacement from (HP)Cr(CO)$_5$ by py and picoline are 5.1(4) and 7.3(8) kcal/mol, significantly less than the estimated HP-Cr bond strength. These results, together with entropies of activation of $\underline{ca.}$ zero, suggested to Peters and coworkers that the displacement of HP from (HP)Cr(CO)$_5$ takes place $\underline{via}$ an interchange mechanism. If the reaction takes place $\underline{via}$ rate-determining solvent dissociation to produce the [Cr(CO)$_5$] intermediate, it should react with nucleophiles with negligible activation barrier. Figure 20 illustrates plots of potential energy $\underline{vs}$ reaction coordinate for dissociative and interchange pathways based on this view.

On the other hand, recent studies (CHAPTER III) of displacement of BZ from photogenerated (η^2-BZ)Cr(CO)$_5$ in L/BZ mixtures have provided strong evidence that displacement of BZ by pip and hex involves rate-determining dissociation of BZ $\underline{via}$ a [Cr(CO)$_5$] intermediate, although for L = py, both dissociative and interchange pathways are accessible.
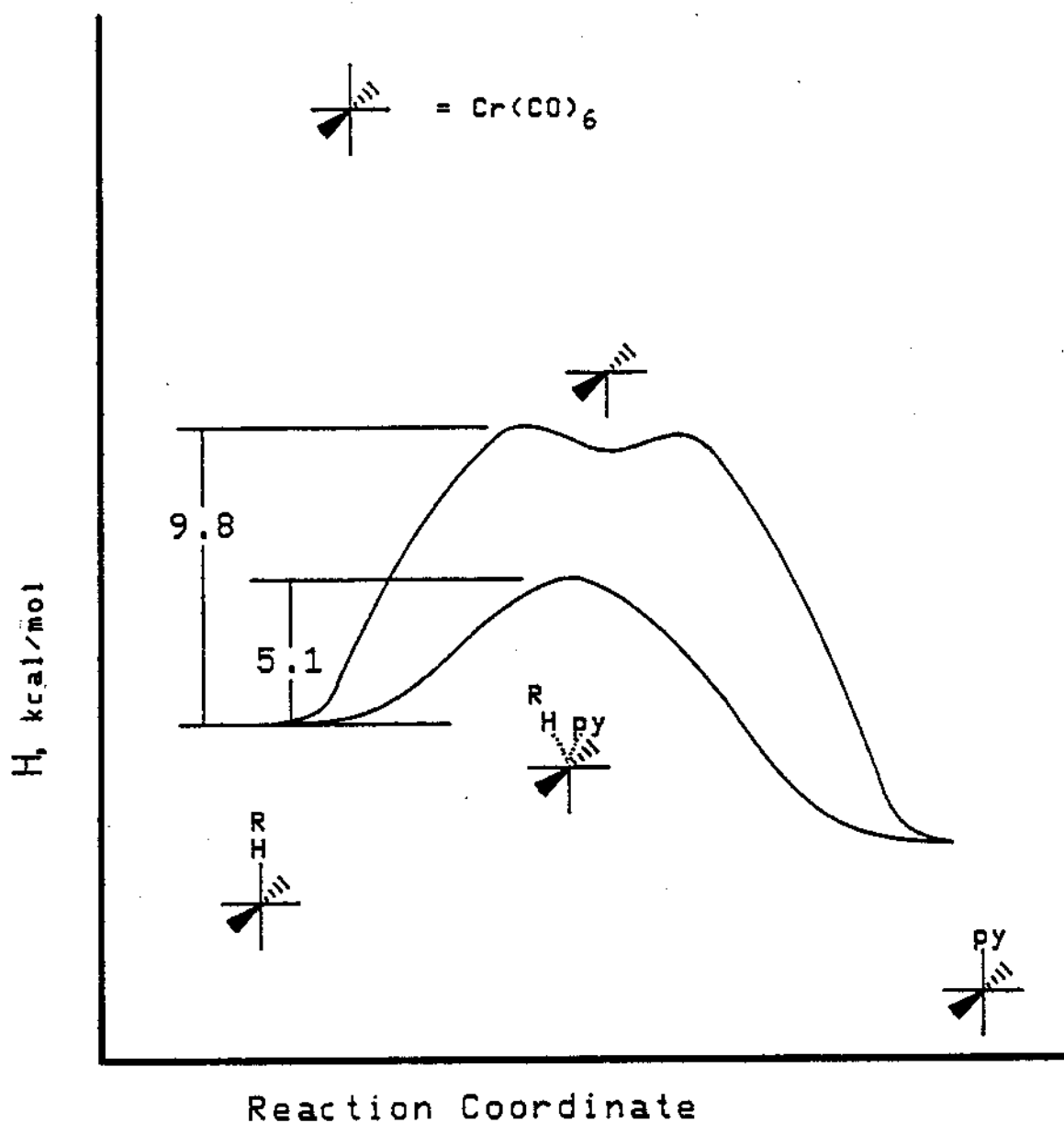
Figure 20. Plots of potential energy vs reaction coordinate
for reaction of (HP)Cr(CO)₅ with py via a dissociative
pathway (top), and via an interchange pathway.

Volumes of activation have been found to be a useful mechanistic indicator in a variety of contexts.[35,97] Since it seems that the mechanisms of solvent displacement reactions depend on both the solvents and the incoming nucleophiles and probably also the metal center, the volumes of activation for solvent displacement reactions in $(solv)M(CO)_5$ (M = Cr, Mo, W; solv = aliphatic, aromatic hydrocarbons) by several incoming ligands were studied in order to obtain an overview of the mechanistic possibilities in these systems.

Furthermore, examinations of the influences of the electronic and steric properties on the solvent-metal interactions are essential for understanding the mechanism of solvent displacement, and the selectivity as well as reactivity of solvated intermediates which exist in many organometallic reactions. Conventional reaction rate studies for various $M(CO)_6$/L/solvents systems have been carried out to probe these influences.

A. The Reaction Stoichiometry and Rate Law Expressions

The λ_{max} for $(solv)M(CO)_5$ (M = Cr, Mo, W; solv = aliphatic, aromatic hydrocarbons) transient generated after flash photolysis in the studied systems falls in the range of 400-530 nm. Monitoring the reaction at a wavelength within this range, under pseudo-first-order kinetics

conditions ([solv], [L] >> [(solv)M(CO)$_5$]), decay signals with one exponential function were obtained. This indicates the conversion of (solv)M(CO)$_5$ to single products which is attributable to LM(CO)$_5$, thus the reaction stoichiometry accompanying flash photolysis of M(CO)$_6$ can be shown in Eq. 16:

$$M(CO)_6 \xrightarrow[+solv]{h\nu} [(solv)M(CO)_5] \xrightarrow[+L]{k_{obsd}} LM(CO)_5 \qquad (16)$$
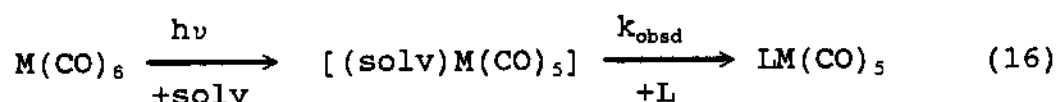
The pseudo-first-order rate constant, k_{obsd}, can be calculated from computer fitting of the exponential decay. From data taken at several concentrations at ambient pressure, it was observed that k_{obsd} obey Eq. 2 for all solvents and L when [L] << [solv] (_vide infra_); thus all rate data can be encompassed within the overall mechanism shown in Scheme I, for which the two reaction pathways obey the rate laws given in Eq. 14, 15.

Eq. 17 can also be employed to represent the overall pseudo-first-order rate constant, in which [solv] is almost constant in the case of [L] << [solv]. The solvent displacement reaction takes place predominantly _via_ a dissociative pathway when $k_1k_2/(k_{-1}[solv]) >> k_3$; and _via_ an interchange pathway when $k_1k_2/(k_{-1}[solv]) << k_3$.

$$k_{obsd} = \{k_1k_2/(k_{-1}[solv]) + k_3\}[L] \qquad (17)$$

B. Volumes of Activation for Solvent Displacement from $(solv)M(CO)_5$ Transients[109]

The volume of activation is related to the rate constant and pressure (Eq. 12, 13) and can be determined from the slope of a plot of ln k $\underline{vs}$ P at a constant temperature (Eq. 13). Table IX lists values for k_{obsd} as a function of pressure at 25.0 °C for all the systems investigated. Representative examples of plots of ln k_{obsd} $\underline{vs}$ P (MPa) were linear over a pressure range of ambient to 1500 atm as shown in Figure 21. The calculated volumes of activation, $\Delta V^{\ddagger}_{obsd}$, from the slopes of plots of ln k_{obsd} $\underline{vs}$ P are listed in Table X. They can be discussed in terms of the influence of the solvent, the incoming nucleophile and the identity of the metal atom.

1. Volumes of activation and the solvent

Noting that the first term in Eq. 17, arising from the dissociative pathway, will contribute to the overall volume of activation in the forms of Eq. 18 and 19:

$$\Delta V^{\ddagger}_{obsd}(dis) = \Delta V^{\ddagger}_1 - \Delta V^{\ddagger}_{-1} + \Delta V^{\ddagger}_2 \qquad (18)$$

$$\Delta V^{\ddagger}_{obsd}(dis) = \Delta V(K_{eq}) + \Delta V^{\ddagger}_2 \qquad (19)$$

Table IX. Rate Constants Observed After Flash Photolysis of
M(CO)$_6$ (M = Cr, Mo, W) in Various Ligand/Solvent
Solutions at 25.0 °C under Various Pressures

M	Solvents	Ligands	[L] (M)	P (atm.)	$10^{-4}k_{obsd}$ (s^{-1})
Cr	n-Heptane	1-hexene	0.2410	50	376.(6)
				250	360.(1)
				500	338.(5)
				750	316.(1)
				1000	300.(1)
				1500	263.(4)
		piperidine	0.01784	50	107.6(17)
				500	102.9(13)
				1000	99.4(6)
				1500	99.2(1)
		2-picoline	0.01188	50	99.4(8)
				500	99.6(9)
				1000	103.7(32)
				1500	107.2(23)
		pyridine	0.0103	50	194.(4)
				500	199.(2)
	Fluorobenzene	1-hexene	0.8799	50	7.74(3)
				500	6.21(1)
				1000	5.42(7)
				1500	4.39(1)
		piperidine	0.5144	1	13.75(7)
				500	12.0(2)
				1000	10.50(5)
				1500	9.54(15)
		pyridine	0.1389	50	9.96(28)
				500	8.26(25)
				1000	7.33(24)
				1500	6.05(4)
		enthylene-diamine	0.0558	50	10.97(36)
				500	9.34(25)
				1000	8.19(20)
				1500	7.17(15)
		1,10-phen-anthroline	0.0500	50	19.2(8)
				500	16.6(6)
				1000	13.0(4)
				1500	11.4(4)
	Chlorobenzene	1-hexene	1.273	50	0.477(1)
				500	0.447(1)

Table IX. Continued

M	Solvents	Ligands	[L] (M)	P (atm.)	$10^{-4}k_{obsd}$ (s^{-1})
				1000	0.394(1)
				1500	0.351(2)
		norborna-diene	1.166	1	0.475(20)
				500	0.430(15)
				1000	0.402(8)
				1500	0.381(6)
		piperidine	1.000	1	2.22(2)
				500	2.20(2)
				1000	2.20(2)
				1500	2.19(4)
		2-picoline	0.6805	1	1.23(8)
				500	1.37(2)
				1000	1.43(7)
				1500	1.49(1)
	Benzene	1-hexene	1.170	50	1.07(2)
				250	0.976(2)
				500	0.852(3)
				750	0.793(8)
		piperidine	0.401	200	2.27(7)
				400	2.18(2)
				600	2.10(6)
				800	2.05(1)
	Toluene	1-hexene	1.404	50	0.711(8)
				500	0.554(1)
				1000	0.472(16)
				1500	0.371(9)
		piperidine	0.8723	1	1.968(7)
				500	1.59(1)
				1000	1.53(3)
				1500	1.44(2)
Mo	n-Heptane	1-hexene	0.0622	50	134.(3)
				500	128.(2)
				1000	125.(2)
				1500	117.(1)
	Fluorobenzene	1-hexene	0.5366	50	0.957(4)
				500	0.893(8)
				1000	0.743(11)
				1500	0.698(8)
		pyridine	0.1389	50	4.59(3)
				500	4.06(8)
				1000	3.60(17)
				1500	3.17(33)

Table IX. Continued

M	Solvents	Ligands	[L] (M)	P (atm.)	$10^{-4}k_{obsd}$ (s^{-1})
		ethylene-diamine	0.1117	50	5.59(14)
				500	4.93(17)
				1000	4.37(28)
				1500	3.88(20)
	Chlorobenzene	1-hexene	1.273	50	0.648(8)
				500	0.595(11)
				1000	0.572(8)
				1500	0.532(7)
		norborna-diene	1.048	1	1.18(6)
				500	1.14(4)
				1000	1.00(4)
				1500	0.99(6)
	Toluene	1-hexene	1.367	50	0.1031(1)
				500	0.097(2)
				1000	0.093(2)
				1500	0.085(1)
W	n-Heptane	1-hexene	(35.0°C)		
			0.0926	50	19.5(3)
				500	17.6(4)
				1000	17.2(4)
				1500	16.6(4)
	Fluorobenzene	1-hexene	1.424	50	0.0619(5)
				500	0.0579(4)
				1000	0.0556(4)
				1500	0.0532(8)
		pyridine	0.5263	50	0.83(2)
				500	0.77(13)
				1000	0.73(5)
				1500	0.71(5)
		1,10-phen-anthroline	0.0500	50	1.12(6)
				500	1.02(2)
				1000	0.95(5)
				1500	0.90(2)
	Chlorobenzene	1-hexene	2.210	50	0.0306(2)
				500	0.0297(8)
				1000	0.0300(1)
				1500	0.0296(1)
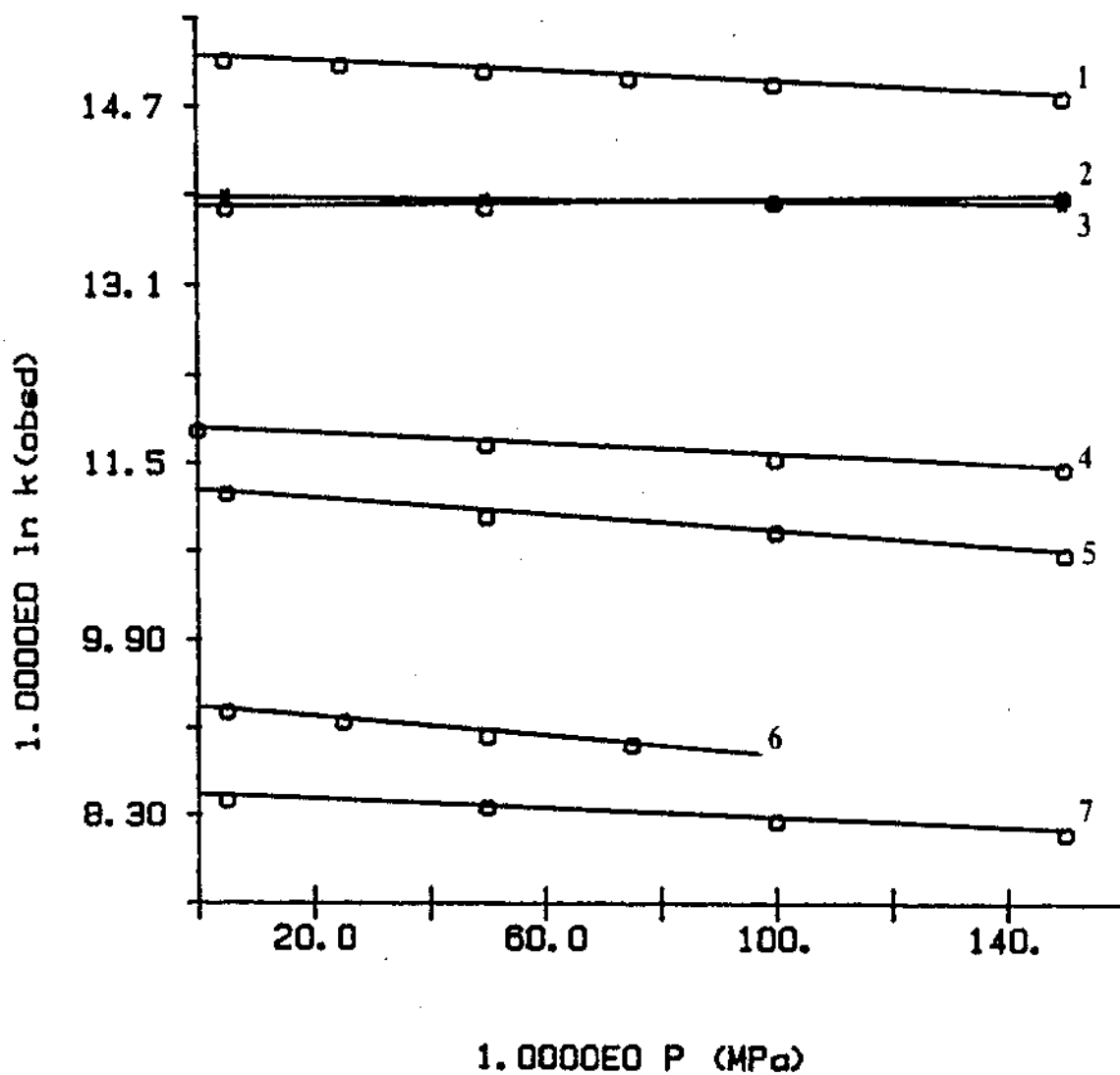
Figure 21. Plots of ln k_{obsd} (s^{-1}) <u>vs</u> P (MPa) for reactions
taking place after flash photolysis of Cr(CO)$_6$ in L/solv
solutions at 25.0 °C. L/solv = hex/HP (1), pic/HP (2),
pip/HP (3), pip/FB (4), hex/FB (5), hex/BZ (6), hex/CB (7).

Table X. Second-order Rate Constants and Volumes of

Activation for Reactions of $(solv)M(CO)_5$ (M = Cr, Mo,

W) With Various Nucleophiles at 25.0 °C

M	Solvents	Ligands	$10^{-5}k$ $(M^{-1}s^{-1})$	$\Delta V^{\ddagger}_{obsd}$ (cm^3/mol)
Cr	n-Heptane	1-hexene	147(1)	+ 6.2(2)
		piperidine	540(10)	+ 1.4(4)
		2-picoline	900(220)	- 1.4(3)
		pyridine	1990(50)	- 1.4(5)
	Fluorobenzene	1-hexene	0.889(3)	+ 9.4(7)
		piperidine	2.94(4)	+ 6.1(3)
		pyridine	7.0(5)	+ 8.2(6)
		ethylenediamine	18.8(4)	+ 7.2(4)
		1,10-phenanthroline	38.5(14)	+ 9.2(7)
	Chlorobenzene	1-hexene	0.0374(1)	+ 5.4(4)
		norbornadiene	0.041(2)	+ 3.6(4)
		piperidine	0.222(2)	+ 0.2(2)
		2-picoline	0.181(11)	- 3.1(6)
	Benzene	1-hexene	0.091(2)	+10.9(10)
		piperidine	0.57(2)	+ 4.2(3)
	Toluene	1-hexene	0.0506(6)	+10.8(7)
		piperidine	0.226(1)	+ 4.8(14)
Mo	n-Heptane	1-hexene	158.0(10)	+ 2.2(3)
	Fluorobenzene	1-hexene	0.178(7)	+ 5.8(8)
		pyridine	3.22(5)	+ 6.3(1)
		ethylenediamine	4.89(11)	+ 6.2(2)
	Chlorobenzene	1-hexene	0.0509(6)	+ 3.2(3)
		norbornadiene	0.0572(8)	+ 3.4(8)
	Toluene	1-hexene	0.00754(1)	+ 3.2(3)
W	n-Heptane	1-hexene	15.8(5)	+ 2.7(4)
	Fluorobenzene	1-hexene	0.00435(4)	+ 2.5(2)
		pyridine	0.1571(8)	+ 2.7(5)
		1,10-phenanthroline	1.39(2)	+ 3.8(4)
	Chlorobenzene	1-hexene	0.00138(1)	+ 0.4(3)

where $\Delta V(K_{eq})$ is the change in molar volume accompanying
desolvation. This value is expected to be positive, since it
involves release of a solvent molecule from the coordination
sphere of $(solv)M(CO)_5$. For a given incoming nucleophile,
$\Delta V^{\ddagger}_2$ will not vary, and thus the change in $\Delta V^{\ddagger}_{obsd}(dis)$ will
depend only on $\Delta V(K_{eq})$. This value may increase with
increasing molar volume of the solvent molecules employed,
but such a trend is not evident for the results obtained.
Table XI lists the volumes of activation for reactions of
$(solv)Cr(CO)_5$ with hex and pip, the molar volumes of
ligands, and the solvents (HP, FB, BZ, TL, CB).

Table XI. Volumes of Activation for Reactions of
$(solv)Cr(CO)_5$ with 1-Hexene and Piperidine, and the
Molar Volumes of the Solvents and Ligands

Solvent	V (cm^3/mol) (ligand)	$\Delta V^{\ddagger}_{obsd}$ (cm^3/mol)				
		HP	FB	BZ	TL	CB
1-Hexene	125.0	6.2(2)	9.4(7)	10.9(10)	10.8(7)	5.4(4)
Piperidine	98.9	1.4(4)	6.1(3)	4.2(3)	4.8(14)	0.2(2)
V $(cm^3/mol$, solvent)		146.6	94.0	88.9	106.3	101.8

Studies (CHAPTER III, section C) of displacement of BZ
from photogenerated $(\eta^2\text{-BZ})\text{Cr(CO)}_5$ in L/BZ mixtures have
provided strong evidence that displacement of BZ by hex and
pip takes place predominantly through the dissociative
pathway. Since the volumes of activation for FB and TL are
very close to that of BZ for both ligands, it is suggested
that the dissociative mechanism is also operative for FB and
TL desolvation reactions. These results may also suggest
that the solvent-Cr interactions in $(\text{solv})\text{Cr(CO)}_5$ for solv =
FB, BZ and TL are similar, i.e. through an "isolated" double
bond.

It is to be noted that values of $\Delta V^{\ddagger}_{obsd}$ for HP and CB
are significantly smaller, by 3-6 cm^3/mol, than for the
other solvents. It also is to be noted that the second-
order rate constants (Table X), for displacement of solvent
from $(\text{solv})\text{Cr(CO)}_5$ by hex at 25.0 °C vary CB < TL < BZ < FB
<< HP; the same trend is noted for pip. Thus aromatic
solvents are displaced much more slowly than is the alkane.
Considering the series of C_6H_5X solvates (X = CH_3, H, Cl, F),
it is observed that rate of displacement of CB does not
correspond to the order of the electron-withdrawing
abilities of X; it is slower than would be anticipated on
this basis. This observed trend in rate constant and the low
$\Delta V^{\ddagger}_{obsd}$ for CB may be attributable to a different mode of
bonding of CB to the metal, via a Cl-Cr coordinate covalent
bond, as opposed to BZ, TL and FB which coordinate to Cr

through a double bond on the ring. There is considerable evidence other than that presented here, in the form of X-ray crystallographic and other data, of the X-M bonding mode for substituted haloalkane and arenes (X = Cl, Br, I).[110-127] Questions concerning the mechanisms of CB displacement from (CB)Cr(CO)$_5$ and the bonding mode of CB will be further examined.

The decrease of $\Delta V^{\ddagger}_{obsd}$ is especially noteworthy for n-heptane, since, if the solvent molar volumes influence $\Delta V^{\ddagger}_{obsd}$, the much larger molar volume for HP than for the other solvents might be expected to result in a more positive $\Delta V^{\ddagger}_{obsd}$ for HP as the solvating molecule. Bonding of n-heptane to Cr is likely to take place through a two-electron three-center "agostic" C-H-Cr interaction,[17-19] and thus may suggest a smaller "collapse" in volume upon C-H-Cr bond formation in the solvates than upon "edgewise" bonding of arene to Cr. On the other hand, the smaller $\Delta V^{\ddagger}_{obsd}$ for HP is also consistent with the accessibility of an interchange solvent displacement pathway (vide infra), as suggested by the studies of Peters and coworkers.[83]

2. Volumes of activation and the incoming nucleophile

The volumes of activation for solvent displacement from (solv)Cr(CO)$_5$ employing 1-hexene as the incoming nucleophile are uniformly larger, by 3-7 cm^3/mol, than are

those observed for piperidine (Table XI). Thus it is reasonable to presume that this difference arise at least in part as a consequence of the contribution of the term $\Delta V^{\ddagger}_2$ in Eq. 18 and 19.

However, examination of rate constants for displacement of HP from (HP)Cr(CO)$_5$ as a function of the identity of the incoming nucleophiles (Table X), together with the thermal activation parameters (vide infra) show that lower volumes of activation also may be correlated with increased rates of HP displacement and with decreasing activation enthalpies and entropies. These data thus might be interpreted in terms of an increasing contribution of $\Delta V^{\ddagger}_3$, the volume of activation for the interchange process governed by k_3 (Scheme I, Eq. 17), as the displacement rates increase.

On the other hand, the relativly smaller range of volumes of activation observed for displacement of FB from (FB)Cr(CO)$_5$ by various incoming nucleophiles does not seem to correlate with the rate constants in the way as observed for HP (Table X). Since it has been demonstrated that displacement of FB by L are dissociative in nature (vide infra), via [Cr(CO)$_5$], the relative rates of FB displacement by L may be taken as a measure of the discriminating ability of [Cr(CO)$_5$] among the various L. Thus, the apparent discriminating ability in HP, which is greater than is observed in FB, likely arises in part from the accessibility of the interchange pathway in n-heptane.

3. Volumes of activation and the metal atom

Table XII illustrates changes in volumes of activation for reactions of various (solv)M(CO)$_5$ transients (solv = HP, FB, BZ, TL, CB; M = Cr, Mo, W) with hex. It is evident that $\Delta V^{\ddagger}_{obsd}$ decreases from Cr to Mo and W for all the solvents employed. These results are most simply suggestive of an increasing contribution of the interchange mechanism down the Group VI-B metals, which is consistent with previous observations. Thus a recent study of chelate ring displacement by Lewis bases in (chelate)M(CO)$_4$ complexes has indicated that volumes of activation decrease significantly from Cr to Mo, a trend interpreted to a change in mechanism from rate-determining chelate ring-opening for Cr to interchange displacement by L for the larger Mo atom.[128] It has also been noted that the relative contribution of the

Table XII. Volumes of Activation (cm^3/mol) for Reactions of (solv)M(CO)$_5$ Transients with 1-Hexene

M	Solvent = HP	FB	BZ	TL	CB
Cr	6.2(2)	9.4(7)	10.9(10)	10.8(7)	5.4(4)
Mo	2.2(3)	5.8(8)	-----	3.2(3)	3.2(3)
W	2.7(4)	2.5(2)	-----	-----	0.4(3)

interchange pathway for CO displacement reactions of Group VI-B metal carbonyls[129,130] increases in the order Cr < Mo, W, related to the order of increasing atomic size (Cr < Mo, W), and the order of increasing effective nuclear charge (Cr < Mo << W).[13] Since the larger atomic size of Mo and W may be expected to diminish the steric discrimination of metal atoms for coordinated molecules, this may also explain the lack of the observed differences in $\Delta V^{\dagger}_{obsd}$ for Mo and W for various solvents and nucleophiles noted for $(solv)Cr(CO)_5$.

C. Reactions of $(alkane)M(CO)_5$ Complexes with L

As discussed in section B, significant selectivity of HP displacement from $(HP)Cr(CO)_5$ by several nucleophiles was observed, which likely arises from the accessibility of the interchange pathway. To probe this point further, displacement of HP by nucleophiles exhibiting a great range of electronic and steric properties has been investigated.

It is now recognized that the interactions of aliphatic hydrocarbons with transition metal are through "agostic" or "σ-complex" bonding,[17-19,100] which may play a role in C-H insertion, β-elimination, ligand-exchange, and hence catalytic reactions. An important step in evaluating whether this type of bonding can play a significant role in these reactions is to determine the strengths of these bonds. Morse, Parker and Burkey have estimated, employing

photoacoustic calorimetry, the (solv)-M bond strengths

(kcal/mol) in (solv)M(CO)$_5$ species as follows:[108]

(heptane)-Mo (8.7 ± 2.7) < (pentane)-Cr (8.9 ± 3.2) <

(heptane)-Cr (9.6 ± 2.3) < (isooctane)-Cr (11.0 ± 2.1) <

(cyclohexane)-Cr (12.6 ± 2.1) < (heptane)-W (13.4 ± 2.8).

They also concluded that "agostic" bond formation is

preferred with secondary relative to primary CH bonds. The

relative strengths of (solv)-M interactions have been

further examined by studies of the displacement rates of

various aliphatic solvents in (solv)M(CO)$_5$ by nucleophiles.

Table XIII lists the pseudo-first-order rate constants

obtained from flash photolysis of M(CO)$_6$ (M = Cr, Mo, W) in

aliphatic hydrocarbons in the presence of various

nucleophiles at different temperatures. The plots of k_{obsd} vs

[L] obey Eq. 2, which predicts linear plots of k_{obsd} vs [L]

as shown in Figure 22. The existence of the small intercepts

(< 1% of the slope) may be attributed to trace amount of

impurities in the solvents, even though the solvents have

been carefully purified especially for heptane and

cyclohexane (vide supra). It may also be attributed to the

reaction of (solv)M(CO)$_5$ with dissolved N$_2$ in solution[73]

since all the reactions were carried out under a N$_2$ blanket.

Therefore, reactions were also studied in the absence of

added nucleophiles, from which the observed slow rates were

found to be in very close agreement with the values of the

intercepts (Table XIII). Thus, the second-order rate

Table XIII. Pseudo-first-order Rate Constants Observed After

Flash Photolysis of $M(CO)_6$ in Alkane Solutions of

Various Nucleophiles at Different Temperatures

M	Solvent	Ligand	Temp (°C)	$10^2[L]$ (M)	$10^{-6}k_{obsd}$ (s^{-1})
Cr	n-Heptane	1-hexene	2.0	6.07	0.32(2)
			24.5		1.01(2)
			25.0	0.0	0.11(6)
				2.03	0.474(6)
				4.06	0.749(9)
				6.09	1.074(5)
				8.12	1.40(1)
				10.15	1.66(2)
				20.30	3.21(7)
				30.45	4.61(14)
			45.0	6.07	2.375(7)
		Benzene	25.0	2.00	0.56(1)
				4.07	1.32(3)
				8.14	2.26(40)
		Chlorobenzene	1.2	1.954	0.232(2)
			25.0		0.74(6)
			45.0	0.977	0.90(8)
		Piperidine	2.3	1.857	1.01(10)
				2.668	1.16(8)
				3.374	1.39(3)
				4.212	1.92(21)
				8.435	2.98(12)
			24.5	1.857	1.12(3)
				2.000	1.05(4)
				2.668	1.74(9)
				3.374	2.25(6)
				4.212	2.33(12)
				4.495	2.80(10)
				6.670	3.64(10)
				9.287	5.37(37)
			25.0	1.784	1.08(2)
			45.8	1.857	2.11(6)
				2.668	2.77(31)
				3.374	3.42(20)
				4.212	4.12(35)
		Ethanol	2.0	1.148	0.29(1)
				5.740	0.98(14)

Table XIII. Continued

M	Solvent	Ligand	Temp (°C)	$10^2[L]$ (M)	$10^{-6}k_{obsd}$ (s^{-1})
			24.5		4.11(10)
			45.0	1.148	1.30(4)
		2,6-Lutidine	1.2	1.33	0.262(7)
			15.0		0.74(4)
			25.0		1.17(10)
			35.0		1.42(9)
			45.0		2.55(9)
		2-Picoline	1.2	1.188	0.54(2)
			15.0		0.92(2)
			25.0		0.994(1)
				1.22	1.10(2)
				2.44	2.05(15)
			35.0	1.188	1.95(21)
			45.0		3.00(17)
		THF	2.0	0.566	0.35(1)
			24.5	2.83	3.50(8)
				5.88	6.60(32)
			45.0	0.566	1.12(2)
		Pyridine	1.2	1.03	0.99(6)
			2.0	0.59	0.56(1)
			15.0	1.03	1.51(2)
			24.5	1.18	2.28(4)
			25.0	1.03	2.16(5)
			35.0		2.84(7)
			45.0		3.86(7)
		Acetonitrile	2.0	1.04	1.31(49)
			24.5	4.16	12.8(3)
			25.0	2.00	6.6(2)
			45.0	1.04	5.9(6)
	n-Octane	no ligand	25.0	0.0	0.142(5)
		1-Hexene		6.06	1.01(1)
				12.13	2.18(10)
				18.20	3.08(6)
				24.26	4.04(8)
	n-Octane-d$_{18}$			0.0	0.71(1)
				11.5	1.82(2)
				25.3	3.60(10)
	iso-Octane			0.0	0.267(3)
				6.12	1.38(3)
				12.24	2.34(16)
				18.36	3.22(15)
				24.48	4.40(12)
	Cyclohexane			0.0	0.15(5)

Table XIII. Continued

M	Solvent	Ligand	Temp (°C)	$10^2[L]$ (M)	$10^{-6}k_{obsd}$ (s^{-1})
				10.06	0.56(1)
				20.12	1.17(2)
				40.24	2.10(9)
				60.36	3.21(14)
		Piperidine	12.9	7.26	1.18(1)
			13.9	2.94	0.47(2)
				4.90	0.73(2)
				8.62	1.26(2)
				13.74	2.08(6)
				17.23	2.57(6)
				21.54	3.22(4)
			14.7	7.26	1.23(2)
			16.8		1.21(2)
			19.8		1.29(1)
			22.7		1.42(2)
			24.5	0.98	0.215(7)
				1.96	0.400(2)
				2.94	0.58(2)
				3.92	0.778(4)
				4.90	0.959(1)
				13.74	2.66(4)
				17.23	3.20(5)
				21.54	4.14(14)
			25.0	2.00	0.380(2)
			25.5	7.26	1.434(2)
			27.7		1.52(1)
			30.7		1.63(2)
			33.5		1.68(2)
			34.4	3.92	0.98(5)
				4.90	1.22(1)
				8.62	2.17(11)
				13.74	3.28(4)
				17.23	4.34(2)
	Methylcyclohexane	Acetonitrile	25.0	2.00	2.85(12)
		1-Hexene		2.00	0.15(4)
		Piperidine		2.00	0.45(2)
		Acetonitrile		2.00	2.98(9)
Mo	n-Heptane	1-Hexene	25.0	0.0	0.122(9)
				5.94	1.236(5)
				11.88	2.08(2)
				16.63	2.70(1)
				23.75	3.97(11)

Table XIII. Continued

M	Solvent	Ligand	Temp (°C)	10^2[L] (M)	$10^{-6}k_{obsd}$ (s^{-1})
W				0.0	0.017(1)
				11.88	0.220(4)
				23.75	0.402(3)
				47.50	0.780(1)
				71.25	1.16(1)
				99.00	1.580(8)
				225.2	3.44(5)

constants, k_{2nd}, have been calculated from the slopes of plots of k_{obsd} vs [L], or have been corrected from the contributions of "impurities" according to Eq. 2. However, this influence on activation parameters was found to be relativly small compared to the experimental errors.

1. Reactions of (HP)Cr(CO)₅ and incoming nucleophiles

Table XIV lists the calculated second-order rate constants, k_{2nd}, at 25.0 °C and the activation parameters (Figure 23) for reactions of (heptane)Cr(CO)₅ with various nucleophiles. It is noted that while the relative rate constants change somewhat ca 20 fold in the order of acetonitrile (22) > pyridine (14) > THF (8) > 2-picoline (6) > 2,6-lutidine (5.4) > ethanol (4.8) > piperidine (3.7) > chlorobenzene (2.2) > benzene (1.8) > 1-hexene (1), the
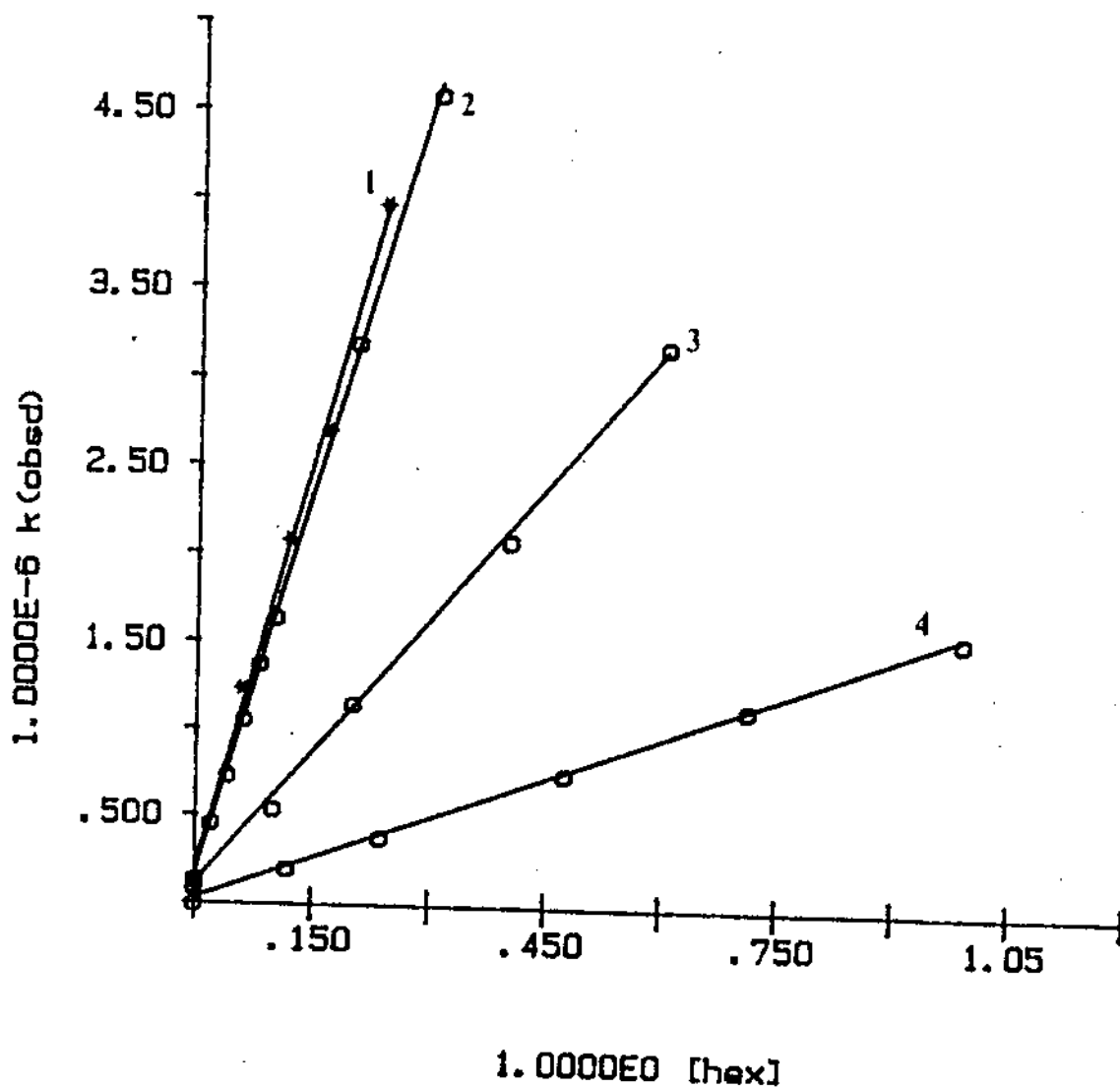
Figure 22. Plots of k_{obsd} vs [L] for reactions taking place
after flash photolysis of $M(CO)_6$/hex/solv solutions at
25.0 °C. M/solv = Mo/HP (1), Cr/HP (2), Cr/CH (3), W/HP (4).

Table XIV. Second-order Rate Constants at 25.0 °C and
Activation Parameters for Reactions of
$(HP)Cr(CO)_5$ with Various Nucleophiles

Ligands	$10^{-7}k_{2nd}$ ($M^{-1}s^{-1}$)	k_{rel}	$\Delta H^{\ddagger}$ (kcal/mol)	$\Delta S^{\ddagger}$ (*)	$\Delta V^{\ddagger}$ (cm^3/mol)
piperidine	5.4(1)	3.7	3.1(5)	-12.5(16)	+1.4(4)
THF	11.8(4)	8.0	4.1(2)	-7.8(6)	-----
pyridine	19.9(5)	13.5	4.8(1)	-4.3(4)	-1.4(5)
acetonitrile	32.(1)	22.0	5.0(6)	-2.9(21)	-----
2-picoline	9.(2)	6.1	6.1(5)	-1.2(18)	-1.4(3)
ethanol	7.0(2)	4.8	6.6(13)	-0.9(44)	-----
1-hexene	1.47(1)	1.0	7.5(1)	-0.3(4)	+6.2(2)
chlorobenzene	3.2(3)	2.2	7.5(1)	+1.4(3)	-----
2,6-lutidine	8.0(7)	5.4	7.9(8)	+4.2(28)	-----
benzene	2.6(4)	1.8	-----	-----	-----

* cal/(deg mol)

activation parameters change in a different order as shown
in Table XIV. However, it is clearly seen that when the
enthalpies of activation increase down the column, the
entropies of activation and the volumes of activation
consistently becomes more positive. This strongly indicates
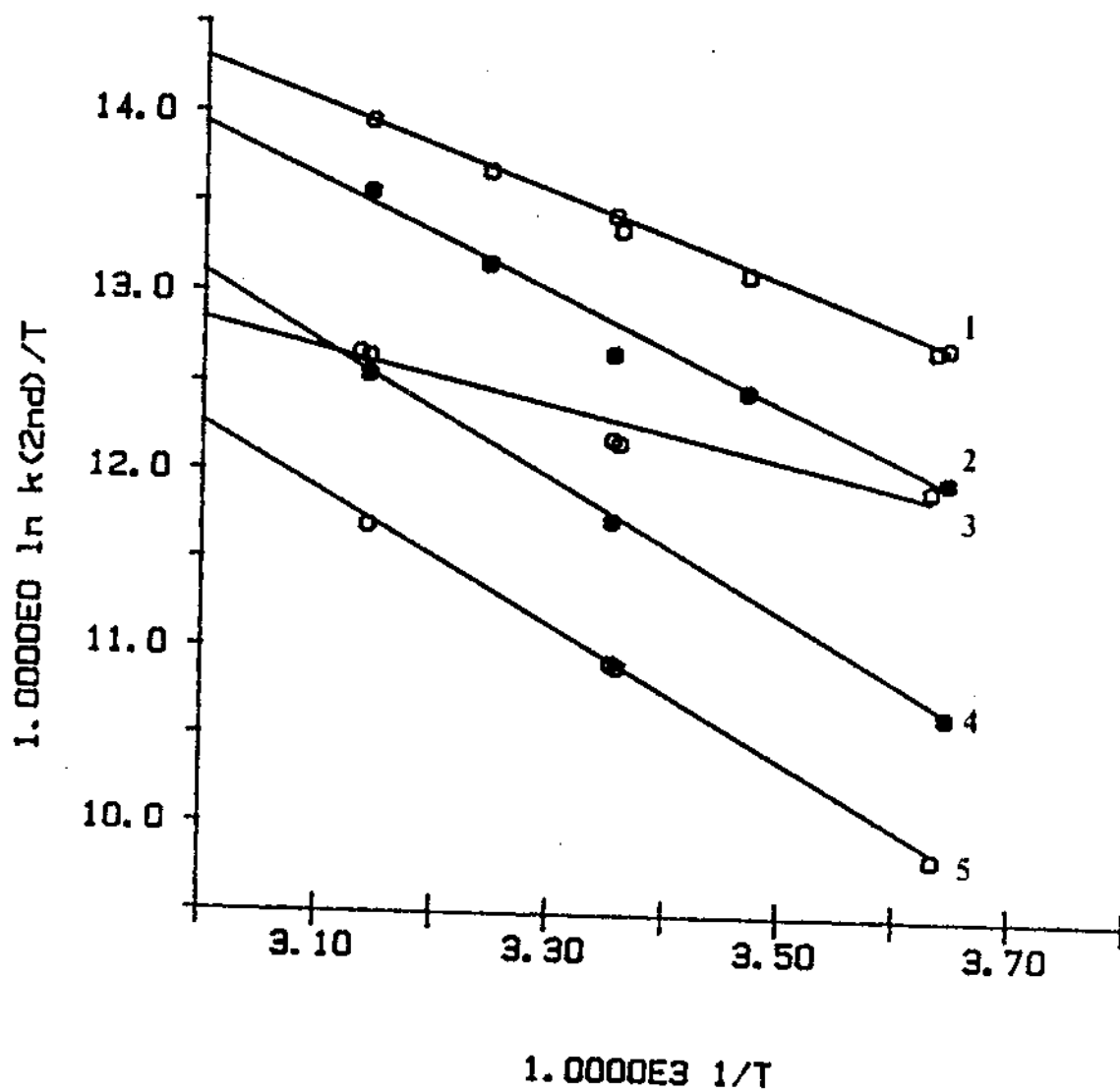
Figure 23. Plots of ln k_{2nd}/T vs 1/T for reactions taking place after flash photolysis of Cr(CO)$_6$ in L/HP solutions. L = py (1), pic (2), pip (3), CB (4), hex (5).

that the reactions are experiencing a gradually change from more interchange pathway to more dissociative pathway down the column in Table XIV.

The observed results also suggest that both steric and electronic properties of the nucleophiles play important roles in the rate of HP displacement. For example, the small nucleophile, CH_3CN, which should exhibits little steric hindrance, afforded the highest rate constant; while 2,6-lutidine presumably more electronic donating but more sterically hindered than pyridine afforded considerable slower rate than pyridine. On the other hand, relatively poor donor nucleophiles (hex, BZ and CB) replace HP from $(HP)Cr(CO)_5$ at much more slower rates.

In essence, it may be concluded that while strong and less steric demanding nucleophiles react with $(HP)Cr(CO)_5$ more via an interchange pathway, weak and bulky nucleophiles may react via a predominately dissociative pathway. Thus, the highest observed enthalpy of activation, 7-8 kcal/mol, may be a rough measurement of the (HP)-Cr bond strength; this value is somewhat lower than the values estimated from photoacoustic calorimetry technique,[83,108] but is within their reported experimental errors.

2. Influences of the identities of the solvent and the metal

The rates of displacement of aliphatic hydrocarbons from $(solv)M(CO)_5$ depend upon the structure of the solvent

Table XV.   Second-order Rate Constants for Reactions of
(solv)M(CO)$_5$ (solv = alkanes; M= Cr, Mo, W) with
Nucleophiles at 25.0 °C

M	Ligands	Solvents	$10^{-7}k_{2nd}$ $(M^{-1}s^{-1})$
Cr	1-Hexene	iso-Octane	1.65(4)
		n-Octane	1.63(4)
		n-Heptane	1.47(1)
		n-Octane-d$_{18}$	1.15(9)
		Methylcyclohexane	0.75(21)
		Cyclohexane	0.52(1)
	Piperidine	n-Heptane	5.4(1)
		Methylcyclohexane	2.24(11)
		Cyclohexane	1.90(1)[a]
	Acetonitrile	n-Heptane	32.4(10)
		Methylcyclohexane	14.9(5)
		Cyclohexane	14.2(6)
Mo	1-Hexene	n-Heptane	1.58(5)
W	1-Hexene	n-Heptane	0.158(1)
	4-Acetyl- pyridine	n-Heptane	6.8(4)
		Methylcyclohexane	2.79(3)[b,c]
		Cyclohexane	3.2(1)[c]

a) $\Delta H^{\ddagger}$ = 3.3(3) kcal/mol; $\Delta S^{\ddagger}$ = -13.9(9) cal/(deg mol).
b) $\Delta H^{\ddagger}$ = 3.3(2) kcal/mol; $\Delta S^{\ddagger}$ = -13.0(6) cal/(deg mol).
c) from reference 131.

and the identity of the metal atom as is shown in Table XV.
It is noted for M = Cr that the rates of solvent
displacement decrease in the order of heptane >
methylcyclohexane > cyclohexane, which is the case for three
different nucleophiles. It is also noteworthy that the
displacement rates for a series of aliphatic hydrocarbons by
hex should reveal information about the relative strengths
of (solv)-Cr bonds since the reaction of (solv)Cr(CO)$_5$ with
hex is more dissociative in nature than the other
nucleophiles. Thus, the slower rate for cyclohexane
displacement is a manifestation of a stronger "agostic" bond
between the cyclic secondary CH and Cr center, which is in
agreement with Burkey and coworkers' results.[108] The slight
increase of rate for methylcyclohexane compared to
cyclohexane may be attributable to the fact that
statistically there is one less -CH$_2$- group in the former
which should increase the rate of reaction via a
dissociative pathway. This behavior seemingly departs from
that observed for metal insertion into alkane CH bonds for
which insertion into primary CH bonds is prefered to
insertion into secondary bonds.[132-134] However, the reverse
behavior relative to insertion may not be surprising since
the solvent displacement process involves primarily C-H-M
bond breaking but the insertion reaction involves C-H bond
breaking, and C-M and H-M bond formation.

While there are insignificant differences among the

rates of displacement of heptane, octane and isooctane, comparison of the rates for n-octane and n-octane-d_{18} afforded a normal kinetic deuterium isotope effect of k_H/k_D = 1.4(1) which is consistent with a solvent displacement process involving rupture of an "agostic" C-H-Cr bond.

The similar rate constants for displacements of heptane, octane and isooctane may suggest that there is no observable preference for "agostic" bonding of secondary CH with Cr center over "agostic" bonding of primary CH with Cr center in open-chain aliphatic molecules. Thus, the stronger interaction of cyclohexane with Cr may not be a result of different electronic properties of $-CH_2-$ in cyclic and open-chain molecules, but most likely results of steric effects and flexibility of the solvent molecule as a whole.

From the relative rates of displacement HP by hex from $(HP)M(CO)_5$, it can be recognized that the relative HP-M bond strengths vary Mo $\leq$ Cr $<$ W, as has been observed previously.[108] However, the entropies of activation for solvent displacement by piperidine and 4-acetylpyridine are quite negative (Table XV), indicating a predominant interchange mechanism, thus rates observed for these nucleophiles cannot be used as means of measuring relative solv-M bond strengths.

D. Reactions of (arene)M(CO)₅ Complexes with L

"Although reaction kinetics remains the single most powerful method for exploring mechanism, no account is complete without reference to complementary techniques".[135] One of these techniques is the application of <u>linear free-energy relationships</u>. This method correlates the experimentally observed changes in reaction rate, or free energy of activation $\Delta G^\dagger$, with changes in molecular structure. Correlating molecular structure with reactivity by substituent constants has gained a lot of attention in organic chemistry.[136-140] Linear free energy relationships have also been employed in organometallic chemistry, which is most commonly found in the correlations of the electronic and steric properties of coordinating ligands with reactivities.[81,141,142]

(Arene)M(CO)₅ species represent a special category of organometallic complexes, <u>i.e.</u> a "simple" combination of a transition metal fragment with a typical aromatic organic solvent. Attempts have been made to correlate the electronic and steric properties of the substituents on benzene ring with the reactivities of (arene)M(CO)₅ (arene = benzene and benzene derivatives; M = Cr, Mo, W), in order to attain a better understanding of the arene-metal interactions in these species.

Table XVI. Pseudo-first-order Rate Constants Observed After
Flash Photolysis of $M(CO)_6$ (M = Cr, Mo, W) in Arene
and n-Butyl-chloride Solutions of hex or pip

M	L	Solvent	Temp (°C)	[L] (M)	$10^{-3}k_{obsd}$ (s⁻¹)
Cr	hex	α,α,α-Trifluoro-toluene	25.0	0.0562	43.2(3)
				0.1125	78.0(4)
				0.2250	127(4)
				0.3375	237(43)
		Fluorobenzene		0.1959	23.2(3)
				0.3919	39.4(10)
				0.5878	55.5(15)
				0.7838	78.1(4)
				0.9797	101(4)
		Cumene		0.1060	1.6(5)
				0.2120	2.9(1)
				0.3190	4.4(2)
				0.5320	6.8(2)
		Mesitylene		0.2028	2.3(5)
				0.4056	4.6(3)
				0.6084	7.0(3)
				1.014	11.0(7)
		t-Butylbenzene		0.1380	1.60(6)
				0.2760	2.7(2)
				0.4140	4.2(1)
				0.6915	7.4(2)
		Cyclohexylbenzene		0.2132	3.8(4)
				0.4264	4.9(2)
				0.6396	7.4(1)
				1.066	12.2(5)
		Ethylbenzene		0.1180	1.5(2)
				0.2360	2.7(3)
				0.3540	3.7(3)
				0.5901	5.8(3)

Table XVI. Continued

M	L	Solvent	Temp (°C)	[L] (M)	$10^{-3}k_{obsd}$ (s^{-1})
		o-Dichlorobenzene		0.3020	2.17(2)
				0.6040	4.2(1)
				0.9060	6.4(2)
				1.510	11.1(1)
		Toluene		0.2254	1.52(4)
				0.4508	2.95(4)
				0.6762	3.98(20)
				1.127	5.79(24)
		m-Xylene		0.2034	0.73(3)
				0.4068	1.38(5)
				0.6102	2.06(8)
				1.017	3.55(6)
		Chlorobenzene		1.342	5.13(9)
		p-Xylene		0.252	0.75(1)
				0.504	1.28(3)
				0.756	2.1(2)
				1.260	3.67(9)
		o-Xylene		0.0959	0.33(1)
				0.4795	1.34(3)
				0.7675	2.1(2)
				0.9594	2.6(1)
		1,2,3,4-Tetramethylbenzene		0.2030	0.22(2)
				0.4060	0.39(1)
				0.6090	0.59(2)
				1.015	1.04(2)
		o-Bromofluorobenzene		0.5644	0.54(2)
				0.8466	0.802(9)
				1.129	1.11(4)
				1.411	1.38(8)

Table XVI. Continued

M	L	Solvent	Temp (°C)	[L] (M)	$10^{-3}k_{obsd}$ (s^{-1})
		Bromobenzene		0.3514	0.078(4)
				0.6190	0.128(2)
				0.8784	0.197(2)
				1.411	0.409(15)
		n-Butylchloride		0.4386	0.077(10)
				0.8771	0.168(18)
				1.305	0.270(4)
				1.641	0.363(1)
	pip	Cumene	26.1	0.1100	7.56(3)
		t-Butylbenzene		0.1063	4.887(7)
		Benzene		0.1070	5.489(5)
		Ethylbenzene		0.1061	6.12(2)
		Toluene		0.1027	2.766(3)
		Chlorobenzene		0.1063	2.398(2)
		Bromobenzene		0.1081	0.290(3)
Mo	hex	Benzene	25.0	0.5904	1.07(6)
		p-Xylene		0.7560	0.25(4)
	pip	Fluorobenzene	26.1	0.0208	3.62(13)
		Benzene		0.1061	2.60(2)
		Ethylbenzene		0.1040	0.413(2)
		Toluene		0.1030	1.062(2)
		Chlorobenzene		0.1025	7.43(3)
		Bromobenzene		0.1015	1.26(1)
W	hex	Chlorobenzene		0.1922	0.034(4)
				0.3494	0.056(8)
				0.5240	0.086(3)
				0.9423	0.156(1)
				1.530	0.26(1)
		Benzene	25.0	1.438	0.048(4)
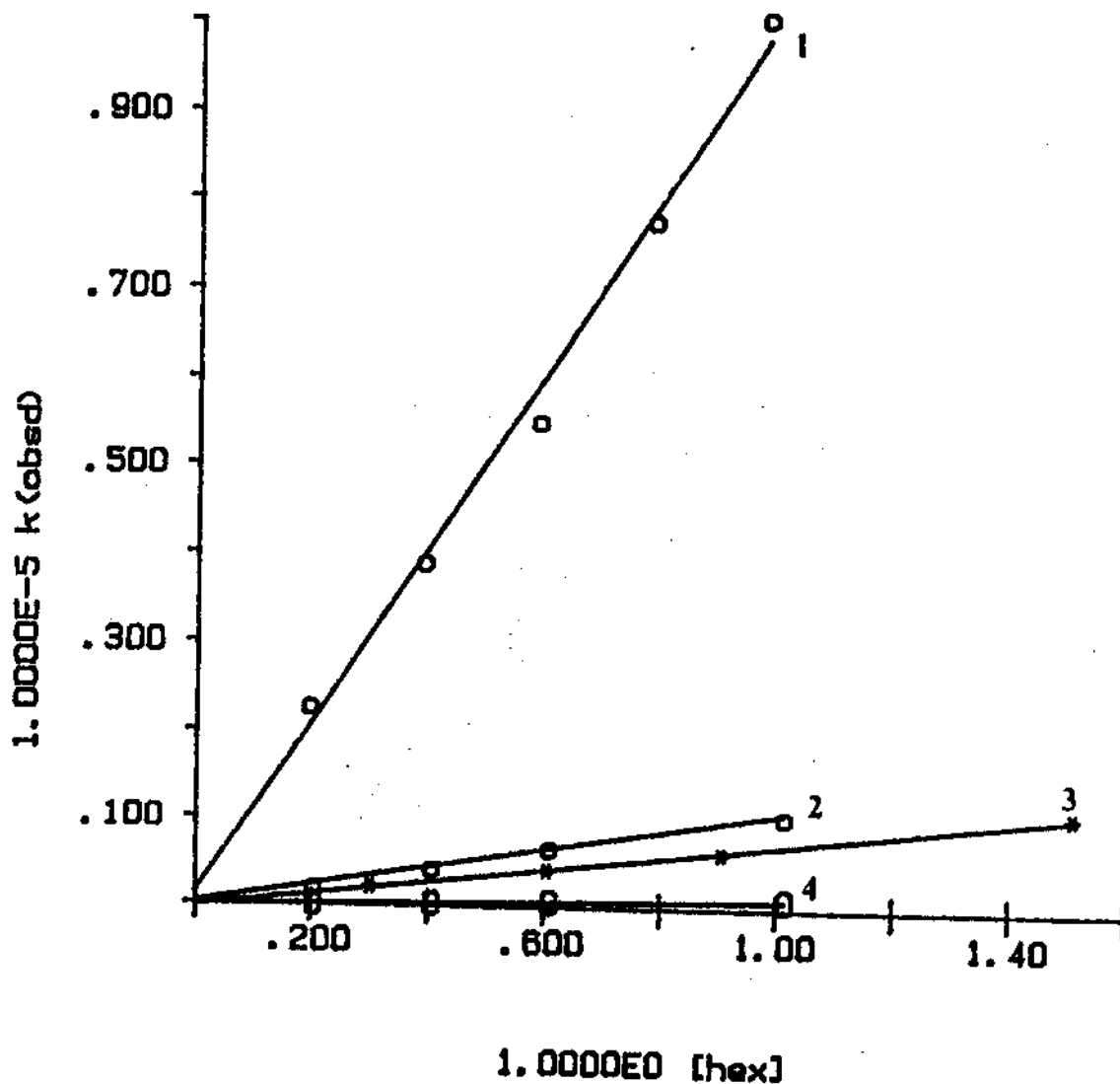
Figure 24. Plots of k_{obsd} vs [hex] for reactions taking place after flash photolysis of $Cr(CO)_6$ in hex/solv solutions at 25.0 °C. solv = fluorobenzene (1), 1,3,5- mesitylene (2), o-dichlorobenzene (3), 1,2,3,4-tetramethylbenzene (4).

Table XVI lists the pseudo-first-order rate constants for reactions of (arene)M(CO)$_5$ with hex and pip. The aromatic solvents ranging from mono-substituted to poly-substituted benzene were employed. These solvents vary largely in both their electronic and steric properties. Plots of k_{obsd} vs [L], as shown in Figure 24, obey Eq. 2. Thus the second-order rate constants (k_{2nd}) calculated from the slopes of these plots, or from $k_{obsd}/[L]$, according to Eq. 2, can be used to correlate reactivities with the structures.

1. Effect of substituents (X) on the reactivities of (C$_6$H$_5$X)Cr(CO)$_5$ complexes

Among the 17 arene solvents examined, 10 of them are monosubstituted benzene (C$_6$H$_5$X). The relative rates for displacement of these solvents from (C$_6$H$_5$X)Cr(CO)$_5$ by hexene according to X can be seen in Table XVII: CF$_3$ > F > CH(CH$_3$)$_2$ > H > C(CH$_3$)$_3$ > C$_6$H$_{11}$ > CH$_2$CH$_3$ > CH$_3$ > Cl > Br. The relative rates vary some 2000-fold. It is evident that the extremely fast rates for α,α,α-trifluorotoluene and fluorobenzene arise from the strong electron-withdrawing effect of -CF$_3$ and -F groups, which reduce the electron density on the benzene ring. On the other hand, the apparently similar rates for cumene, benzene, t-butylbenzene, cyclohexylbenzene and ethylbenzene seem to be caused by a combination of

electronic and steric effects of these substituents. In an effort to separate these effects, a set of "aromatic" substituent constants (σ_m, σ_p, MR) developed by Hansch and coworkers[143] have been employed. Bearing in mind the fact that the arene-Cr interaction is most likely to take place through an "isolated" C=C bond,[1,23,27-34,93,99] the sum of σ_m and σ_p, which are the electronic effect constants for two connecting carbons, is taken as the electronic effect constant ($\underline{E}$). The MR values, originating from molar refractivity data,[144] have been used as the steric effect constant ($\underline{S}$). These substituent constants are collected in Table XVIII.

When correlating rate constants (k_{2nd}) with these substituent constants, Eq. 20 was employed, where a, b, c

$$\log k_{2nd} = a\underline{E} + b\underline{S} + c \tag{20}$$

are constants to be determined. However, the fitting of the k_{2nd} values for reactions of $(C_6H_5X)Cr(CO)_5$ with 1-hexene for 10 monosubstituted benzenes in Table XVII to Eq. 20, through multilinear regression, afforded a correlation coefficient, R, of 0.072. This result is apparently due to the "abnormally" slow rate constants observed for CB and BB when considering their strong electron withdrawing effect on benzene ring (Table XVIII). Consequently, exclusion of these two members from the C_6H_5X series afforded a correlation coefficient, R, of 0.977 for 1-8 solvents. Thus, Eq. 21 was

Table XVII. Rate Constants Calculated for Reactions of $(C_6H_5X)Cr(CO)_3$ with hex at 25.0 °C

Solvent	No.	-X	$10^{-3}k_{2nd}$ ($M^{-1}s^{-1}$)	$10^{-4}k'$ (s^{-1})
α,α,α-trifluorotoluene	1	$-CF_3$	670(70)	550(57)
Fluorobenzene	2	$-F$	99(4)	106(4)
Cumene	3	$-CH(CH_3)_2$	12.3(4)	8.84(4)
Benzene	4	$-H$	10.9(10)	12.2(11)
t-Butylbenzene	5	$-C(CH_3)_3$	10.6(4)	6.8(3)
Cyclohexylbenzene	6	$-C_6H_{11}$	10.2(8)	6.0(5)
Ethylbenzene	7	$-CH_2CH_3$	8.9(2)	7.3(2)
Toluene	8	$-CH_3$	4.6(4)	4.3(4)
Chlorobenzene	9	$-Cl$	3.82(7)	3.75(7)
Bromobenzene	10	$-Br$	0.32(3)	0.30(3)

Table XVIII. Aromatic Substituent Constants

-X	σ_m	σ_p	$\underline{E}$ ($= \sigma_m + \sigma_p$)	$\underline{S}$ ($= MR$)
$-CF_3$	0.43	0.54	0.97	5.02
$-F$	0.34	0.06	0.40	0.92
$-CH(CH_3)_2$	-0.07	-0.15	-0.22	14.98
$-H$	0.00	0.00	0.00	1.03
$-C(CH_3)_3$	-0.10	-0.20	-0.30	19.62
$-C_6H_{11}$	0.07[a]	-0.22	-0.29	26.69
$-CH_2CH_3$	-0.07	-0.15	-0.22	10.30
$-CH_3$	-0.07	-0.17	-0.24	5.65
$-Cl$	0.37	0.23	0.60	6.03
$-Br$	0.39	0.23	0.62	8.88

a) this value is not available from the reference, so it was assumed to be the same as that of $-CH(CH_3)_2$.

determined through multilinear regression to be:

$$\log k_{2nd} = 1.75\underline{E} + 0.0185\underline{S} + 4.11 \qquad (21)$$

Examination of rate constants for reaction of $(C_6H_5X)Cr(CO)_5$ with piperidine produced very similar results (Eq. 22) with R = 0.94:

$$\log k_{2nd} = 1.76\underline{E} + 0.0285\underline{S} + 4.73 \qquad (22)$$

These results at least suggest the following points: (a) A similar mechanism operates for the solvent displacement reactions for C_6H_5X solvents 1-8, which is most likely $\underline{via}$ a dissociative pathway as observed for BZ (Chapter III), a member of the group; (b) The rates of the reaction increase with the increasing of the electron-withdrawing ability and the size of the substituent X; thus the corresponding $(\eta^2\text{-}C_6H_5X)\text{-}Cr(CO)_5$ bond strengths decrease when the electron density in the benzene ring decreases, and when the steric hindrance from the substituent increases; (c) The "mode" of CB and BB interactions with Cr are different from those of solvents 1-8. It is very likely that CB and BB bond with Cr through the halogen atoms ($\underline{cf}$ section B.1),[110-127] while solvents 1-8 bond with Cr through an "isolated" double bond ($\underline{cf}$ Chapter III, E).[1,23,27-34,93,99]

If the interaction of CB-Cr in $(CB)Cr(CO)_5$ is through Cl-Cr bonding, this bond strength should depend on the electron density on the chlorine atom instead of the benzene

ring in CB. This point is further supported by the slower rate constant (k_{2nd} = 2.37(8) x 10^2 $M^{-1}s^{-1}$) observed for n-butylchloride (BuCl) desolvation from (BuCl)Cr(CO)$_5$ by hex (vide supra) than that of CB (k_{2nd} = 3.82(7) x 10^3 $M^{-1}s^{-1}$) from (CB)Cr(CO)$_5$, since C_6H_5- group is less electron releasing than $CH_3CH_2CH_2CH_2-$ group.

Since displacements of 1-8 solvents take place via a dissociative pathway, under the reaction conditions employed, [solv] >> [L]; thus from Eq. 14:

$$k_{2nd} = k_1k_2/(k_{-1}[solv]_o) \tag{23}$$

[solv]$_o$ is the concentration of a neat solvent, which may vary slightly according to its density and molecular weight. Therefore, the rate constants used in linear free energy relationship should be k' which can be calculated from k_{2nd} and [solv]$_o$ according to Eq. 24 (Table XVII):

$$k' = k_1k_2/k_{-1} = k_{2nd}[solv]_o \tag{24}$$

However, employing k' afforded only a slightly different result (Eq. 25) from k_{2nd} for L = hex (Eq. 21) with correlation coefficient R = 0.979:

$$\log k' = 1.70\underline{E} + 0.0069\underline{S} + 5.14 \tag{25}$$

Figure 25 shows correlations of log k' with the electronic and steric substituent constants. Figure 26 presents a plot of log k'(cal) - log k'(exp) vs E, S, where k'(cal) and k'(exp) are the values calculated according to Eq. 25 and the experimental values, respectively. As shown in this figure, the observed rate constants for CB and BB extremely far deviated from the plan defined by solvents 1-8 according to Eq. 25. These results clearly demonstrate that CB and BB do not belong to the 1-8 series, and thus are evidences of different bonding modes for CB and BB with Cr vs solvent 1-8 with Cr in $(C_6H_5X)Cr(CO)_5$ complexes.

2. Effects of multi-substituents

As noted from Table XIX, the introduction of methyl substituents generally lowers the rate of reaction, this trend may arise from the increase of electron density in the ring system due to the electron-releasing nature of methyl group.[143] However, the strength of arene-Cr interaction also seems to depend on the relative position of methyl substituents. It is to be noted that the rate constant for mesitylene displacement is considerably greater than that observed for any other methyl substituted benzene. Straightforward examination of the structures of these arenes suggests that the difference in rates arises from the absence of an unsubstituted "isolated" double bond in the
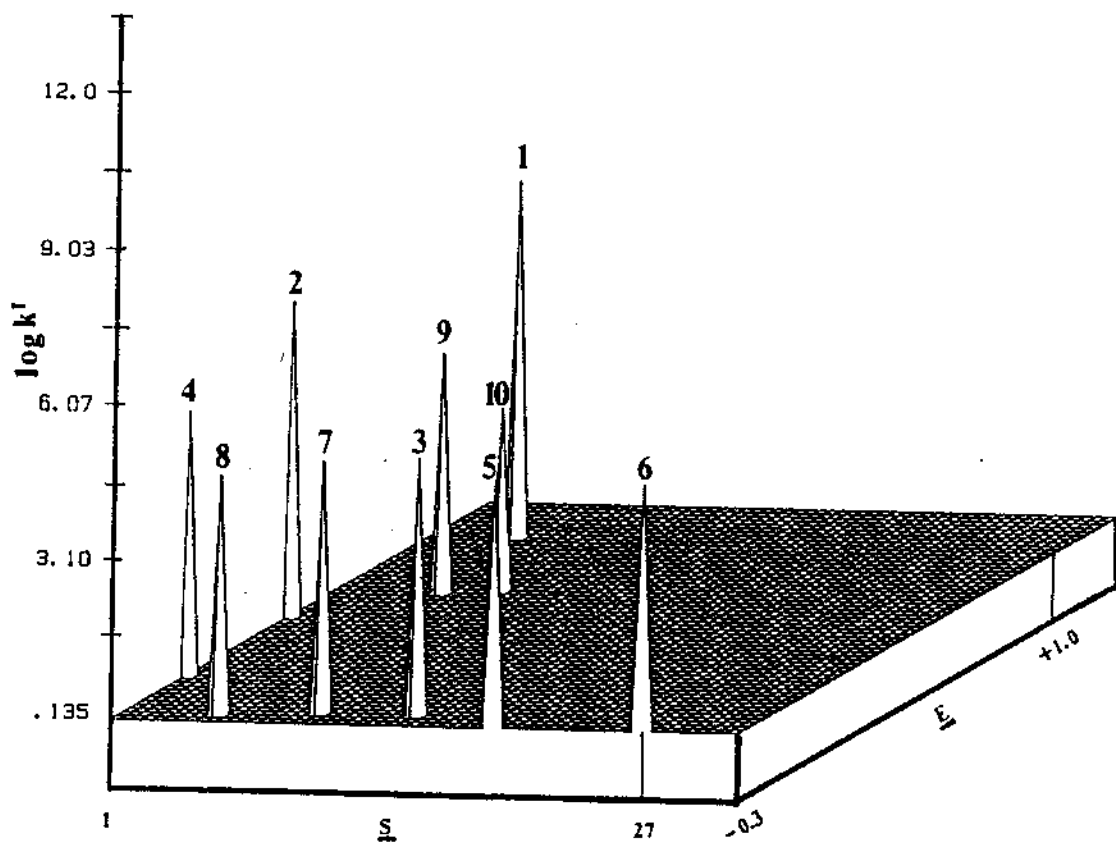
Figure 25. Three-dimensional plots of log k' vs E and S, where the height of each "stick" represents the corresponding value of log k', in which k' is defined by Eq. 24.
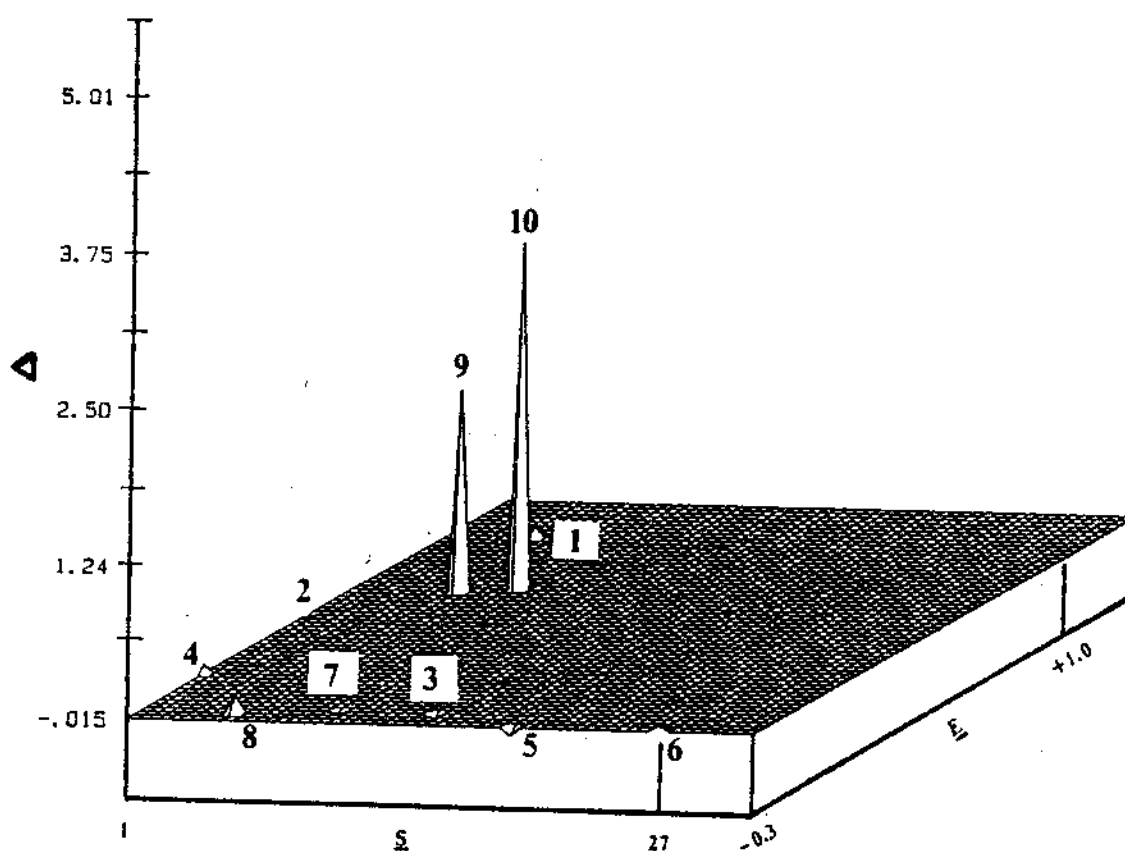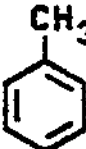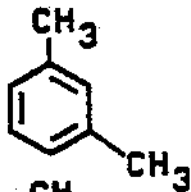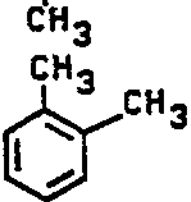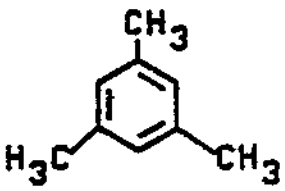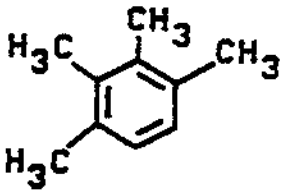
Figure 26. Three-dimensional plots of log k'(cal) - log k'
(exp) vs E and S, where the height of each "stick"
represents the corresponding difference between predicted
value of log k' and experimental value of log k'.

Table XIX. Second-order Rate Constants Calculated for
Reactions of (arene)Cr(CO)$_5$ (arene = BZ and
methyl-substituted benzene) with hex at 25.0 °C

Arene	Structure	$10^{-3}k_{2nd}$ ($M^{-1}s^{-1}$)
Benzene		10.9(10)
Toluene		4.6(4)
m-Xylene		3.48(7)
p-Xylene		3.0(1)
o-Xylene		2.64(1)
Mesitylene		10.7(3)
1,2,3,4-tetra-methylbenzene		1.02(4)

mesitylene molecule. Thus, arenes may prefer bonding with
Cr(CO)$_5$ _via_ an unsubstituted double bond; this preference
may be a result of steric crowding between the methyl group
attached to the double bond and the coordinated CO's in the
Cr(CO)$_5$ moiety. Furthermore, employing 2$\underline{E}$ and 2$\underline{S}$ (_cf_ p 104)
for two methyl substituents in xylene molecules, values of
k_{2nd} and k' were predicted (Eq. 21, 25) to be 3.0 x 10^3
(M^{-1}s^{-1}), 2.6 x 10^4 (s^{-1}), in close agreement with 3.0 x 10^3
(M^{-1}s^{-1}), 2.5 x 10^4 (s^{-1}) respectively determined
experimentally for that of p-xylene's k_{2nd} and k'. This may
suggest that the arene-Cr interaction primarily involves
bond formation from _ortho-_ and _meta-_ carbons in
monosubstituted benzenes.

Assuming that bonding of Cr with halogenated benzene
takes place through -Cl or -Br atoms, the relative rates
among halogenated benzenes (Table XX) may be explained in
terms of electron-withdrawing effects of second halogen in
o-dichlorobenzene and o-bromofluorobenzene.

3. Reactions of (arene)Mo(CO)$_5$ and (arene)W(CO)$_5$ complexes

The order of rates for arene displacement from Mo
solvates (Table XXI) differs from that observed for their Cr
counterparts. This can be seen from the relative faster rate
for CB than for BZ, in their displacement by both piperidine
and 1-hexene. This order of rate constants is apparently

Table XX. Second-order Rate Constants Calculated for
Reactions of (arene)Cr(CO)$_5$ (arene = halogenated-
benzene) with hex at 25.0 °C
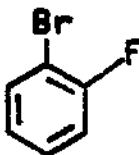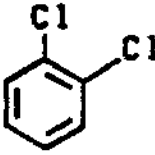
Arene	$10^{-3}k_{2nd}$ (M^{-1}s^{-1})
Fluorobenzene	99(4)
Bromobenzene	0.32(3)
o-Bromofluorobenzene	1.00(2)
Chlorobenzene	3.82(7)
o-Dichlorobenzene	7.4(2)

Table XXI Second-order Rate Constants for Reactions of
(arene)M(CO)$_5$ (M = Mo, W) with pip and hex

M	L	Solvent	Temp. (°C)	$10^{-3}k_{2nd}$ ($M^{-1}s^{-1}$)
Mo	pip	Fluorobenzene	26.1	174.(6)
		Chlorobenzene		72.5(3)
		Benzene		25.6(2)
		Bromobenzene		12.4(1)
		Toluene		10.31(2)
		Ethylbenzene		3.97(2)
	hex	Fluorobenzene	25.0	17.8(7)
		Chlorobenzene		5.09(6)
		Benzene		1.8(1)
		Toluene		0.754(1)
		p-Xylene		0.33(5)
W	hex	Fluorobenzene		0.435(4)
		Chlorobenzene		0.138(1)
		Benzene		0.033(3)

directly related to the electronic withdrawing abilities of substituents. However, application of the linear free energy relationship (Eq. 20) to the two limited series of Mo solvates in Table XIX afforded Eq. 26, 27 for L = piperidine and hexene respectively:

$$\log k_{2nd} = 0.86\underline{E} - 0.11\underline{S} + 4.79 \qquad (R = 0.86) \qquad (26)$$

$$\log k_{2nd} = 1.29\underline{E} - 0.092\underline{S} + 3.59 \qquad (R = 0.87) \qquad (27)$$

These preliminary results from limited data suggest that the bonding in CB-Mo(CO)$_5$ is probably the same as is that for other arenes, i.e. via "isolated" double bond; the negative values for the steric coefficients in Eq. 26, 27 may indicate an interchange mechanism for arene displacement from (arene)Mo(CO)$_5$. In this view, steric crowding is expected to raise the energy of the 7-coordinate transition state, and have a negative effect on the rate of reaction. The order of rate constants observed for FB, CB, BZ displacement from (arene)W(CO)$_5$ by 1-hexene are similar to their Mo analogous.

Therefore, these results are in agreement with the conclusion derived from volumes of activation studies (Section B.3) as to the reaction pathway related to the identity of metal atoms.

Chapter Summary

Studies on reactions of (solv)M(CO)$_5$ with Lewis bases were carried out employing (i) activation parameters, in particular, volumes of activation; (ii) comparisons of rate constants; and (iii) linear-free-energy-relationship. The results demonstrate that the mechanisms for these reactions depend on the electronic and steric properties of the solvents and incoming nucleophiles, and the identities of the metal atoms. Meanwhile, the strengths of (solv)-M

bonding interactions are sensitive to the structures of the solvent molecules and the identities of the metal centers.

The results favor dissociative desolvation pathways for most arene solvents in $(solv)Cr(CO)_5$ species and are consistent with the accessibility of an interchange pathway for $(heptane)M(CO)_5$. Different types of $(arene)-Cr(CO)_5$ interactions were suggested for chlorobenzene and bromobenzene vs fluorobenzene and other non-halogenated arenes, i.e. via σ-halogen-Cr bond formation in CB and BB solvates vs η^2-arene-Cr bond formation solvates of the other arenes. The data also support the increasing importance of interchange pathways for solvent displacement from the solvates of Mo and W vs that of Cr.

These results underscore the similarities between solvent substitution mechanisms for $(solv)M(CO)_5$ transients and ligand substitution pathways of the metal hexacarbonyls and their substitution products.

CHAPTER V

COMPETITIVE MECHANISMS FOR SOLVENT DISPLACEMENT
FROM (SOLVENT)M(CO)$_5$ TRANSIENTS

Interpretation of activation parameters and
correlation of reaction rates with structures of solvents
and incoming nucleophiles have been employed in studies of
mechanisms of solvent displacement from (solv)M(CO)$_5$ by
Lewis bases (Chapter IV). However, the determination of
reaction rate laws and the individual rate constants are
very often the most indicative and important means to
approach the elucidation of a reaction mechanism. In this
respect, the key to studies of solvent displacement reaction
by L is to examine the reaction rates as a function of
concentrations of both incoming nucleophile and the solvent.
One such an approach has been carried out in the studies of
reactions of (BZ)Cr(CO)$_5$ with L (= pip, hex, py), where
mixtures of L/BZ with various [L]/[BZ] ratios have been
employed (Chapter III). However, in order to vary
concentrations of both L and the solvent independently, a
second solvent has to be introduced into the system. Such an
approach was also adopted in studies of reactions of
(CB)Cr(CO)$_5$ with pip, where pip/CB/HX mixtures were
employed. In such systems, the resolution of reaction rate
laws will inevitably become more complex (<u>vide supra</u>), but

will afford more information about mechanistic pathways.

We shall consider a system $M(CO)_6$/L/solv1/solv2, where solv1 and solv2 are the first and second solvents respectively. Flash photolysis with CO dissociation from $M(CO)_6$ produces an $M(CO)_5$ intermediate which will very rapidly react with L, solv1 and solv2[62,63,71-75] to form $LM(CO)_5$, $(solv1)M(CO)_5$ and $(solv2)M(CO)_5$ respectively (Scheme III). If $LM(CO)_5$ is the final stable product, the solvents in the solvated species $(solv1)M(CO)_5$ and $(solv2)M(CO)_5$ will eventually be replaced by L. If the solvents are very weak nucleophiles, the solvent exchange processes may take place through dissociative pathways, while the solvent displacement by L can take place via competitive dissociative and interchange pathways (vide supra). Overall possible reaction pathways thus will be as shown in Scheme III.

In practice, solv1 and solv2 can be chosen so reaction of $(solv2)M(CO)_5$ is much faster than reaction of $(solv1)M(CO)_5$; thus both $[M(CO)_5]$ and $(solv2)M(CO)_5$ species can be considered as steady-state intermediates on the time scale for reaction of $(solv1)M(CO)_5$. In this case solv2 is considered to be relatively "inert" and acts as a dilution medium.

After applying the steady-state approximation to $[M(CO)_5]$ and $[(solv2)M(CO)_5]$ in Scheme III, the pseudo-first-order rate law for disappearance of the $(solv1)M(CO)_5$

Scheme III
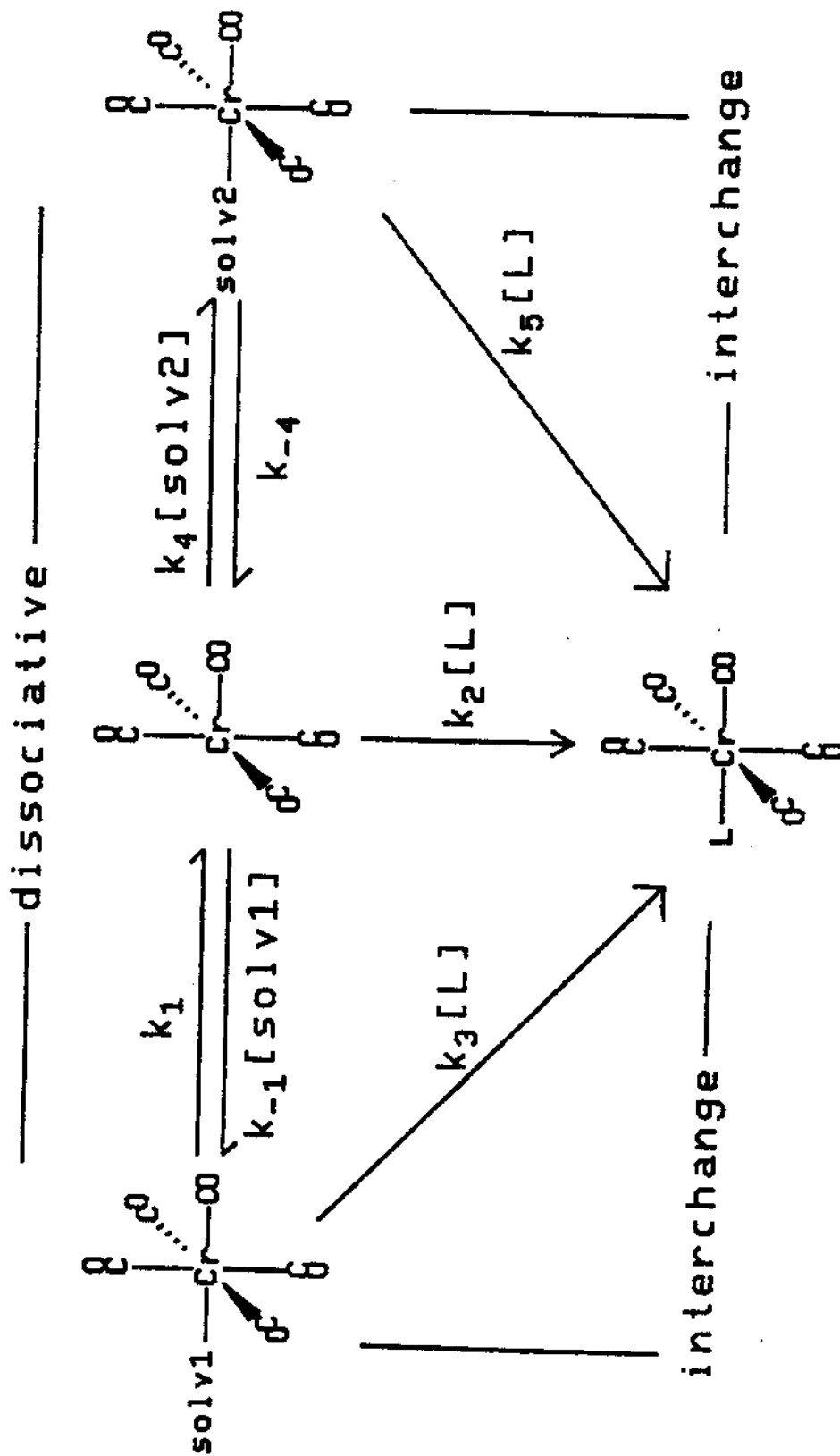
transient can be derived as in Eq. 28:

$$k_{obsd} = k_3[L] + \tag{28}$$

$$\frac{k_1\{k_2(k_{-4}+k_5[L]) + k_4k_5[solv2]\}[L]}{(k_{-4}+k_5[L])k_{-1}[solv1] + \{k_2(k_{-4}+k_5[L]) + k_4k_5[solv2]\}[L]}$$

Rearrangement of Eq. 28 can afford Eq. 29:

$$k_{obsd} = k_3[L] + \frac{k_1(k_2 + k'_4)[L]}{k_{-1}[solv1] + (k_2 + k'_4)[L]} \tag{29}$$

$$\text{where} \quad k'_4 = \frac{k_4k_5[solv2]}{k_{-4} + k_5[L]} \tag{30}$$

Based on these results, it is noted when $k_4 \approx 0$, $k_5 \approx 0$ or [solv2] ≈ 0, then $k'_4 \approx 0$ (Eq. 30). In these events the rate law will be identical to that observed in the absence of solv2 (Eq. 10, p 54).

The present work reports studies of competitive mechanistic pathways for solvent displacement in $(HP)M(CO)_5$ (M = Cr, Mo, W), $(FB)Cr(CO)_5$ and $(CB)Cr(CO)_5$, employing the combination of L/solvent and L/solv1/solv2 systems. The results will be discussed for the cases of (i) $k_3 \neq 0$; $k_5 \approx 0$, (ii) $k_3 = 0$; $k_5 \neq 0$, and (iii) $k_3 \neq 0$; $k_5 \neq 0$.

A. Reactions of (HP)M(CO)$_5$ with hex[145]

The activation parameters for reaction of (HP)M(CO)$_5$ with L, to afford LM(CO)$_5$, have implicated the accessibility of an interchange pathway (<u>vide supra</u>). For L = hex, a relatively weak nucleophile, the dissociative and interchange pathways may be competitive. According to Eq. 10, where solv = HP, L = hex, and [HP] >> [hex] with [M(CO)$_5$] relatively non-discriminating between HP and hex (<u>vide supra</u>), the pseudo-first-order rate constant for reaction in hex/HP one solvent system is,

$$k_{obsd} = (k_3 + \frac{k_1 k_2}{k_{-1}[HP]}) \, [hex] \qquad (31)$$

a rate law consistent with that observed experimentally (Chapter IV.C), since at low [hex], [HP] will be relatively constant.

The possible presence of the two terms in Eq. 10 (p 54) or Eq. 31 has been explored through a comparison of the rate of HP displacement from (HP)M(CO)$_5$ by hex in hex/HP solutions <u>vs</u> that observed when this solution is diluted (1:1, v/v) with MCH$_f$ (= perfluoromethylcyclohexane). MCH$_f$ interacts much more weakly with [M(CO)$_5$] than does HP, as is indicated by the rate constants for displacement of MCH$_f$ (solv2) and HP (solv1) from (solv)Cr(CO)$_5$, 3.0(9) x 10^9 M^{-1}s^{-1} (L = cyclohexane),[73] <u>vs</u> 1.47(1) x 10^7 M^{-1}s^{-1} (L = hex at

25.0 °C, p 95). Thus, $[(MCH_f)M(CO)_5]$ will be a steady-state intermediate in the presence of HP and hex on the time scales of the reactions of $(HP)M(CO)_5$ with L. Table XXII lists the observed pseudo-first-order rate constants for reactions of $(HP)M(CO)_5$ with L to afford $LM(CO)_5$ (cf Eq. 16 on p 73, where solv = HP). The data in the absence of hex are also given to allow corrections from the contribution of "impurities" (vide supra, Chapter IV. C). The corrected rate constants before (k) and after (k') the MCH_f dilution are shown in Table XXIII.

The dilution of hex/HP by MCH_f by a 1:1 ratio (v/v) reduced the concentrations of both [hex] and [HP] by half (Table XXII). It is noted that if displacement of HP by hex takes place via an interchange pathway the constants before (k_I) and after (k'_I) the MCH_f dilution are

$$k_I = k_3[hex] \qquad (32)$$

and $\qquad k'_I = k_3[hex]/2 \qquad (33)$

respectively. On the other hand, if the reaction takes place via a dissociative pathway (i.e. $k_3 = 0$), the constants before (k_D) and after (k'_D) the MCH_f dilution are

$$k_D = \frac{k_1 k_2 [hex]}{k_{-1}[HP] + k_2[hex]} \qquad (34)$$

and according to Eq. 29,

$$k'_D = \frac{k_1(k_2 + k'_4)[hex]}{k_{-1}[HP] + (k_2 + k'_4)[hex]} \qquad (35)$$

Table XXII. Rate Constants Observed After Flash Photolysis of $M(CO)_6$ (M = Cr, Mo, W) in hex/HP and hex/HP/MCH$_f$ Solutions at 35.0 °C

[hex] (M)	[HP] (M)	$\frac{[hex]}{(HP)}$	$10^{-6}k_{obsd}$ (s^{-1})		
			M = Cr	Mo	W
in n-heptane					
0.0	6.8	0.0	0.165(3)	0.14(1)	0.045(4)
0.1188	6.8	57.0	2.72(11)	3.04(10)	0.332(1)
in n-heptane/MCH$_f$(1:1)					
0.0	3.4	0.0	0.28(2)	0.22(4)	0.030(1)
0.0594	3.4	57.0	2.23(13)	2.06(6)	0.222(2)

Table XXIII. Rate Constants for Reaction of $(HP)M(CO)_5$ (M = Cr, Mo, W) with 1-Hexene at 35.0 °C

M	$10^{-6}k$ (s^{-1})	$10^{-6}k'$ (s^{-1})	$10^{-7}k_3$ (M^{-1}s^{-1})	C_{inter}%
Cr	2.56(11)	1.95(15)	1.0(4)	46(20)
Mo	2.90(11)	1.84(10)	1.8(4)	74(18)
W	0.287(5)	0.192(3)	0.16(1)	66(5)

Comparison of Eq. 34 and 35 gives:

$$k'_D - k_D = \frac{k_1 k_{-1} k'_4 [HP][hex]}{(k_{-1}[HP] + k_2[hex])(k_{-1}[HP] + (k_2 + k'_4)[hex])}$$

(36)

or

$$k'_D \geq k_D \qquad (\text{when } k'_4 \geq 0) \qquad (37)$$

However, the observed rate constants k and k' (Table XXIII) indicate that

$$k/2 < k' < k \qquad (38)$$

These results indicate that the reactions take place _via_ the competitive interchange and dissociative pathways, _i.e._ the rate law obey Eq. 10 (p 54) or 31 in the hex/HP solution.

Furthermore, if we assume that $k'_4 \approx 0$ (when $k_4 \approx 0$ or $k_5 \approx 0$, _cf_ Scheme III, and Eq. 30), then $k'_D \approx k_D$ (Eq. 36) the second-order rate constants for interchange pathways, $k_3 = 2(k - k')/[hex]$, and the relative contribution of interchange and dissociative pathways to the overall rate of reaction can be estimated as $C_{inter}\%$, which are listed in Table XXIII. It can be seen from these "semi-quantitative" results, that the contribution of the interchange pathways for Mo and W are greater than that for Cr, which is

consistent with the observation discussed before (Chapter IV, section B.3). However, the assumptions that $k_4 \approx 0$ or $k_5 \approx 0$ are not necessarily valid to afford quantitative calculations.

These experiments were carried out at 35.0 °C rather than at 25.0 °C because MCH_f and HP were observed not to be miscible at temperatures below 26.4(1) °C. Further experiments employing this dilution method can provide extensive information about the competitive mechanisms. However, these experiments are limited not only by the miscible concentration range of HP/MCH_f mixtures but also by the accessibility of extremely fast rates for these systems from the available flash photolysis equipment.

B. Studies of Reactions of (FB)Cr(CO)₅ with pip in FB and FB/HP solutions

Volumes of activation and studies based on linear free energy relations have suggested a dissociative mechanism for reactions of (FB)Cr(CO)₅ with L ($k_3 = 0$, cf Scheme I, p 42, where solv = FB; Scheme III, p 119, where solv1 = FB). To verify this conclusion with respect to reaction rate laws, parallel mechanistic studies were carried out in pip/FB and pip/FB/HP (FB = solv1; HP = solv2) mixtures in which [pip]/[FB] ratios were widely varied. The time-resolved

spectra, obtained after flash photolysis of $Cr(CO)_6$ in pip/FB solutions, are very similar to those obtained in a pip/BZ solution (Figure 9). Figure 27 shows a plot of absorbance vs time monitoring 490 nm after flash photolysis of $Cr(CO)_6$ in a pip/FB solution ([pip] = 1.55 M); the inset depicts a plot of ln $(A_t - A_\infty)$ vs time which demonstrates the reaction of $(FB)Cr(CO)_5$ with pip to afford $(pip)Cr(CO)_5$ obeys pseudo-first-order kinetics. A plot of absorbance vs time monitoring 490 nm after flash photolysis of $Cr(CO)_6$ in a pip/FB/HP solution ([pip] = 0.1416 M), and the corresponding plot of ln $(A_t - A_\infty)$ vs time are shown in Figure 28. However, in this case, the kinetics behavior which is consistent with two first-order processes was observed. The slower process, whose rate constant can be calculated from the slope of the linear portion on the long-time range of plot of ln $(A_t - A_\infty)$ vs time, is attributed to the disappearance of $(FB)Cr(CO)_5$. The faster process (rate constant > 10^7 s^{-1}) likely reflects the disappearance of $(HP)Cr(CO)_5$ which was initially formed rapidly after flash photolysis of $Cr(CO)_6$ in the presence of a large concentration of HP. On the basis of the rate constants for reactions of $(HP)Cr(CO)_5$ with L (Chapter IV, section C.1), the disappearance of $(HP)Cr(CO)_5$ is attributable to its reactions with pip and FB to afford $(pip)Cr(CO)_5$ and $(FB)Cr(CO)_5$ respectively. Due to its very fast rate of reaction, the $(HP)Cr(CO)_5$ species will exist only as a
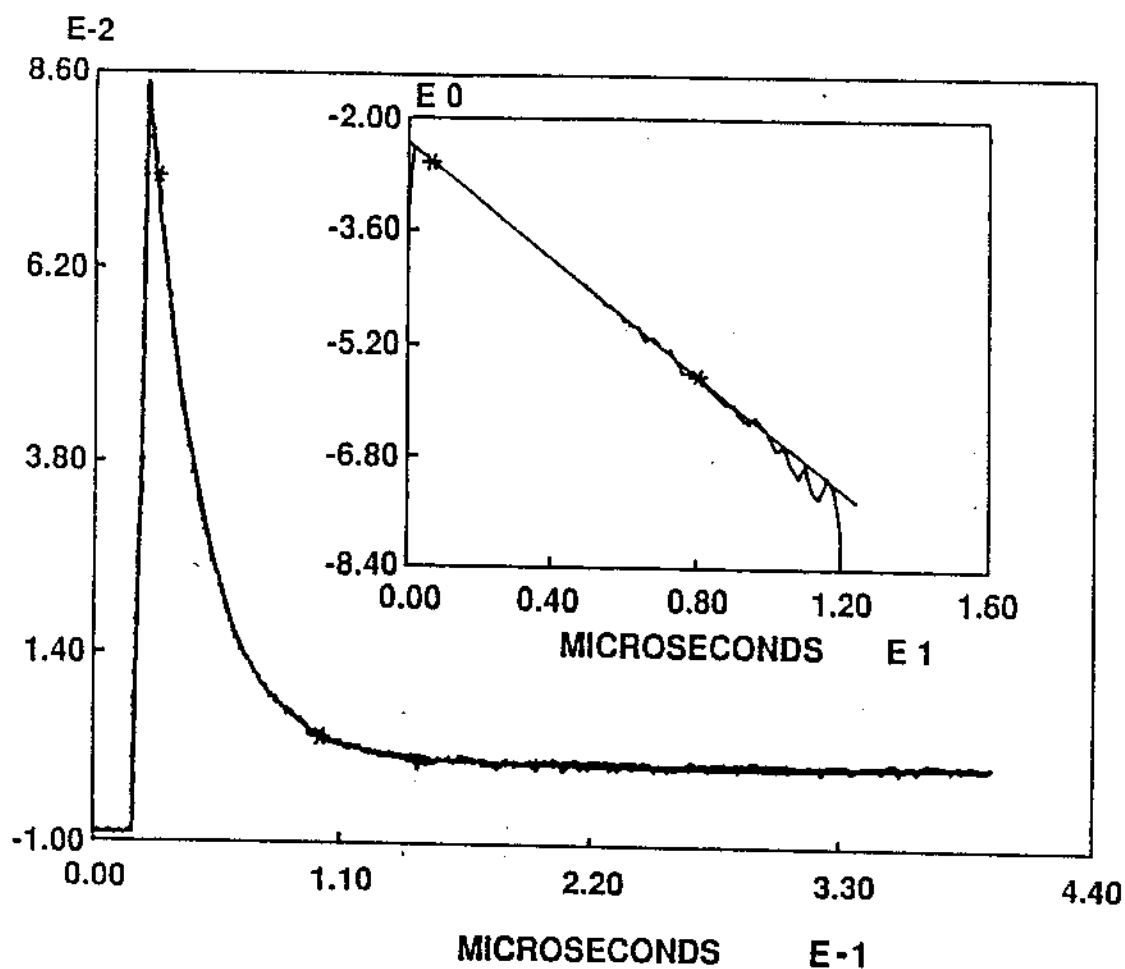
Figure 27. Plot of absorbance vs time monitoring 490 nm after flash photolysis of Cr(CO)$_6$ in a 1.55 M pip/FB solution at 25.0 °C; the inset depicts a plot of ln (A$_t$ - A$_\infty$) vs time.
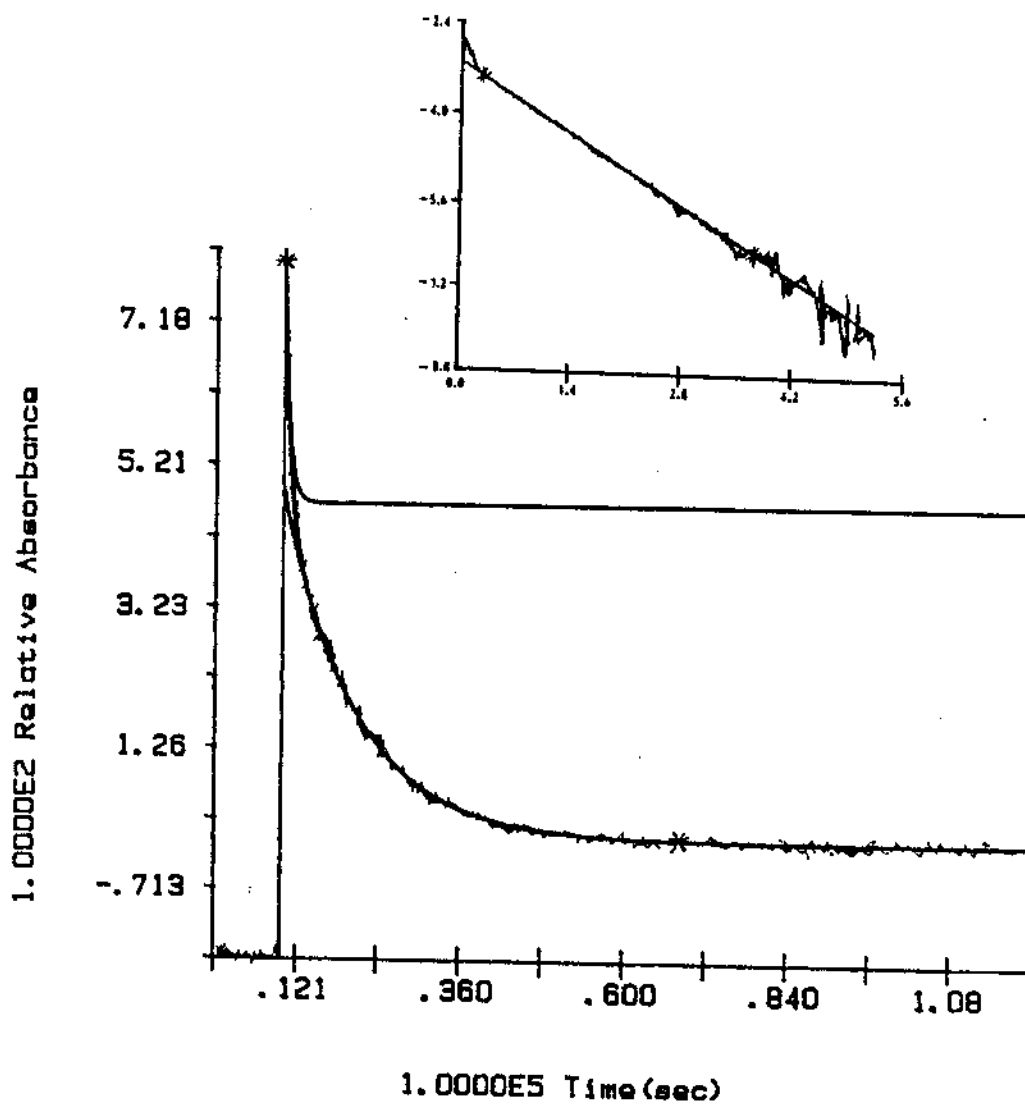
Figure 28. Plot of absorbance vs time monitoring 490 nm after flash photolysis of Cr(CO)$_6$ in a 0.1416 M pip/FB/HP solution at 25.0 °C; the inset depicts a plot of ln (A$_t$ - A$_\infty$) vs time.

steady-state intermediate during the period for reaction of (FB)Cr(CO)$_5$ with pip to form (pip)Cr(CO)$_5$.

The pseudo-first-order rate constants for reaction of (FB)Cr(CO)$_5$ with pip at four temperatures are listed in Table XXIV. As noted from these data, because all the pip/FB solutions were diluted by HP by 1/24 (v:v) ratio, both [pip] and [FB] were reduced to 1/25 of their former values, but [FB]/[pip] ratios were not changed.

Comparisons of these two sets of rate constants indicate slight increases of rate constants upon dilution by HP. These results are different from that observed for hex/HP/MCH$_f$ experiments (section A) where decreases in rate upon the dilutions were observed. Plots of k_{obsd} $\underline{vs}$ [pip]/[FB] for data obtained in both pip/FB and pip/FB/HP mixtures exhibited curvatures similar to those shown in Figure 12, 14 ($\underline{cf}$ Chapter III, sections B, C). However, the reciprocal plots, $1/k_{obsd}$ $\underline{vs}$ [FB]/[pip], for both systems are found to be linear (Figure 29). Even though the two reciprocal plots produced different slopes, they afforded the same intercept. Values of the intercepts and slopes from the reciprocal plots for data at four temperatures are shown in Table XXV.

If $k_3 = 0$, $\underline{i.e.}$ the reaction of (FB)Cr(CO)$_5$ with pip takes place exclusively $\underline{via}$ a dissociative pathway ($\underline{vide}$ $\underline{supra}$), according to Eq. 10 (p 54, where solv = FB, L = pip), the rate constant in pip/FB solutions, k_{obsd}, can be

Table XXIV. Pseudo-first-order Rate Constants for Reactions
(FB)Cr(CO)$_5$ with pip in pip/FB and pip/FB/HP Solutions
at various Temperatures

[pip]	[FB]	$\dfrac{[FB]}{[pip]}$	$10^{-5}k_{obsd}$ (s^{-1})			
			Temp.($^{\circ}$C):			
(M)	(M)		35.0	25.0	15.0	2.3

in pip/FB mixtures

1.550	9.010	5.814	6.71(2)	4.06(2)	2.46(1)	1.17(2)
1.900	8.590	4.520	8.04(6)	4.80(5)	2.92(2)	1.34(1)
2.590	7.869	3.039	10.56(9)	6.41(3)	3.85(3)	1.75(1)
3.540	6.848	1.935	14.09(2)	7.94(14)	4.86(4)	2.25(3)
4.997	5.334	1.068	17.9(4)	10.52(9)	6.18(6)	2.74(3)
6.590	3.668	0.5566	-----	-----	-----	3.23(6)

in pip/FB/HP mixtures ([HP] = 6.57 M)

0.0620	0.3604	5.814	8.73(4)	4.96(2)	2.90(8)	1.38(4)
0.0760	0.3436	4.520	10.70(2)	5.96(5)	3.48(7)	1.70(4)
0.1036	0.3148	3.039	13.7(1)	7.4(2)	4.4(1)	1.96(5)
0.1416	0.2739	1.935	16.8(2)	9.20(2)	5.3(1)	2.35(6)
0.1999	0.2134	1.068	20.8(4)	11.3(4)	6.6(2)	2.84(3)
0.2636	0.1467	0.5566	-----	-----	-----	3.3(1)
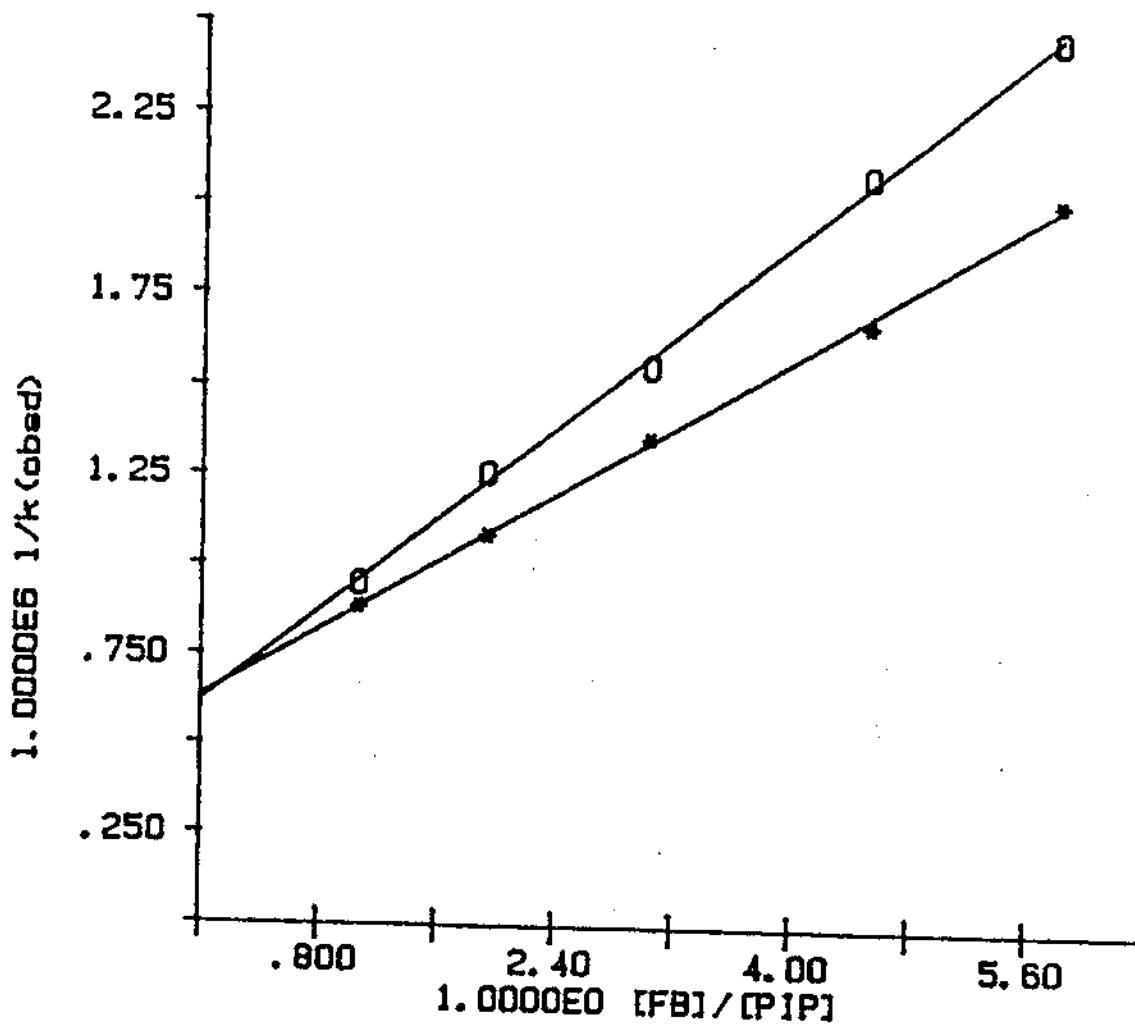
Figure 29. Plots of $1/k_{obsd}$ vs [FB]/[pip] for reactions taking place after flash photolysis of $Cr(CO)_6$ in pip/FB (o) and pip/FB/HP (*) solutions at 25.0 °C.

Table XXV. The Slopes and Intercepts from Plots of $1/k_{obsd}$
vs [FB]/[pip] for Reactions of (FB)Cr(CO)$_5$ with pip in
FB and FB/HP Solutions at Various Temperatures

Temp. (°C)	10^7Slope (s)		10^7Intercept (s)	
Solvents =	FB	FB/HP	FB	FB/HP
35.0	1.99(3)	1.38(4)	3.4(1)	3.2(2)
25.0	3.19(7)	2.36(4)	6.2(2)	6.3(2)
15.0	5.19(6)	4.01(9)	10.5(2)	10.9(3)
2.3	10.4(1)	7.9(1)	25.1(4)	26.6(4)

related to [pip] and [FB] by Eq. 39:

$$\frac{1}{k_{obsd}} = \frac{1}{k_1} + \frac{k_{-1}}{k_1 k_2} \frac{[FB]}{[pip]} \qquad (39)$$

In pip/FB/HP solutions, according to Eq. 29 and 30 (where
solv1 = FB, solv2 = HP, L = pip) the rate constant, k'_{obsd},
for reaction of (FB)Cr(CO)$_5$ with pip can be related to
[pip], [FB] and [HP] by Eq. 40:

$$\frac{1}{k'_{obsd}} = \frac{1}{k_1} + \frac{k_{-1}}{k_1(k_2 + k'_4)} \frac{[FB]}{[pip]} \qquad (40)$$

where $\quad k'_4 = \dfrac{k_4 k_5 [HP]}{k_{-4} + k_5 [pip]}$ (41)

According to the kinetics conditions employed, [HP] was kept constant (= 6.57 M); and pip was kept in very low concentrations ([pip] < 0.3 M). Assuming $k_5[pip] \ll k_{-4}$ in Eq. 41, k'_4 ($\approx k_4 k_5 [HP]/k_{-4}$) is almost constant. Eq. 39 and 40 are very well in agreement with the observed results on three points: (i) the linearity of plots of $1/k_{obsd}$ vs [FB]/[pip] and $1/k'_{obsd}$ vs [FB]/[pip] (Figure 29), (ii) the common intercept (= $1/k_1$) of these plots (Table XXV, Figure 29), and (iii) the greater values of slopes [= $k_{-1}/(k_1 k_2)$] for plots of $1/k_{obsd}$ vs [FB]/[pip] than slopes {= $k_{-1}/[k_1(k_2 + k'4)]$} for $1/k'_{obsd}$ vs [FB]/[pip] (Table XXV, Figure 29).

These results are consistent with a mechanism described in Scheme III when $k_3 = 0$ and $k_5 \neq 0$. In other words, while the reaction of $(FB)Cr(CO)_5$ with pip takes place exclusively via a dissociative pathway, the interchange pathway for displacement of HP by pip from $(HP)Cr(CO)_5$ is accessible. This kinetics evidence strongly support the conclusions obtained from previous studies on the basis of volumes of activation and free-energy-relationships (Chapter IV, section B, D).

The calculated rate constants from these values of intercepts and slopes of the reciprocal plots (Eq. 39, 40) are collected in Table XXVI. The activation parameters for

FB dissociation from $(FB)Cr(CO)_5$ $(\Delta H^{\dagger}_1, \Delta S^{\dagger}_1)$, the comparative activation parameters $(\Delta H^{\dagger}_2 - \Delta H^{\dagger}_{-1}, \Delta S^{\dagger}_2 - \Delta S^{\dagger}_{-1})$, and the competition ratios (k_2/k_{-1}) (Table XXVI) are very similar to that observed for BZ dissociation from $(BZ)Cr(CO)_5$ (Chapter III, section C), these results further suggest similar bonding interaction and bond strengths for FB and BZ with $Cr(CO)_5$.

The ratios (k'_4/k_2) calculated from the values of the slopes of plots of $1/k_{obsd}$ vs $[FB]/[pip]$ (Eq. 39) and plots of $1/k'_{obsd}$ vs $[FB]/[pip]$ (Eq. 40) are also listed in Table XXVI. According to Eq. 41,

$$k'_4 < k_4 k_5 [HP]/k_{-4} \qquad (42)$$

and $\quad k'_4/k_2 < k_4 k_5 [HP]/(k_{-4} k_2) \qquad (43)$

$$\approx k_{inter}/k_{dis} \qquad \text{(for HP)}$$

where $k_{inter} = k_5$;

$$k_{dis} \approx k_{-4} k_2/(k_4 [HP])$$

thus k'_4/k_2 ratios can also be taken as a rough measure of relative importance of interchange and dissociative pathways for HP displacement by pip from $(HP)Cr(CO)_5$. Unfortunately, accurate quantitative calculations for the competitive rate

Table XXVI. The Rate Constants for Reactions of $(FB)Cr(CO)_5$ with pip at Various Temperatures

Temp. (°C)	$10^{-6}k_1{}^{a)}$ (s^{-1})	$k_2/k_{-1}{}^{b)}$	k'_4/k_2
35.0	2.95(9)	1.70(8)	0.44(6)
25.0	1.62(6)	1.94(12)	0.35(5)
15.0	0.95(2)	2.02(6)	0.29(4)
2.3	0.40(1)	2.41(6)	0.31(4)

a) $\Delta H^{\ddagger}_1 = 9.6(2)$ kcal/mol;

$\Delta S^{\ddagger}_1 = +2.2(8)$ cal/(deg mol).

b) $\Delta H^{\ddagger}_2 - \Delta H^{\ddagger}_{-1} = -1.6(3)$ kcal/mol;

$\Delta S^{\ddagger}_2 - \Delta S^{\ddagger}_{-1} = -4.1(11)$ cal/(deg mol).

constants in HP displacement reaction are still not accessible. However, it can be seen from Table XXVI that the k'_4/k_2 ratios exhibit little change at various temperatures, indicating small values of enthalpies of activation for both the interchange and the dissociative pathways. In fact, the enthalpy of activation for the displacement of HP by pip from $(HP)Cr(CO)_5$ was determined to be only 3.1(5) kcal/mol (Table XIV).

C. Mechanisms for Reaction of (CB)Cr(CO)₅ with L

Studies of displacement of CB by pip from (CB)Cr(CO)₅ in pip/CB/HX solutions (Chapter III, section B) have revealed that rates of CB desolvation were inhibited with increasing [CB] thus the desolvation mechanism involved reversible CB-Cr bond breaking. However, it is now clear that both [Cr(CO)₅] and (HX)Cr(CO)₅ could be the reactive intermediates based on the evidence obtained from studies in hex/HP/MCH$_f$ and pip/FB/HP systems (sections A, B). It was also conclusively demonstrated that the bonding in (CB)-Cr(CO)₅ is through Cl atom instead of through an "isolated" double bond from studies of volumes of activation and linear free energy relations. Thus the last two "uncertainties" which were discussed at the end of section B of Chapter III still remain: the negative entropy of activation for CB "dissociation", $\Delta S^{\ddagger}_1$ = -2.9(4) cal/(deg mol) (Table V); and the accessibility of an interchange pathway (Scheme I, p 42) for CB displacement by pip from (CB)Cr(CO)₅ in CB. These questions will be further investigated in the present section.

1. Reactions of (CB)Cr(CO)₅ in hex/CB mixtures

It has been demonstrated that 1-hexene is a weak incoming nucleophile, by which solvent displacement is more

likely to occur _via_ a dissociative pathway (Chapter IV,
section C.1). To avoid the complication due to the
introduction of a "second solvent", binary mixtures of
hex/CB were employed to probe the mechanisms of CB
displacement by hex from photogenerated $(CB)Cr(CO)_5$
transient. The concentrations of hex and CB have been
largely varied in these experiments and the observed pseudo-
first-order rate constants for three temperatures are listed
in Table XXVII.

Curved plots of k_{obsd} _vs_ [hex]/[CB] and linear
reciprocal plots of $1/k_{obsd}$ _vs_ [CB]/[hex] for these data were
observed. These results are consistent with a dissociative
mechanism (Scheme I, p 42, where solv = CB, L = hex) for CB
displacement by hex from $(CB)Cr(CO)_5$. Thus the rate law
obeys Eq. 6 or 7 (p 42, 43), where solv = CB, L = hex. Table
XXVIII lists the rate constants k_1, and "competition ratios"
(k_2/k_{-1}) calculated from the values of intercepts and slopes
of plots of $1/k_{obsd}$ _vs_ [CB]/[hex] according to Eq. 7. The
activation parameters $\Delta H^{\ddagger}_1 = 14.0(4)$ kcal/mol and $\Delta S^{\ddagger}_1 =$
+10.1(15) cal/(deg mol), for CB dissociation from
$(CB)Cr(CO)_5$ are strong evidences to support the dissociative
mechanism, with a late transition state for CB-Cr bond
fission. However, there are inconsistencies between $\Delta H^{\ddagger}_1$'s
and $\Delta S^{\ddagger}_1$'s from this study and that in pip/CB/HX mixtures
(Chapter III, section B): 14.0(4) kcal/mol _vs_ 9.8(1)
kcal/mol; and +10.1(15) cal/(deg mol) _vs_ -2.9(4) cal/(deg

Table XXVII. Pseudo-first-order Rate Constants for Reactions
Taking Place After Flash Photolysis of $Cr(CO)_6$ at
Various Temperatures in hex/CB Solutions

[hex] (M)	[CB] (M)	[CB]/[hex]	Temp. (°C)	$10^{-3}k_{obsd}$ (s^{-1})
1.342	8.166	6.085	3.8	1.032(6)
1.900	7.510	3.953		1.546(7)
2.426	6.855	2.826		1.90(1)
3.279	5.756	1.755		2.73(2)
4.314	4.551	1.055		4.00(1)
1.342	8.166	6.085	15.2	2.56(1)
1.900	7.510	3.953		3.67(2)
2.426	6.855	2.826		4.81(1)
3.279	5.756	1.755		7.02(7)
4.314	4.551	1.055		9.94(11)
1.342	8.166	6.085	25.0	5.13(9)
1.900	7.510	3.953		7.60(3)
2.426	6.855	2.826		10.00(5)
3.279	5.756	1.755		14.54(4)
4.314	4.551	1.055		21.1(2)

Table XXVIII. The Rate Constants and Activation Parameters
for Reactions of $(CB)Cr(CO)_5$ with hex at Various
Temperatures

Temp. (°C)	$10^{-4}k_1{}^{a)}$ (s^{-1})	$k_2/k_{-1}{}^{b)}$
25.0	5.88(18)	0.58(2)
15.2	2.38(13)	0.73(5)
3.8	0.89(10)	0.80(12)

a) $\Delta H^{\ddagger}_1 = 14.0(4)$ kcal/mol; $\Delta S^{\ddagger}_1 = +10.1(15)$ cal/(deg mol).

b) $\Delta H^{\ddagger}_2 - \Delta H^{\ddagger}_{-1} = -2.4(5)$ kcal/mol;

$\Delta S^{\ddagger}_2 - \Delta S^{\ddagger}_{-1} = -9.1(18)$ cal/(deg mol).

mol). Even though two different nucleophiles were employed
in these studies (hex vs pip), if the reactions proceeded by
the dissociative mechanism, values of $\Delta H^{\ddagger}_1$ and $\Delta S^{\ddagger}_1$ should be
independent of this difference as is the case for the
reactions of $(BZ)Cr(CO)_5$ with hex and pip (Chapter III,
section C). Therefore, the reaction mechanism for
$(CB)Cr(CO)_5$ with pip is somehow different from that with
hex, and most likely, the reaction in the former takes
places via competitive dissociative and interchange
pathways.

2. Reactions of (CB)Cr(CO)₅ in pip/CB mixtures

The displacements of BZ from (BZ)Cr(CO)$_5$ by hex and pip have been found to takes place _via_ dissociative pathway; while for py, the reaction was suggested to proceed _via_ competitive dissociative and interchange pathways because of the different intercept in the plots 1/k$_{obsd}$ _vs_ [BZ]/[L] for L = py from that for L = hex and pip (Chapter III, section C). We have also demonstrated that CB displacement by hex takes place most likely _via_ a dissociative pathway (section C.1); thus it is natural to compare the intercepts in these reciprocal plots for data obtained in hex/CB and pip/CB mixtures (Table XXIX, Figure 30).

Table XXIX. Pseudo-first-order Rate Constants for Reactions Taking Place After Flash Photolysis of Cr(CO)$_6$ in pip/CB Solutions at 25.0 °C

[pip] (M)	[CB] (M)	[CB]/[pip]	$10^{-4}k_{obsd}$ (s^{-1})
1.000	8.82	8.82	2.22(2)
1.535	8.32	5.42	3.36(4)
2.094	7.78	3.72	4.31(1)
2.594	7.29	2.81	5.08(2)
3.626	6.27	1.73	7.06(4)
5.035	4.95	0.983	9.18(18)
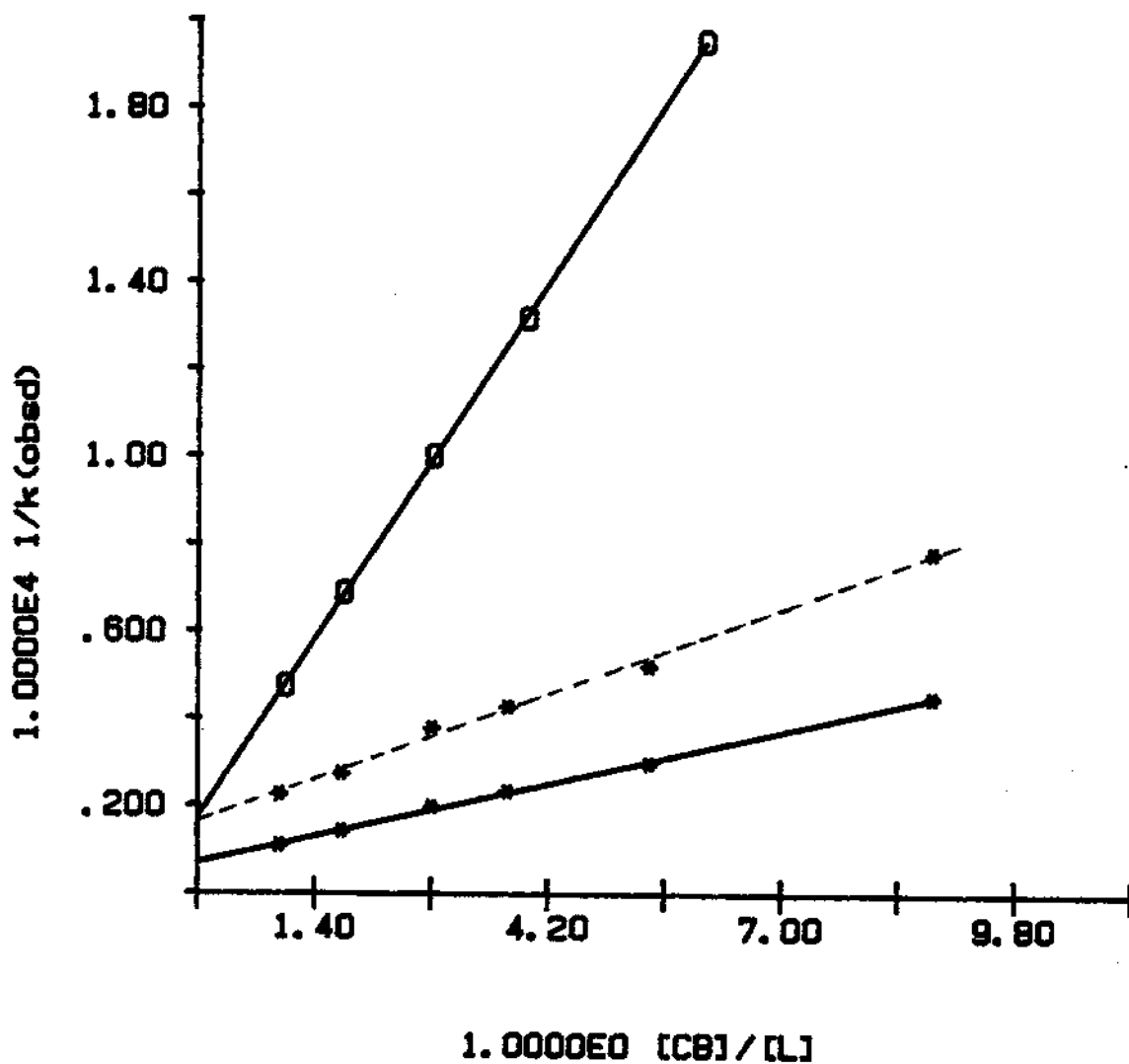
Figure 30. Plots of $1/k_{obsd}$ vs [CB]/[L] for reactions taking place after flash photolysis of $Cr(CO)_6$ in L/CB solutions at 25.0 °C. L = hex (o), L = pip (*). (----), Plots of $1/(k_{obsd} - k_3[pip])$ vs [CB]/[pip].

Comparison of these two plots is shown in Figure 30 for data at 25.0 °C. It is noted that plot of $1/k_{obsd}$ vs [CB]/[pip] for data obtained from pip/CB solutions (Table XXIX) afforded a significantly smaller value of the intercept than that of $1/k_{obsd}$ vs [CB]/[hex]. These results further support the accessibility of the interchange pathway for CB displacement by pip from $(CB)Cr(CO)_5$. The overall mechanisms should be described as in Scheme I (p 42). Thus, the subtraction of a value, k_3[pip], from k_{obsd} so that the two intercepts are coincident affords a linear plot of $1/(k_{obsd} - k_3[pip])$ vs [CB]/[pip] (Figure 30, cf Eq. 10, 11, p 54). It was found:

$$k_3 \approx 9.4 \times 10^3 \ M^{-1}s^{-1}$$

which is the second order rate constant for the interchange pathway (Scheme I, p 42).

3. Reactions of $(CB)Cr(CO)_5$ in pip/CB/HP solutions

The apparent linearity of a $1/k_{obsd}$ vs [solv]/[L] plot for data in a L/solv mixtures is necessary but not sufficient evidence for a dissociative mechanism. So other "control experiments" should be carried out to "confirm" the proposed mechanism. Thus the competitive dissociative and interchange pathways for CB displacement by pip were further investigated by employing the "dilution" technique.

The pseudo-first-order rate constants observed for

Table XXX. Pseudo-first-order Rate Constants for
Reactions Taking Place After Flash Photolysis of
Cr(CO)$_6$ at 25.0 °C in pip/CB/HP Solutions ([CB]/[pip]
= 2.811; [HP] ≈ 6.5(2) M)

[pip] (M)		$10^{-4}k_{obsd}$ (s^{-1})
2.594	(in pip/CB mixture)	5.08(2)
0.0519		2.59(3)
0.1037		2.75(6)
0.1556		2.90(3)
0.2075		3.08(6)

reaction of (CB)Cr(CO)$_5$ with pip in pip/CB/HP solutions are
listed in Table XXX. In these solutions [CB]/[pip] ratio was
kept constant (= 2.811) while concentratiuons of pip and CB
were varied in a low range. It is noted that when the
"binary" pip/CB solution was diluted 50-fold by HP, the rate
constants were reduced about 2-fold. This evidence by itself
is another indication of a competitive mechanism for CB
displacement by pip from the (CB)Cr(CO)$_5$ complex.

Furthermore, the rate constant, k_3, for the
interchange pathway also can be calculated. According to
Scheme III and Eq. 10 (p 54), and Eq. 29, where L = pip,

solv1 = CB, and solv2 = HP, the difference in rate constant k_{obsd} and k'_{obsd}, obtained in the pip/CB and pip/CB/HP (concentration of pip = [pip]') solutions respectively, obeys Eq. 44:

$$k_{obsd} - k'_{obsd} = k_3([pip] - [pip]') - \alpha \qquad (44)$$

in which (also <u>cf</u> Eq. 32-36)

$$\alpha = \frac{k_1 k_{-1} k'_4 [CB][pip]}{(k_{-1}[CB] + k_2[pip])(k_{-1}[CB] + (k_2 + k'_4)[pip])}$$

$$= \frac{k_1 (k_{-1}/k_2)(k'_4/k_2)}{(k_{-1}/k_2 + [pip]/[CB])((k_{-1}/k_2)([CB]/[pip]) + k'_4/k_2 + 1)}$$

$$(45)$$

Rearrangement of Eq. 44 afforded Eq. 46,

$$k_3 = (k_{obsd} - k'_{obsd} + \alpha)/([pip] - [pip]') \qquad (46)$$

The value of α can be estimated based on known rate constants and "competition ratios" at 25.0 °C. We obtained that $k_1 = 5.9 \times 10^3$ s^{-1}, from studies in hex/CB mixtures (Table XXVIII); $k_{-1}/k_2 = 0.31$, from studies in pip/BZ, hex/BZ and hex/CB (Table VII, XXVIII); $k'_4/k_2 = 0.35$, from studies in pip/FB and pip/FB/HP (Table XXVI). For [CB]/[pip] = 2.811,

$$\alpha = 4.33 \times 10^2 \ s^{-1}$$

Substitution of this value together with values of k_{obsd}, k'_{obsd} and $[pip]'$ into Eq. 46 afforded an average value of k_3:

$$k_3 = 9.3(6) \times 10^3 \ M^{-1}s^{-1}$$
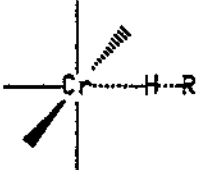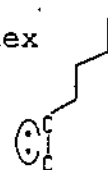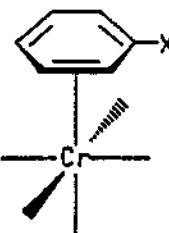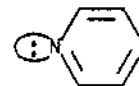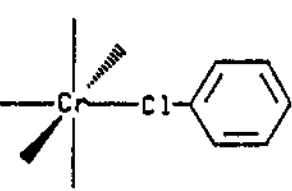
which is in fairly good agreement with the result obtained according to plot of $1/(k_{obsd} - k_3[pip])$ vs $[CB]/[pip]$, 9.4 x $10^3 \ M^{-1}s^{-1}$ (section C.2). On the basis of this rate constant, it can be calculated that the contribution of the interchange pathway to the overall rate of CB displacement by pip in pip/CB at high pip concentration ($[pip] = 2.594$ M) is ca. 50%.

These self-consistent kinetics results for CB displacement by L from $(CB)Cr(CO)_5$, obtained in hex/CB (section C.1), pip/CB (section C.2) and pip/CB/HP (section C.3) solutions, lead us to the following conclusions: The CB displacement by L from $(CB)Cr(CO)_5$ takes place via a dissociative pathway for L = hex; via the competitive dissociative and interchange pathways for L = pip.

D. Mechanisms of Solvent Displacement and the Type of Solvent-Metal Bonding in $(solv)M(CO)_5$ Complexes

Throughout Chapter III-V, mechanisms of solvent displacement by Lewis bases from $(solv)M(CO)_5$ transients have been discussed based on results obtained by employing

Table XXXI. Mechanisms of Solvent Displacement From

(solv)Cr(CO)₅

Solvent	L	Mechanism(s)	Solv-Cr bonding
HP	Lewis Bases	D & I	
	:L		
FB	Lewis Bases	D	
BZ	hex	D	
	:C		
	pip	D	
	py	D & I	X = H, F, CH₃, etc.
CB	hex	D	
	pip	D & I	

X = H, F, CH_3, etc.

several kinetics techniques. Studies of solvent displacement from $(solv)Cr(CO)_5$, where solv = HP, FB, BZ and CB, have been the most extensive. Comparisons of mechanisms of solvent displacement by L from $(solv)Cr(CO)_5$ according to the solvent and the incoming nucleophile (L) are presented in Table XXXI.

It is noted that the mechanistic accessibility of dissociative (D) and interchange (I) pathways are related to the type of solvent-Cr bonding in the $(solv)Cr(CO)_5$ complexes. The "agostic" C-H-Cr interactions in $(HP)Cr(CO)_5$ and other $(alkane)Cr(CO)_5$ species involve "three-center-two-electron" bonds. The observed accessibility of interchange pathway for HP displacement, which involves a "7-coordinate" transition state, may be attributed to the "electron-deficient" nature of the species and the smaller steric demand engendered through "head-on" "agostic" bonding.[20] The observed mechanistic behaviors for BZ and CB displacement further demonstrate the importance of "steric demand" caused by both the coordinating solvents and the incoming nucleophiles. For example, the displacements of BZ by hex and pip take place exclusively via the dissociative pathway, since the corresponding interchange pathway requires a very congested 7-coordinate transition state. This is because of the η^2-bonding mode of BZ and hex to Cr center. The bonding of pip to the Cr center should be more sterically hindered than that of py if one envisions the

interaction of these molecules with Cr $\underline{via}$ lone pairs of electrons on N atoms (Table XXXI). This is evident from the accessibility of the interchange pathway for BZ displacement by py from (BZ)Cr(CO)$_5$. On the other hand, the Cl- "head-on" coordination in (CB)Cr(CO)$_5$, less steric demanding than "C=C" coordination, allows the reaction of (CB)Cr(CO)$_5$ with pip to take place $\underline{via}$ competitive dissociative and interchange pathways.

The larger sizes of Mo and W atoms in (solv)M(CO)$_5$ complexes are much less sterically demanding than is the Cr atom to both coordinating solvents and incoming nucleophiles. Therefore, it was more frequently observed that solvent displacements by L from (solv)Mo(CO)$_5$ and (solv)W(CO)$_5$ take place $\underline{via}$ the interchange pathways.

CHAPTER VI

KINETICS AND MECHANISMS FOR INTERMOLECULAR AND INTRAMOLECULAR SOLVENT DISPLACEMENTS BY OLEFINS FROM cis-(SOLVENT)(L)W(CO)$_4$ (L = CO, PHOSPHINES)

The interactions of olefins at coordinatively unsaturated transition metal centers are important steps in numerous catalytic processes involving transformations of those olefins, e.g. hydrogenation, isomerization, polymerization, metathesis, hydrosilylation and hydroformylation.[1,2] On the other hand, 1-hexene (hex), as a weak and "bulky" incoming nucleophile, has been successfully employed to probe the mechanisms of solvent displacement reaction from (solv)M(CO)$_5$ (M = Cr, Mo, W) transients, where the most extensive kinetics studies have been carried out for M = Cr (Chapter III-V). It was found that displacement of solvent from (solv)Cr(CO)$_5$ species by hex is likely to occur via a dissociative pathway. It was also suggested that for M = Mo, W the solvent displacement reactions tend to take place via an interchange pathway for most incoming nucleophiles, due to the larger atomic sizes and greater effective nuclear charges (Chapter IV, section B.3). However, no detailed mechanistic studies have been done for Mo and W systems.[77]

Introduction of another coordinating ligand (L) to replace one CO group will change both the electronic and steric properties of metal carbonyl complexes, and so influence the solvent-metal interactions in these solvated species. When L (phosphine or phosphite) is <u>cis</u>- to the coordinating solvent, its steric effect, so called "steric acceleration",[60,80,92,146] almost always "forces" the intermolecular solvent displacement to take place <u>via</u> dissociative pathways.

However, previous evidence suggested that the interchange pathway for intermolecular solvent displacement reaction is more likely accessible at high ligand concentrations (Chapter III, section C; Chapter V, section C.2,3). A plausible means for studying an interchange pathway is to investigate intramolecular solvent displacement reactions by employing potentially chelating ligands. For example, in the solvated species <u>cis</u>-(CB)(η^1-P-ol)W(CO)$_4$ (P-ol = Ph$_2$P(CH$_2$)$_n$CH=CH$_2$; n = 1-4),[87] one should expect a high "effective local concentration" of the uncoordinated (C=C) linkage in the potentially chelating bidentate P-ol ligands.[84] Interchange pathways might be accessible in the intramolecular CB displacement to afford (η^3-P-ol)W(CO)$_4$. The high "effective local concentration" is also expected to vary with the chelating ring size, which will also change the accessibility of the interchange pathway.

We will first discuss the solvent displacement by hex from (BZ)W(CO)$_5$ and <u>cis</u>-(CB)(L)W(CO)$_4$ (L = Ph$_2$PMe) to probe the effect of L on solvent-metal interactions. Reactions of <u>cis</u>-(CB)(η^1-P-ol)W(CO)$_4$ to form (η^3-P-ol)W(CO)$_4$ complexes will then be investigated to study "chelating effects" on intramolecular solvent displacement reactions.

A. Mechanisms of Benzene Displacement and Benzene-W Bonding in the (Benzene)W(CO)$_5$ Complex

BZ displacement by hex from (BZ)Cr(CO)$_5$ has been found to take place <u>via</u> a dissociative pathway; and the BZ-Cr(CO)$_5$ bonding was suggested to take place through an "isolated" C=C bond. However, the mechanism of BZ displacement from (BZ)W(CO)$_5$ and the bonding in BZ-W(CO)$_5$ were not fully understood. Stolz, Haas and Sheline suggested, on the basis of carbonyl stretching data in low temperature glasses (-80°C, -180°C), that the bonding in (BZ)W(CO)$_5$ involves the whole aromatic ring.[98] In the same study, they also suggested different types of bonding at low temperature (-180°C) and at room temperature (20°C) for some heterocyclic aromatic systems (furan, thiophene). On the other hand, BZ-W bonding at room temperature has to be studied by employing kinetics techniques due to the thermal instability of (BZ)W(CO)$_5$ complex. To probe these aspects, kinetic studies for reactions of (BZ)W(CO)$_5$ with hex have been carried out.

The pseudo-first-order rate constants obtained after flash photolysis of $W(CO)_6$ in hex/BZ binary solutions at four temperatures are listed in Table XXXII. It is noted, from both the curved plots of k_{obsd} vs [hex]/[BZ] and the linear reciprocal plots of $1/k_{obsd}$ vs [BZ]/[hex] (Figure 31) for these data, that the rates of the reaction are inhibited when [BZ] is increased. Furthermore, the rate constant in the "dilution experiment" by $\underline{n}$-heptane (Table XXXII), for [BZ]/[hex] = 2.502 at 15.0 °C, indicates a slight increase upon dilution (cf Scheme III; Eq. 36, p 124; Eq. 39, 40, p 132). These results are not inconsistent with a dissociative mechanism as described in Scheme IV, for displacement of BZ by hex from $(BZ)W(CO)_5$.

Scheme IV

$$W(CO)_6$$
$$\downarrow hv$$

$$(BZ)W(CO)_5 \underset{k_{-1}[BZ]}{\overset{k_1}{\rightleftharpoons}} [W(CO)_5] \xrightarrow{k_2[hex]} (hex)W(CO)_5$$
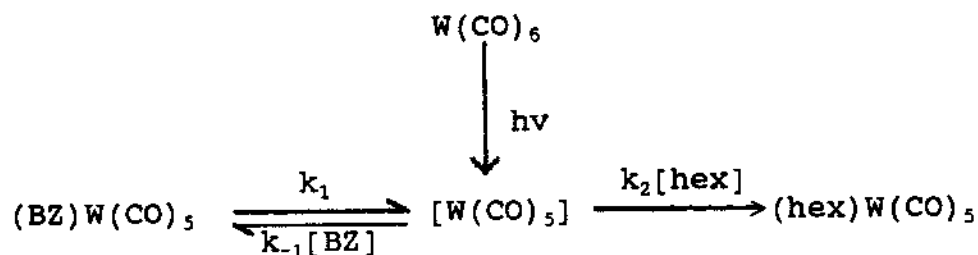
Table XXXIII lists the rate constants of BZ dissociation from $(BZ)W(CO)_5$ (k_1) and "competition ratios" (k_2/k_{-1}) calculated from the values of intercepts and slopes

Table XXXII. Pseudo-first-order Rate Constants for Reactions
Taking Place After Flash Photolysis of $W(CO)_6$ in
hex/BZ Solutions at Various Temperatures

[hex] (M)	[BZ] (M)	$\frac{[BZ]}{[hex]}$	$10^{-2}k_{obsd}$ (s^{-1}) Temp.(°C): 35.0	25.0	15.0	5.0
1.438	9.133	6.351	1.08(6)	0.483(1)	0.23(2)	0.094(6)
			1.1(1)	0.478(2)	0.235(7)	0.094(3)
1.980	8.396	4.241	1.618(4)	0.681(2)	0.3288(3)	0.130(5)
			1.602(3)	0.704(2)	0.3171(4)	0.129(3)
2.867	7.175	2.502	2.54(1)	1.091(2)	0.5172(7)	0.210(9)
			2.68(2)	1.119(3)	0.4969(5)	0.20(1)
0.115	0.287	2.502	(in hex/BZ/HP)		0.61(2)	
4.238	5.269	1.243	4.52(1)	1.982(7)	0.7902(9)	0.31(3)
			4.37(1)	2.063(7)	0.826(1)	0.31(3)
4.646	4.612	0.992	5.53(2)	2.48(1)	1.002(3)	0.421(2)
			5.52(1)	2.39(1)	1.005(1)	0.439(1)
5.166	3.908	0.756	6.64(2)	3.05(1)	1.15(1)	0.528(2)
			6.68(2)	3.01(1)	1.18(2)	0.532(3)
5.867	2.923	0.505	8.25(7)	3.55(1)	1.314(3)	0.562(1)
			8.21(2)	3.72(2)	1.467(5)	0.533(1)
6.783	1.643	0.242	10.3(5)	4.82(1)	2.30(2)	0.867(3)
			10.6(3)	4.78(1)	2.17(2)	0.913(3)
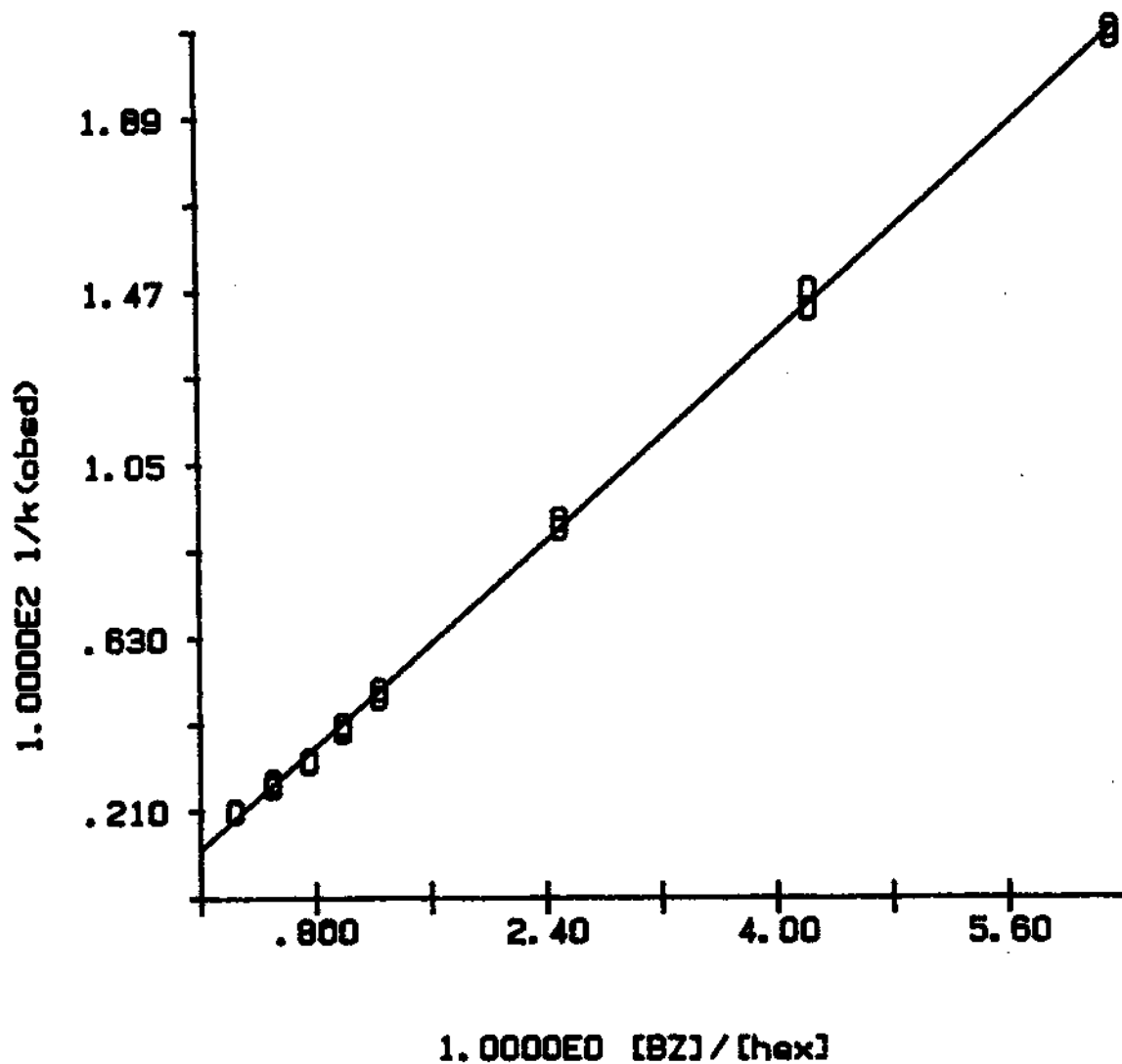
Figure 31. Plots of 1/k_{obsd} vs [BZ]/[hex] for reaction taking place after flash photolysis of W(CO)$_6$ in hex/BZ solutions at 25.0 °C.

of the reciprocal plots (Figure 31). The activation

parameters $\Delta H^{\ddagger}_1$ = 14.9(4) kcal/mol and $\Delta S^{\ddagger}_1$ = +4.8(13)

cal/(deg mol), for BZ dissociation are consistent with the

dissociative mechanism (Scheme I).

Comparisons of activation parameters in Table XXXIII

with that in Table VIII for (BZ)Cr(CO)$_5$ reactions raise some

interesting points.

Table XXXIII. The Rate Constants and Activation Parameters
for Reactions of (BZ)W(CO)$_5$ with hex at Various
Temperatures

Temp. (°C)	$10^{-2}k_1^{a)}$ (s^{-1})	$k_2/k_{-1}^{b)}$
35.0	18.3(10)	0.41(3)
25.0	8.2(5)	0.40(3)
15.0	3.0(3)	0.51(5)
5.0	1.23(9)	0.51(6)

a) $\Delta H^{\ddagger}_1$ = 14.9(4) kcal/mol;

  $\Delta S^{\ddagger}_1$ = +4.8(13) cal/(deg mol).

b) $\Delta H^{\ddagger}_2 - \Delta H^{\ddagger}_{-1}$ = -1.5(6) kcal/mol;

  $\Delta S^{\ddagger}_2 - \Delta S^{\ddagger}_{-1}$ = -6.9(20) cal/(deg mol).

(i) The BZ-W bond strength is <u>ca.</u> 5-7 kcal/mol stronger than the BZ-Cr bond which is consistent with the general trend observed for group VIB metals.[13]

(ii) The entropy of activation for BZ dissociation from $(BZ)W(CO)_5$ is not too different from $(BZ)Cr(CO)_5$, which might suggest somewhat similar bonding interactions in the transition states for BZ dissociation from these two metal centers. This result is not inconsistent with a ground-state BZ-W interaction involves the whole aromatic ring, <u>via</u> A_{2u}, the lower occupied π orbital in benzene ring, and the d_{z^2} orbital from W atom.[98]

(iii) The comparative activation parameters, $\Delta H^{\dagger}_2 - \Delta H^{\dagger}_{-1} = -1.5(6)$ kcal/mol and $\Delta S^{\dagger}_2 - \Delta S^{\dagger}_{-1} = -6.9(20)$ cal/(deg mol) for W species <u>vs</u> $\Delta H^{\dagger}_2 - \Delta H^{\dagger}_{-1} = +3.0(4)$ kcal/mol and $\Delta S^{\dagger}_2 - \Delta S^{\dagger}_{-1} = +8.8(15)$ cal/(deg mol) for Cr species, indicate the considerably different selectivities of $M(CO)_5$ (M = Cr, W) intermediates between nucleophiles (BZ <u>vs</u> hex).

B. The reaction of cis-(CB)(Ph₂PMe)W(CO)₄ with hex

Studies of this reaction should bridge the previous studies on solvated pentacarbonyl complexes (section A) with the future studies (section C) on intramolecular solvent displacement reactions of <u>cis</u>-(CB)(η^1-P-ol)W(CO)₄. 1-Hexene was chosen as an "ideal" nucleophile not only because of its successful role in previous studies but also because it

resembles the terminal olefins in potential chelating ligand (P-ol's). The Ph$_2$PMe also resembles the P-ol's series from the point of view of its shortest alkane chain (cf Table I).

The calculated pseudo-first-order rate constants, k$_{obsd}$, obtained after flash photolysis in hex/CB mixtures at various temperatures and pressures are collected in Table XXXIV. Previous flash photolysis studies have demonstrated, by kinetic infrared spectroscopy[60] and through kinetics results,[80] that upon photolysis of cis-(pip)(L)W(CO)$_4$ complexes (L = phosphines, phosphites), two solvated species, cis-(solv)(L)W(CO)$_4$ and trans-(solv)(L)W(CO)$_4$ are produced. The trans isomer reacts much more slowly than its cis analogues.[60,80,92,146] On the ms time-scale employed in present studies, reaction of cis-(CB)(L)W(CO)$_4$ with hex is observed, while the trans isomer, not investigated, reacts much more slowly.

The most mechanistic information was obtained for both thermal and pressure studies in hex/CB solutions varying from predominant CB to predominant hex concentrations. The plot of k$_{obsd}$ vs [hex]/[CB] at 25.0 °C exhibits the familiar curvature which goes through the origin. The linear plot of 1/k$_{obsd}$ vs [CB]/[hex] is shown in Figure 32, which is consistent the widely observed dissociative mechanisms (Scheme V) for these solvated substituted carbonyls.[80,92,146]

The rate constant for CB dissociation from cis-(CB)(Ph$_2$PMe)W(CO)$_4$ (k$_1$) and the competition ratio (k$_2$/k$_{-1}$) can

Table XXXIV. Pseudo-first-order Rate Constants for Reactions
in hex/CB Mixtures Taking Place After Flash Photolysis
of <u>cis</u>-(pip)(Ph$_2$PMe)W(CO)$_4$ at various Temperatures
and Pressures

Temp. (°C)	Press. (atm)	[CB] (M)	[hex] (M)	$10^{-3}k_{obsd}$ (s^{-1})
5.5	1	5.875	3.116	2.25(5)
		5.549	3.449	2.45(5)
		4.431	4.389	3.72(28)
		2.760	5.727	5.58(8)
25.0		8.053	1.437	4.70(10)
		7.643	1.775	6.08(4)
		6.858	2.416	8.58(8)
		5.464	3.543	14.6(4)
		2.855	5.645	29.6(2)
35.3	50	6.147	2.992	22.6(10)
		5.377	3.644	30.2(10)
		4.347	4.457	37.9(11)
		2.778	5.738	58.4(11)
		1.361	6.815	79.0(27)
	500	6.147	2.992	18.2(6)
		5.377	3.644	23.6(11)
		4.347	4.457	31.3(24)
		2.778	5.738	48.1(14)
		1.361	6.815	62.0(68)
	1000	6.147	2.992	15.1(8)
		5.377	3.644	19.6(2)
		4.347	4.457	26.3(15)
		2.778	5.738	38.3(11)
		1.361	6.815	51.8(7)
	1500	6.147	2.992	13.9(2)
		5.377	3.644	16.6(4)
		4.347	4.457	21.6(16)
		2.778	5.738	32.7(17)
		1.361	6.815	43.8(19)
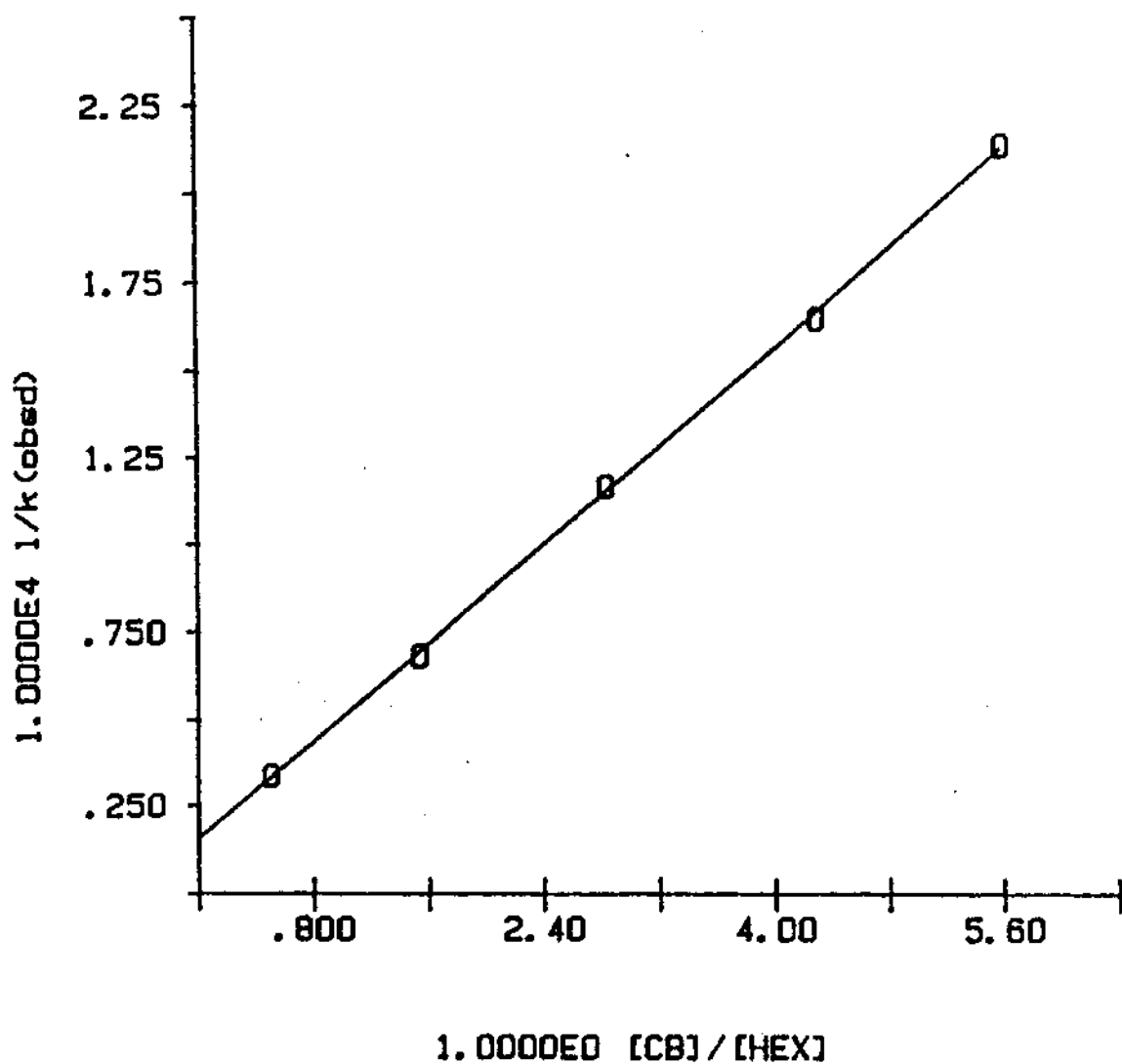
Figure 32. Plots of $1/k_{obsd}$ vs [CB]/[hex] for reaction
taking place after flash photolysis of
cis-(pip)(Ph$_2$PMe)W(CO)$_4$ in hex/CB solutions at 25.0 °C.

Scheme V
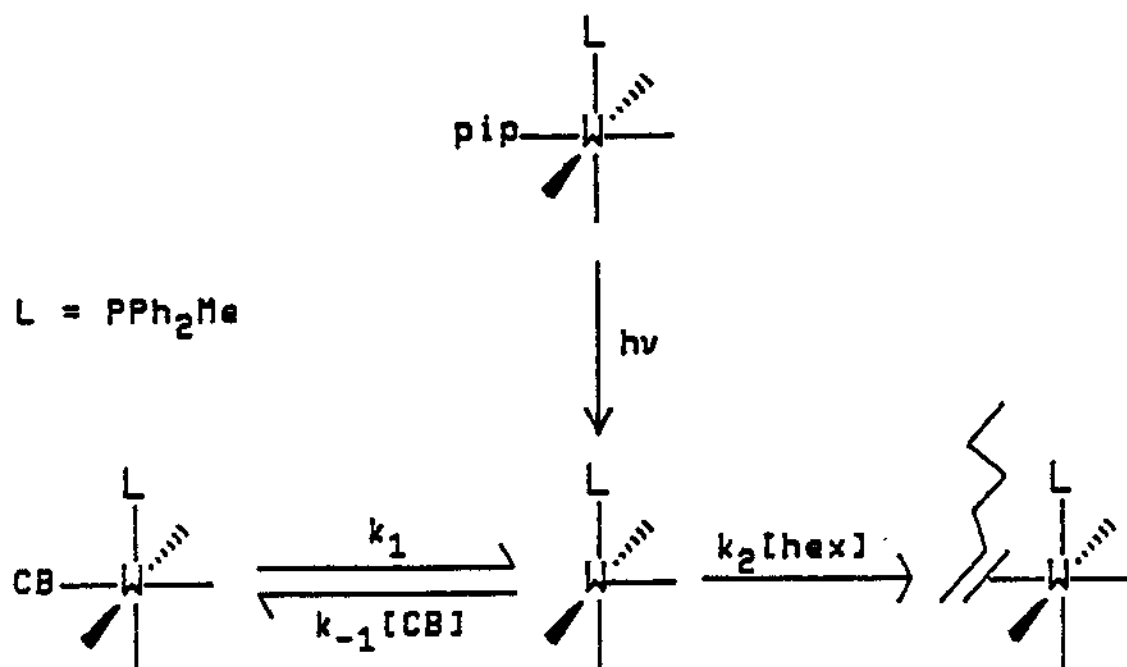
L = PPh$_2$Me

The rate constant for CB dissociation from cis-(CB)(Ph$_2$PMe)W(CO)$_4$ (k_1) and the competition ratio (k_2/k_{-1}) can be calculated from values of the intercept and slope of plots of $1/k_{obsd}$ vs [CB]/[hex] (cf Eq. 7, p 43). However, for more accurate determination of k_1 values, which is calculated from the intercept, solutions with ratios of [CB]/[hex] less than 2 were employed in the studies with different temperatures and pressures. The calculated rate constants and corresponding activation parameters are presented in Table XXXV.

Table XXXV. Rate Constants at Various Temperatures and
Pressures and Activation Parameters for Reactions
of $\underline{cis}$-(CB)(PPh$_2$Me)W(CO)$_4$ with hex

Temp. (°C)	Press. (atm)	$10^{-4}(k_1k_2/k_{-1})$ (s^{-1})	$10^{-4}k_1$ (s^{-1})	k_2/k_{-1}
5.5	1	0.51(2)	1.2(2)	0.42(9)
25.0	1	2.81(4)	6.8(7)	0.41(5)
35.3	50	5.9(2)	10.8(7)	0.55(5)
	500	4.7(1)	8.9(5)	0.53(4)
	1000	3.95(5)	7.2(2)	0.55(2)
	1500	3.41(4)	5.9(2)	0.58(3)

$\Delta H^{\ddagger}_1$ = 12.1(8) kcal/mol

$\Delta S^{\ddagger}_1$ = +3.8(26) cal/(deg mol)

$\Delta V^{\ddagger}_1$ = +10.7(2) cm^3/mol

$\Delta H^{\ddagger}_1 + \Delta H^{\ddagger}_2 - \Delta H^{\ddagger}_{-1}$ = 13.6(3) kcal/mol

$\Delta S^{\ddagger}_1 + \Delta S^{\ddagger}_2 - \Delta S^{\ddagger}_{-1}$ = +7.3(10) cal/(deg mol)

$\Delta V^{\ddagger}_1 + \Delta V^{\ddagger}_2 - \Delta V^{\ddagger}_{-1}$ = +9.7(8) cm^3/mol

$\Delta H^{\ddagger}_2 - \Delta H^{\ddagger}_{-1}$ = 1.5(11) kcal/mol

$\Delta S^{\ddagger}_2 - \Delta S^{\ddagger}_{-1}$ = +3.5(36) cal/(deg mol)

$\Delta V^{\ddagger}_2 - \Delta V^{\ddagger}_{-1}$ = -1.0(10) cm^3/mol

The observed positive volume of activation for CB dissociation $\Delta V^{\ddagger}_1 = +10.7(2)$ cm^3/mol further supports the dissociative mechanism. However, the relatively small entropy of activation ($\Delta S^{\ddagger}_1 = +3.8(26)$ cal/(deg mol)) resembles the behavior observed for (BZ)Cr(CO)$_5$ studied in Chapter III (section C, D). This may suggest the CB-W bonding via an "isolated" double bond in cis-(CB)(L)W(CO)$_4$ complex, instead of the bonding in (CB)-Cr(CO)$_5$ via Cl atom, since in the later case larger positive entropies of activation were observed (Table XXVIII). These differences seem to arise from the steric influences of substituted ligand (L) and the sizes of metal centers.

In this event, the lower value of enthalpy of activation for CB dissociation from cis-(CB)(Ph$_2$PMe)W(CO)$_4$, $\Delta H^{\ddagger}_1 = 12.1(8)$ kcal/mol (Table XXXV), compared to that of BZ dissociation from (BZ)W(CO)$_5$ (14.9(4) kcal/mol) may be attributed to several causes: (i) The steric and electronic effects from the cis- coordinating ligand which will weaken the CB-W bond; (ii) the different bonding mode as a result of (i); (iii) the electron withdrawing nature of Cl atom which reduces the electron density in CB ring system and so weakens the CB-W interaction if the bonding is through an "isolated" double bond.

It is noted that the comparative activation parameters, $\Delta A^{\ddagger}_2 - \Delta A^{\ddagger}_{-1}$ (A = H, S, V), all afforded small values (Table XXXV), indicating the poor distinguishability

of <u>cis</u>-vacant [(L)W(CO)$_4$] species between the nucleophiles (hex and CB). Therefore values of ($\Delta A^{\dagger}_1$ + $\Delta A^{\dagger}_2$ - $\Delta A^{\dagger}_{-1}$) can be considered to be very close to $\Delta A^{\dagger}_1$.

C. Mechanisms of CB Displacement <u>via</u> Chelate Ring-Closure in <u>cis</u>-(CB)(η^1-P-ol)W(CO)$_4$ Transients

1. Formation of cis-(CB)(η^1-P-ol)W(CO)$_4$ transients

Ring-displacement and ring-closure reactions, related to bidentate complexes (L-L)M(CO)$_4$ (L = P, As, S, N, C=C), constitute an important area in organometallic reactions. Their kinetics and mechanisms have been extensively studied.[13,147-149] Intermolecular (bimolecular) and intramolecular (unimolecular) solvent displacement reactions in <u>cis</u>-(solv)(L'-L")W(CO)$_4$ species also have been observed for several systems.[87,150-152] It was found that the solvated species, <u>cis</u>-(solv)(η^1-L'-L")W(CO)$_4$, generated after flash photolysis of <u>cis</u>-(pip)(η^1-L'-L")W(CO)$_4$ or (η^2L'-L")W(CO)$_4$ (L' = P; L" = N), (η^3L'-L")W(CO)$_4$ (L' = P; L" = C=C), reacted according to rate law described in Eq. 47 in the presence of an incoming nucleophile (L).

$$\text{Rate} = (k_{rc} + k_{bm}[L])[\text{cis-(solv)}(\eta^1\text{-L'-L")W(CO)}_4] \qquad (47)$$

Thus, $k_{obsd} = k_{rc} + k_{bm}[L]$ (48)

Where k_{rc} and k_{bm} are the first (or pseudo-first-order) rate constant for ring-closure reaction and the second-order rate constant for "bimolecular" solvent displacement reaction respectively (Scheme VI).

As shown in Scheme VI, cis-(solv)$(\eta^1$-L'-L")W(CO)$_4$ species can be generated by either flash photolysis of cis-(pip)$(\eta^1$-L'-L")W(CO)$_4$ or the ring-closed (L'-L")W(CO)4 complexes when L' = P and L" = N or C=C. In other words, photolysis of these complexes will lead to N-W or olefin-W bond fission instead of P-W or OC-W bond fission in these complexes.[60,80,87,145,150-152] The mechanisms of the intermolecular solvent displacement reaction, governed by k_{bm}, were found to be dissociative in nature (vide supra), whereas the mechanism for intramolecular solvent displacement via chelate ring-closure, governed by k_{rc} was not fully understood.

Studies of cis-(CB)$(\eta^1$-P-ol)W(CO)$_4$ (P-ol = Ph$_2$P(CH$_2$)$_n$CH=CH$_2$; n = 1-4) were carried out by employing flash photolysis of cis-(pip)$(\eta^1$-P-ol)W(CO)$_4$, where P-ol = HDPP (n = 4), PDPP (n = 3), PRDPP (n = 1) and $(\eta^3$-BDPP)W(CO)$_4$ (n = 2) (see Table I).

Figure 33 shows a typical kinetics traces of absorbance vs time, monitoring 470 nm, after flash

Scheme VI
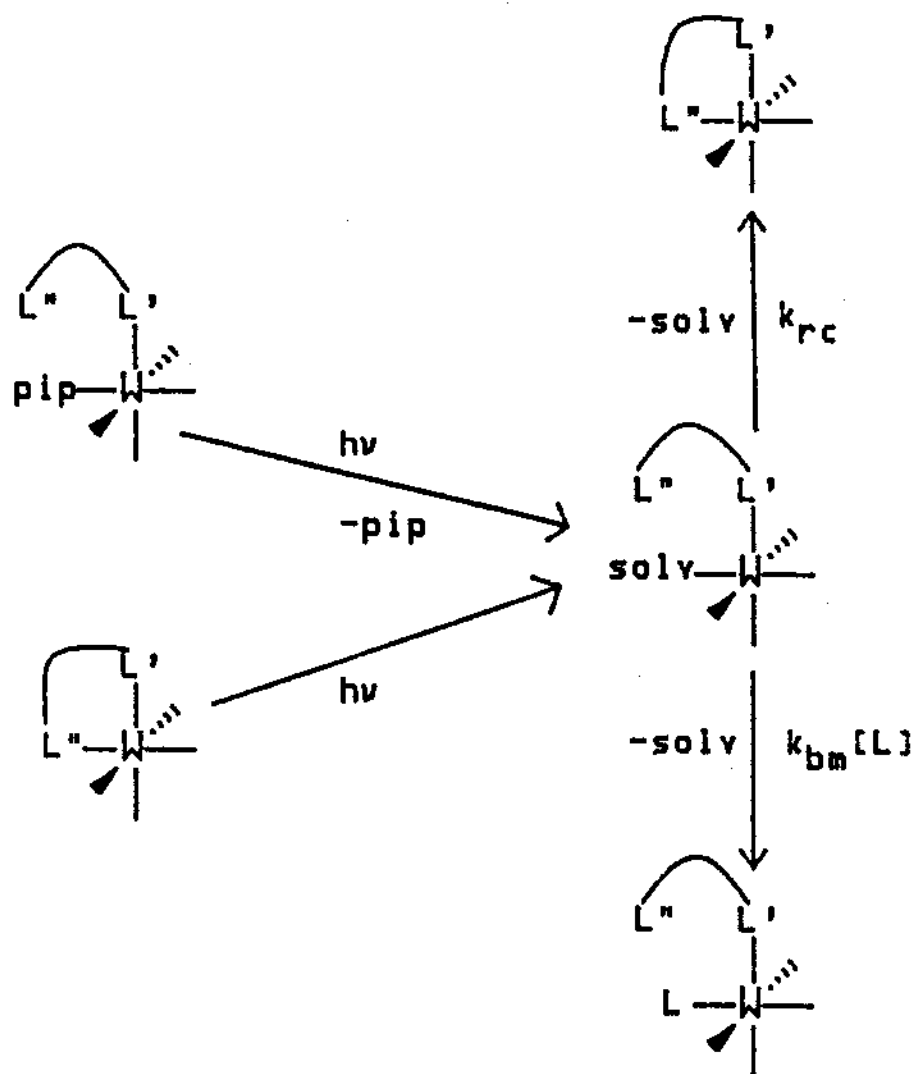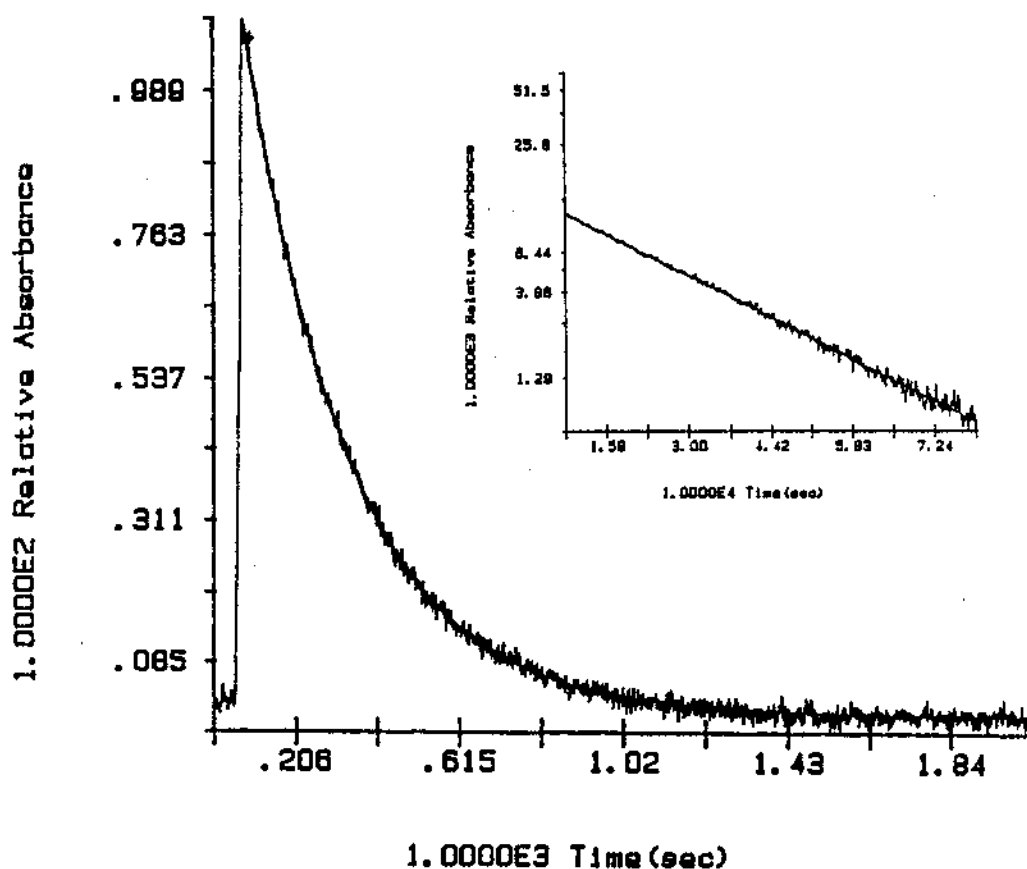
Figure 33. Plot of absorbance vs time, monitoring 470 nm, for reaction taking place after flash photolysis of cis-(pip)(η^1-HDPP)W(CO)$_4$ in CB solution at 25.0 °C; The inset shows a plot of ln (A$_t$ - A$_\infty$) vs time.

photolysis of cis-(pip)(HDPP)W(CO)$_4$ in CB solution at 25.0
°C. The inset shows this decay plotted as ln (A$_t$ - A$_\infty$) vs t.
Such traces exhibit pseudo-first-order kinetics behavior.
The ring-closed reaction products for these reactions, (η^3-
P-ol)W(CO)$_4$, have been previously identified through NMR and
IR spectroscopy.[87]

2. Possible mechanistic pathways

The two possible pathways for intramolecular CB
displacement are dissociative and interchange pathways which
are illustrated in Scheme VII.

Scheme VII

dissociative pathway

interchange pathway
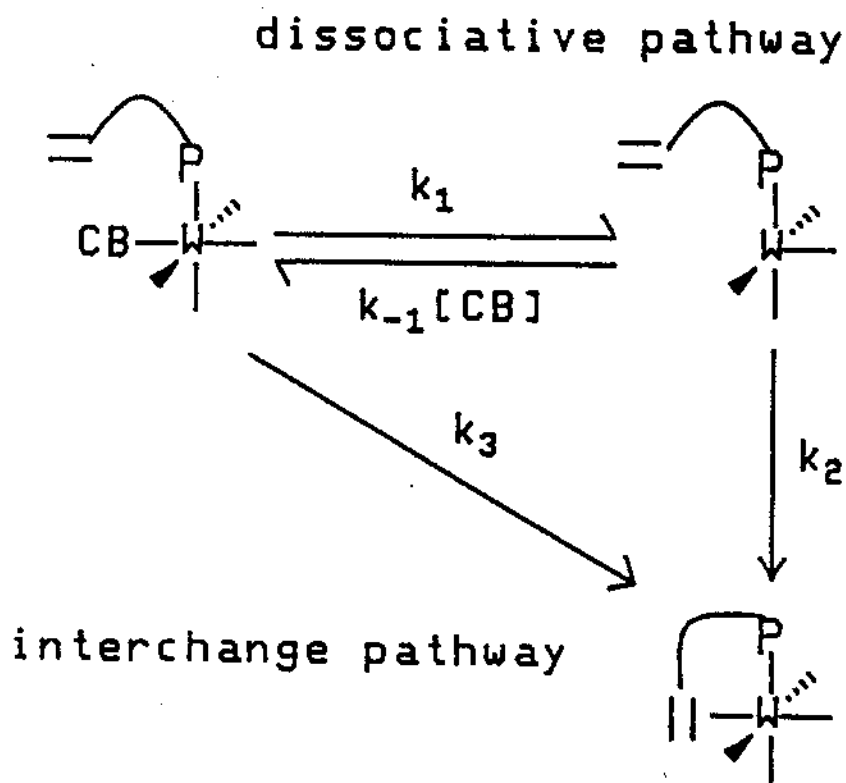
For a dissociative pathway, as in the case of cis-
(CB)(Ph$_2$PMe)W(CO)$_4$ reacting with hex, the rate law should
obey Eq. 49 or 50:

$$k_{obsd} = \frac{k_1 k_2}{k_{-1}[CB] + k_2} \tag{49}$$

$$\frac{1}{k_{obsd}} = \frac{1}{k_1} + \frac{k_{-1}}{k_1 k_2}[CB] \tag{50}$$

For an interchange pathway, the rate constant is simply k$_3$,
i.e.

$$k_{obsd} = k_3 \tag{51}$$

To investigate these two pathways the solvent
concentration ([CB]) has to be varied. However, the only way
to achieve this is to introduce another "inert" solvent even
though there might be some complications. We chose
n-heptane again. The corresponding possible reaction
pathways in CB/HP solutions can be illustrated in Scheme
VIII. While the rate for the interchange pathway is
unchanged (Eq. 51), the pseudo-first-order rate constant for
the dissociative pathway is related to the concentrations of
solvents as in Eq. 52 which is similar to Eq. 50.

$$\frac{1}{k_{obsd}} = \frac{1}{k_1} + \frac{k_{-1}}{k_1(k_2 + k'_4[HP])}[CB] \tag{52}$$

where $k'_4 = \dfrac{k_4 k_5}{k_{-4} + k_5}$ \hfill (53)

In deriving these rate law expressions, steady-state assumptions were made for $(\eta^1\text{-P-ol})W(CO)_4$ and cis-$(HP)(\eta^1\text{-P-ol})W(CO)_4$ intermediates (cf Chapter V, section B). However, $k'_4[HP] < k_2$ was found to be true for similar systems (Chapter V, section B); the present results also indicate that k_{obsd} varies as a function of [CB] and seems independent of [HP] (vide infra), which suggest that $k'_4[HP]$ term is not important in Eq. 52. For this reason, we will assume, at this moment, Eq. 49 and 50 operate for the dissociative pathways.

Scheme VIII
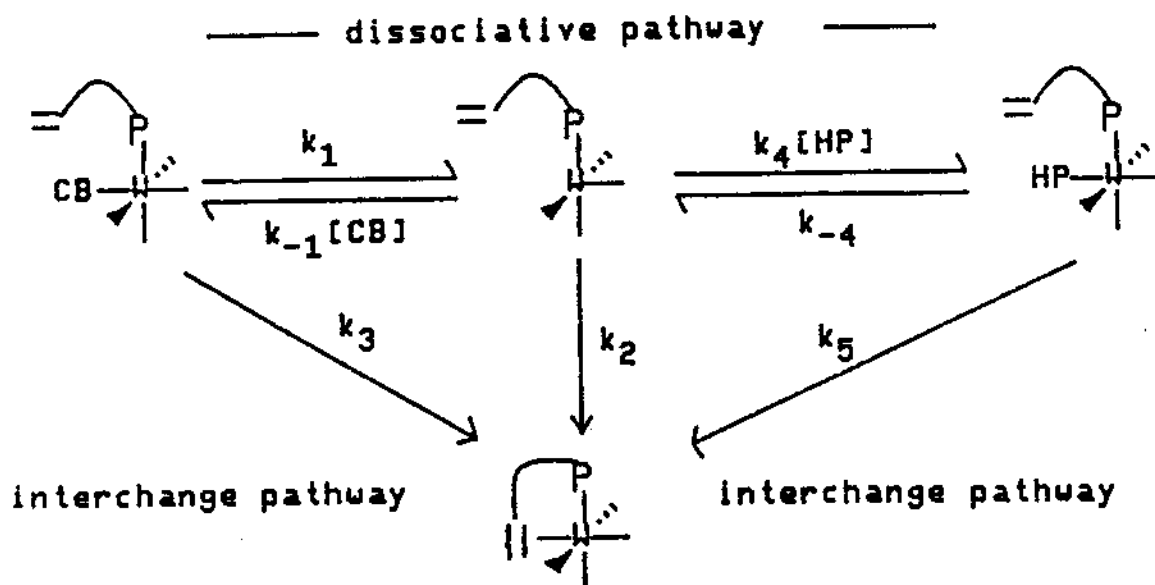
3. The kinetics behavior and reaction rate laws

Table XXXVI lists the calculated pseudo-first-order rate constants for reactions of cis-(CB)$(\eta^1$-P-ol)W(CO)$_4$ at various [CB], temperatures, and pressures. To obtain the maximum mechanistic information, the CB displacement reactions from cis-(CB)$(\eta^1$-P-ol)W(CO)$_4$ were carried out over a wide range of CB concentrations.

Plots of k_{obsd} vs 1/[CB] for reactions of four complexes at 25.0 °C are shown in Figure 34, which all exhibit different degrees of curvature. This might be suggestive of a mechanism consisting of one or more reversible steps such as the dissociative pathway in Scheme VII. Thus, according to Eq. 50, plots of 1/k_{obsd} vs [CB] are expected to be linear. However, these reciprocal plots were found not to be linear, as expected for a dissociative mechanism (Figure 35). To understand this behavior, the data were also plotted in another form, i.e., k_{obsd} vs [CB], which are shown in Figure 36. It seems that when [CB] $-->$ ∞, k_{obsd} approach a non-zero constant which is independent of [CB].

The rough forms of these plots, however, are consistent with a mechanism involving both dissociative and interchange pathways in Scheme VII, i.e. the competitive intramolecular solvent displacement mechanisms. The rate law should be a combination of Eq. 49 and 51:

Table XXXVI. Pseudo-first-order Rate Constants Obtained
After Flash Photolysis of <u>cis</u>-(pip)(η^1-P-ol)W(CO)$_4$
(P-ol = HDPP, PDPP, PRDPP) and (η^3-BDPP)W(CO)$_4$ in
CB ([CB]$_o$ = 9.73 M) and CB/HP Mixtures at Various
Temperatures and Pressures

Complexes	Temp. ($^{\circ}$C)	Press. (atm)	[CB] (M)	$10^{-3}k_{obsd}$ (s^{-1})
HDPP	5.5	1	9.73	0.66(4)
			8.65	0.76(8)
			8.00	0.77(6)
			6.94	0.86(3)
			5.11	1.04(3)
	14.5		9.73	1.61(8)
			8.65	1.75(4)
			8.00	1.81(4)
			6.94	1.93(2)
			5.11	2.35(6)
	25.0		9.73	3.79(6)
			8.58	4.07(4)
			7.43	4.51(2)
			6.28	4.95(12)
			5.08	5.71(7)
			3.90	6.8(2)
			2.77	8.3(5)
			1.58	12.1(3)
			0.415	30.2(8)
	35.3	50	9.73	7.47(4)
			8.40	8.13(12)
			7.35	8.67(16)
			6.54	9.61(20)
			5.09	11.46(29)
		500	9.73	6.13(1)
			8.40	6.69(20)
			7.35	7.33(9)
			6.54	7.77(11)
			5.09	9.31(14)
		1000	9.73	5.00(10)
			8.40	5.60(13)
			7.35	5.85(11)
			6.54	6.23(8)

Table XXXVI. Continued

Complexes	Temp. (°C)	Press. (atm)	[CB] (M)	$10^{-3}k_{obsd}$ (s^{-1})
			5.09	7.56(14)
		1500	9.73	4.13(9)
			8.40	4.34(15)
			7.35	4.91(12)
			6.54	5.24(8)
			5.09	5.94(12)
PDPP	5.5	1	9.73	0.435(1)
			8.65	0.467(2)
			8.00	0.486(6)
			6.94	0.531(15)
			5.11	0.646(6)
	14.5		9.73	1.06(4)
			8.65	1.14(6)
			8.00	1.18(7)
			6.94	1.29(2)
			5.11	1.56(1)
	25.0		9.73	2.67(4)
			8.58	2.86(3)
			7.43	3.15(10)
			6.28	3.48(10)
			5.08	4.05(14)
			3.90	4.59(4)
			2.77	5.66(2)
			1.58	8.34(7)
			0.415	22.11(16)
	35.3	50	9.73	5.33(14)
		500		4.15(20)
		1000		3.51(6)
		1500		2.87(2)
BDPP	5.5	1	9.73	1.779(3)
			8.65	1.811(4)
			6.94	1.907(3)
			5.11	1.981(6)
	14.5		9.73	3.49(8)
			8.65	3.557(4)
			8.00	3.63(12)
			6.94	3.77(7)
			5.11	4.01(28)
	25.0		9.73	7.93(4)
			8.58	8.11(2)
			7.43	8.37(6)
			6.28	8.60(8)

Table XXXVI. Continued

Complexes	Temp. (°C)	Press. (atm)	[CB] (M)	$10^{-3}k_{obsd}$ (s^{-1})
			5.08	8.98(2)
			3.90	9.84(4)
			2.77	10.73(4)
			1.58	14.0(2)
			0.415	31.2(15)
	35.3	50	9.73	15.1(7)
		500		13.8(5)
		1000		12.5(5)
		1500		11.3(9)
PRDPP	5.5	1	9.73	4.32(12)
			8.00	4.52(2)
			6.94	4.79(1)
			5.11	5.22(3)
	25.0		9.73	20.17(7)
			8.58	21.2(4)
			7.43	21.9(2)
			6.28	23.60(3)
			5.08	25.3(6)
			3.90	27.6(7)
			2.77	32.1(2)
			1.58	42.2(5)
			0.415	93.8(36)
	35.3	50	9.73	38.4(6)
			8.52	39.7(7)
			7.42	43.0(11)
			6.38	47.5(7)
			5.07	50.4(13)
		500	9.73	31.6(10)
			8.52	34.5(4)
			7.42	34.6(8)
			6.38	37.9(22)
			5.07	41.5(21)
		1000	9.73	27.9(8)
			8.52	29.8(11)
			7.42	32.0(14)
			6.38	32.6(5)
			5.07	35.5(15)
		1500	9.73	24.6(6)
			8.52	25.4(19)
			7.42	25.8(9)
			6.38	27.0(11)
			5.07	29.7(32)
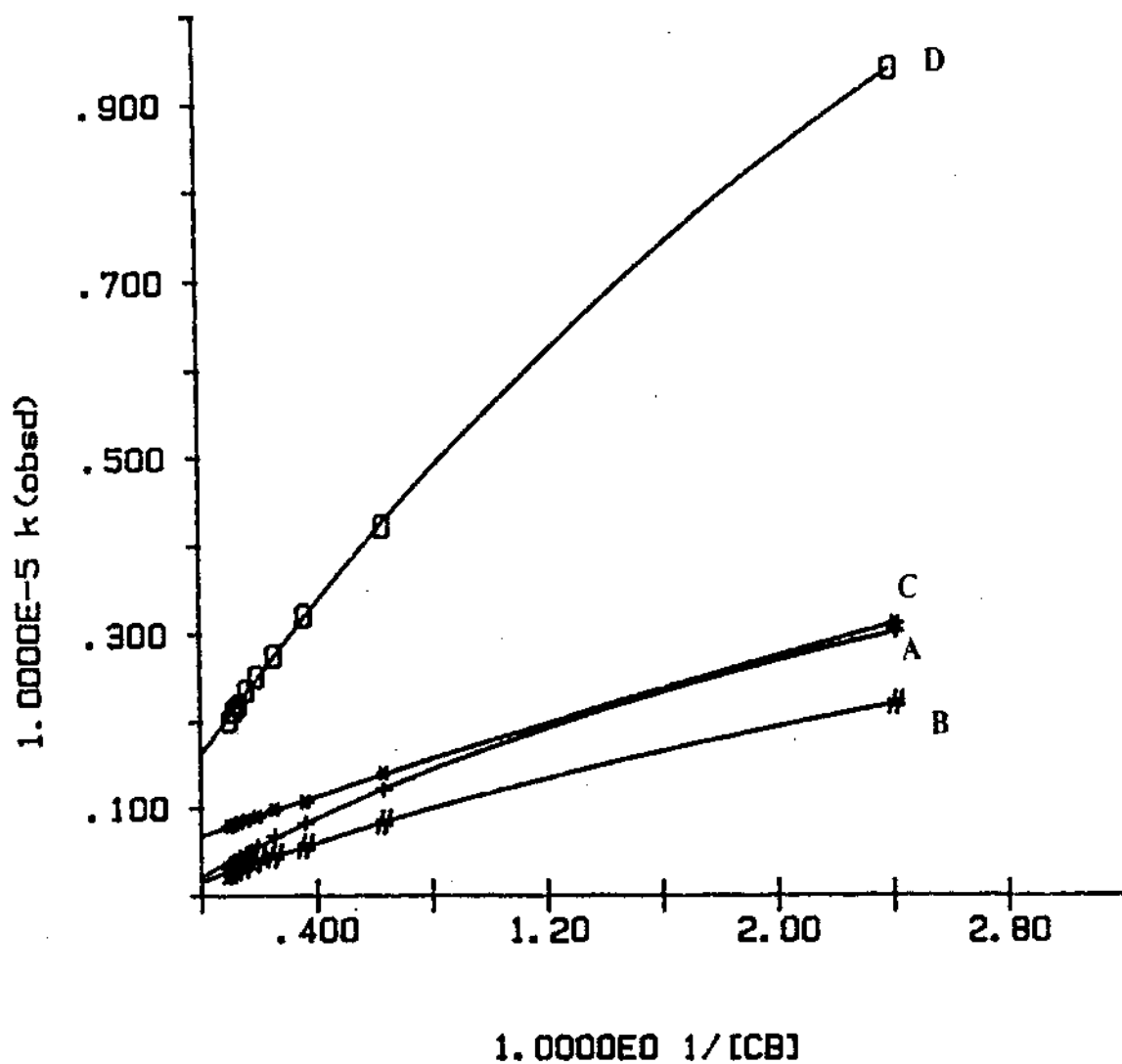
Figure 34. Plots of k_{obsd} vs 1/[CB] for reactions of cis-(CB)(η^1-P-ol)W(CO)$_4$ in CB/HP solutions at 25.0 °C. P-ol = HDPP (A), PDPP (B), BDPP (C), PRDPP (D).
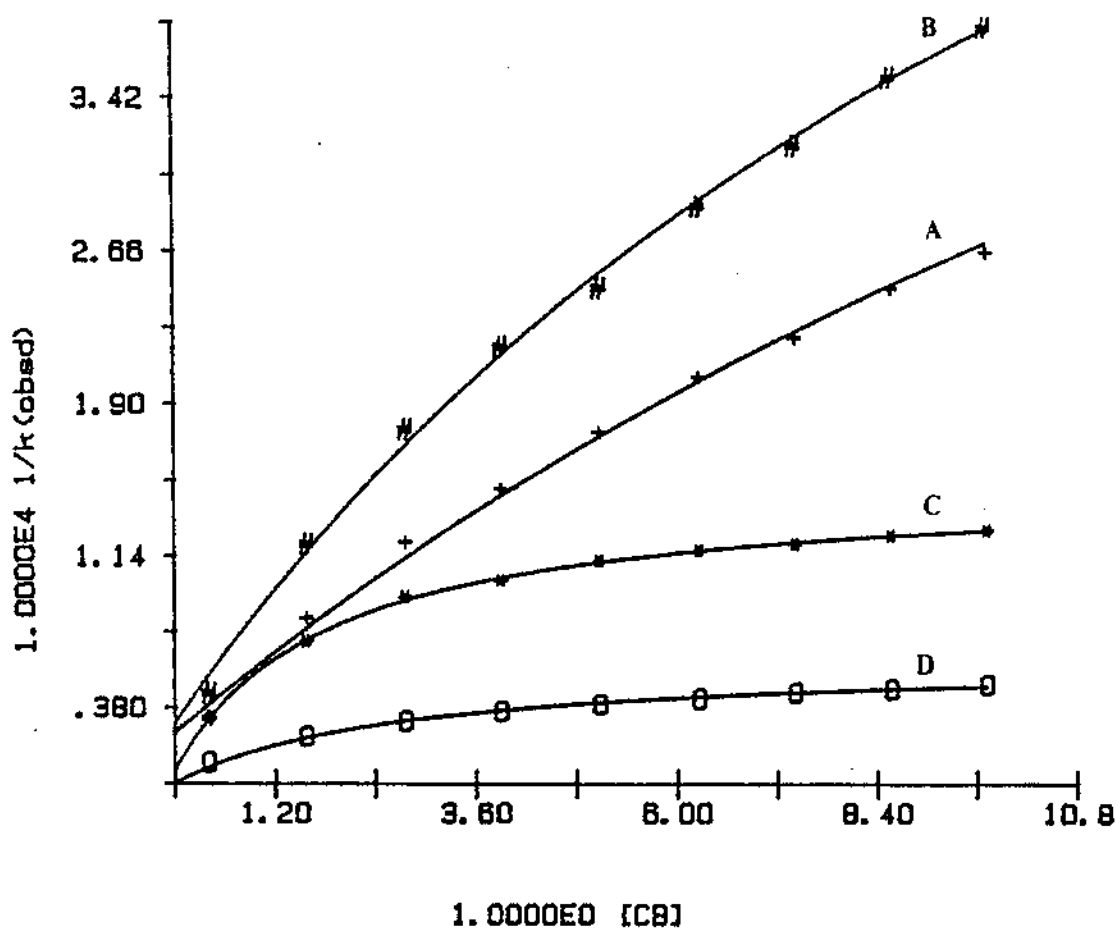
Figure 35. Plots of $1/k_{obsd}$ vs [CB] for reactions of cis-(CB)(η^1-P-ol)W(CO)$_4$ in CB/HP solutions at 25.0 °C. P-ol = HDPP (A), PDPP (B), BDPP (C), PRDPP (D).
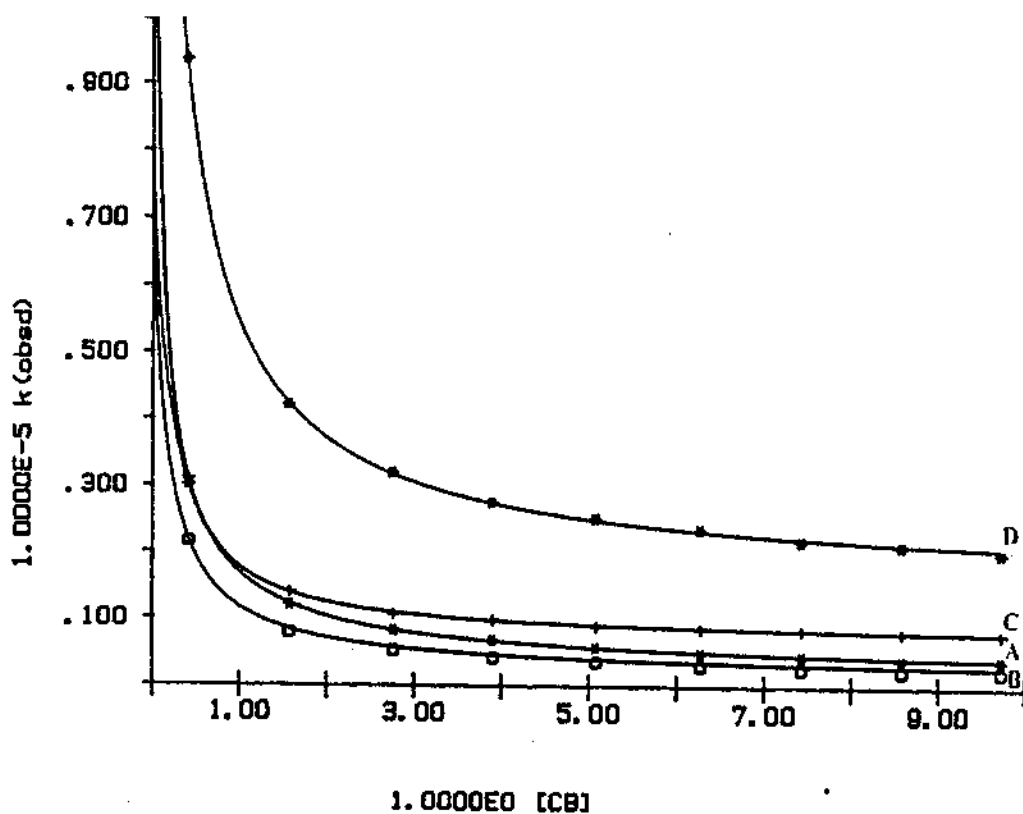
Figure 36. Plots of k_{obsd} vs [CB] for reactions of
cis-(CB)(η^1-P-ol)W(CO)$_4$ in CB/HP solutions at 25.0 °C.
P-ol = HDPP (A), PDPP (B), BDPP (C), PRDPP (D).

$$k_{obsd} = k_3 + \frac{k_1 k_2}{k_{-1}[CB] + k_2} \qquad (54)$$

or

$$\frac{1}{k_{obsd} - k_3} = \frac{1}{k_1} + \frac{k_{-1}}{k_1 k_2}[CB] \qquad (55)$$

In order to determine whether or not the reaction obeys the rate law Eq. 54 or 55, $1/(k_{obsd} - k_3)$ was plotted against [CB] where values of k_3 were determined through a computer fitting procedure so that the best linear correlation coefficients were obtained for these plots. Figure 37a-d illustrate the comparisons of plots of $1/(k_{obsd} - k_3)$ vs [CB] and $1/k_{obsd}$ vs [CB] for all the complexes. The fact that such linear plots can be obtained, not only strongly supports the competitive mechanisms (Scheme VI), but also enable estimate of the rate constants k_3, k_1, and "competition ratios" (k_2/k_{-1}) according to Eq. 55. For all the complexes, the intercept is very small (Figure 37c) and therefore the error is too great for calculating accurate k_1 and k_2/k_{-1} values. However, for HDPP, PDPP and PRDPP complexes, the k_2/k_{-1} values at 25.0 °C were estimated to be 0.50(7), 0.47(10) and 0.46(13) respectively, which are almost the same ($\approx 0.48(2)$) within experimental error. These results suggest that the rate of reaction of a C=C linkage attacking at the vacant coordinating site do not depend on the ring-size,
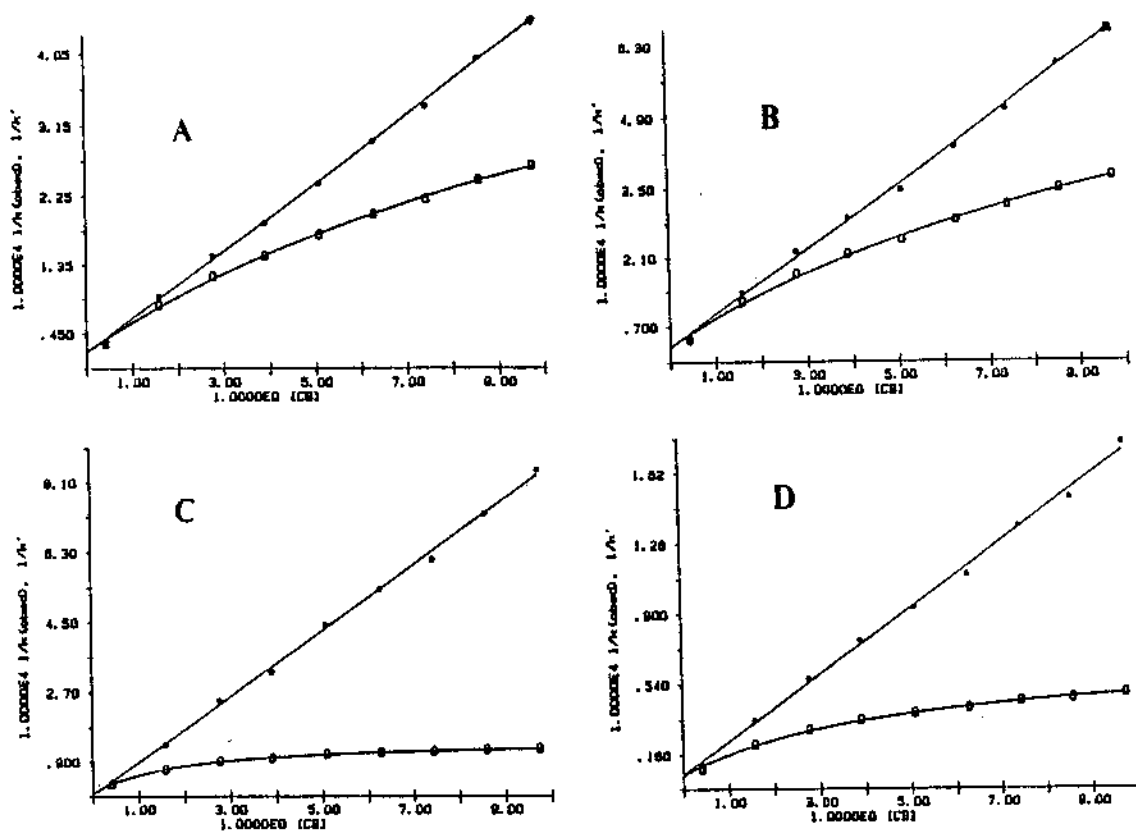
Figure 37. Comparisons of plots of $1/(k_{obsd} - k_3)$ vs [CB] and $1/k_{obsd}$ vs [CB] for reactions of cis-(CB)(η^1-P-ol)W(CO)$_4$ in CB/HP solutions at 25.0 °C. P-ol = HDPP (A), PDPP (B), BDPP (C), PRDPP (D).

indicating little bond formation involved in the transition state of this process. It is not unreasonable to expect that, for BDPP complex, k_2/k_{-1} should have the similar value. Thus the values of $k_1 k_2/k_{-1}$ determined from the slopes of plots of $1/(k_{obsd} - k_3)$ vs [CB] should represent the relative k_1 values (vide infra).

Since $k_2/k_{-1} \approx 0.48$, or $k_{-1} \approx 2k_2$, if we examine Eq. 54, when [CB] is high (> 5 M), $k_{-1}[CB] >> k_2$, Eq. 54 can be simplified to Eq. 56:

$$k_{obsd} = k_3 + \frac{k_1 k_2}{k_{-1}} \frac{1}{[CB]} \qquad (56)$$

The same sets of data as shown in Figure 34, but in the region of [CB] > 5 M ($1/[CB]$ < 0.2 or $k_{-1}[CB]$ > $10k_2$), are fitted as straight lines for plots of k_{obsd} vs $1/[CB]$ and shown in Figure 38. The values of k_3 and $k_1 k_2/k_{-1}$ at 25.0 °C calculated from intercepts and slopes of these plots according Eq. 56, are listed in Table XXXVII together with those values determined from $1/(k_{obsd} - k_3)$ vs [CB] fitting. Comparisons of these rate constants show good agreement considering the experimental errors involved.

It is noteworthy that the data for $[CB]_0 = 9.73$ M (in neat CB) fit into all the rate law expression (Eq. 54-56) which correlated rate constants obtained in CB/HP mixtures. These results indeed indicate $k'_4 \approx 0$ (so $k_5 \approx 0$) in Eq. 52, 53.
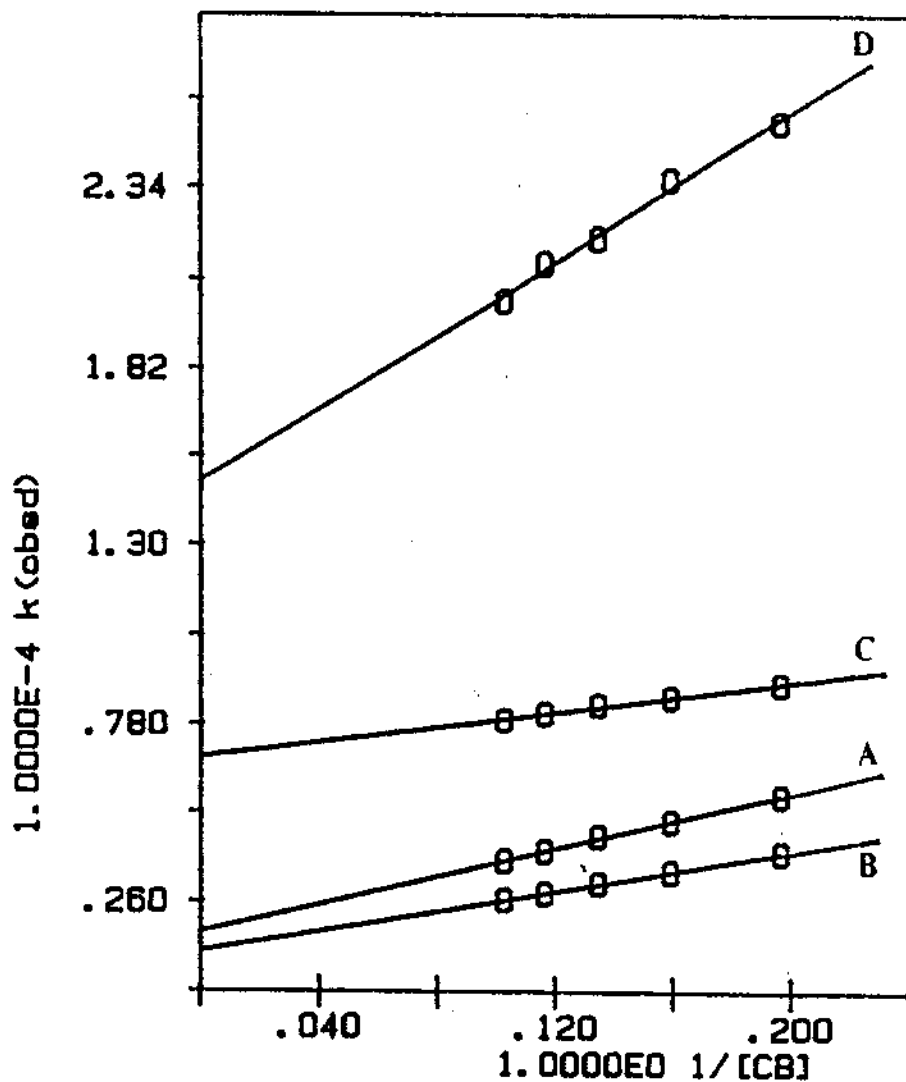
Figure 38. Plots of k_{obsd} vs $1/[CB]$ (when $[CB] > 5$ M) for reactions of cis-$(CB)(\eta^1\text{-P-ol})W(CO)_4$ in CB/HP solutions at 25.0 °C. P-ol = HDPP (A), PDPP (B), BDPP (C), PRDPP (D).

Table XXXVII. Rate Constants at Various Temperatures and Pressures for Reactions of cis-(CB)(η^1-P-ol)W(CO)$_4$ (P-ol = HDPP, PDPP, BDPP, PRDPP)

Complexes	Temp. (°C)	Press. (atm)	$10^{-3}k_3$ (s^{-1})	$10^{-4}(k_1k_2/k_{-1})$ (s^{-1})	$10^{-4}k_1$ (s^{-1})
HDPP	5.5	1	0.28(4)	0.39(3)	----
	14.5		0.83(3)	0.78(2)	----
	25.0		1.72(9)	2.03(6)	----
			1.6[a]	2.29(2)[a]	4.6(6)[a]
	35.3	50	2.99(22)	4.30(15)	----
		500	2.68(11)	3.37(7)	----
		1000	2.31(24)	2.64(16)	----
		1500	2.09(24)	1.99(16)	----
PDPP	5.5	1	0.204(2)	0.266(1)	----
	14.5		0.52(1)	0.535(7)	----
	25.0		1.16(3)	1.47(7)	----
			1.2[a]	1.54(2)[a]	3.2(6)[a]
BDPP	5.5	1	1.57(4)	0.21(3)	----
	14.5		2.92(4)	5.6(3)	----
	25.0		6.82(7)	1.11(5)	----
			6.7[a]	1.18(2)[a]	----
PRDPP	5.5	1	3.26(8)	9.8(6)	----
	25.0		14.8(4)	5.4(3)	----
			14.5[a]	5.9(1)[a]	13(3)[a]
	35.3	50	24.6(24)	13.5(16)	----
		500	21.7(15)	10.1(10)	----
		1000	20.8(14)	7.6(1)	----
		1500	19.0(6)	5.3(4)	----

a) Value calculated from best linear fit for $1/[k_{obsd} - k_3]$ vs [CB] plots.

4. Mechanisms of the reactions and chelating ring-sizes

Values of k_3 and k_1k_2/k_{-1} were also determined from plots of k_{obsd} vs $1/[CB]$ according to Eq. 56 for reactions taking place at other temperatures and pressures to obtain the corresponding activation parameters. These rate constants are listed in Table XXXVII. The calculated rate constants at 25.0 °C and activation parameters are summarized in Table XXXVIII.

The relative rates for CB dissociation, determined according to k_1k_2/k_{-1} in Table XXXVII (vide supra), increase slightly except for PRDPP, as the olefin chain length is increasing in the order of BDPP < PDPP < HDPP. This indicates a steric effect known as "steric acceleration".[60,80,92,146] The "unusual" fast rate for CB dissociation from the PRDPP complex (Table XXXVII, XXXVIII) may suggest that the "nearby" -CH=CH$_2$ group exhibits a specific effect on CB dissociation, either electronically or sterically, or both. One can also visualize an interaction through hydrogen bonded to the sp^2 carbon atom such as is shown in Figure 39a. The faster rate of CB dissociation in cis-(CB)(Ph$_3$P)W(CO)$_4$[80,146] may also be attributed to the similar kind interaction (Figure 39b).

The relative rates for ring closure by direct attack (of the olefin end) at the coordinated CB (k_3) largely depend on the chelate ring sizes formed: PRDPP > BDPP > HDPP

Table XXXVIII. Rate Constants (at 25.0 °C) and Activation Parameters[a] for Reactions of cis-(CB)(η^1-P-ol)W(CO)$_4$ (P-ol = HDPP, PDPP, BDPP, PRDPP)

Complexes	HDPP	PDPP	BDPP	PRDPP
$10^{-3}k_3$ (s^{-1})	1.72(6)	1.16(3)	6.82(7)	14.8(4)
$10^{-4}k_1$ (s^{-1})	4.6(6)	3.2(6)	-----	13(3)
k_2/k_{-1}	0.50(7)	0.47(10)	-----	0.46(13)
R	0.82	0.77	5.99	2.69
C_{inter}%	45%	43%	86%	73%
$\Delta H^\ddagger_3$	12.7(11)	14.1(7)	11.9(6)	11.2(6)
$\Delta S^\ddagger_3$	-1.4(40)	+2.9(23)	-1.2(20)	-2.1(22)
$\Delta V^\ddagger_3$	+6.5(3)	-----	+5.13(1)[b]	+4.4(6)
$\Delta H^\ddagger_1 + \Delta H^\ddagger_2 - \Delta H^\ddagger_{-1}$	13.4(4)	15.3(2)	13.4(13)	14.4(3)
$\Delta S^\ddagger_1 + \Delta S^\ddagger_2 - \Delta S^\ddagger_{-1}$	+6.0(12)	+11.8(8)	+5.2(46)	+11.4(12)
$\Delta V^\ddagger_1 + \Delta V^\ddagger_2 - \Delta V^\ddagger_{-1}$	+13.5(2)	+10.7(8)[b]	-----	+16.2(6)
$\Delta H^\ddagger_{rc}$[c]	13.1(1)	13.7(4)	12.1(1)	13.2(1)

a) Units for activation parameters: H, kcal/mol; S, cal/(deg mol); V, cm^3/mol.
b) Value estimated from ln k_{obsd} vs. P plot.
c) Ref. 87, 150.
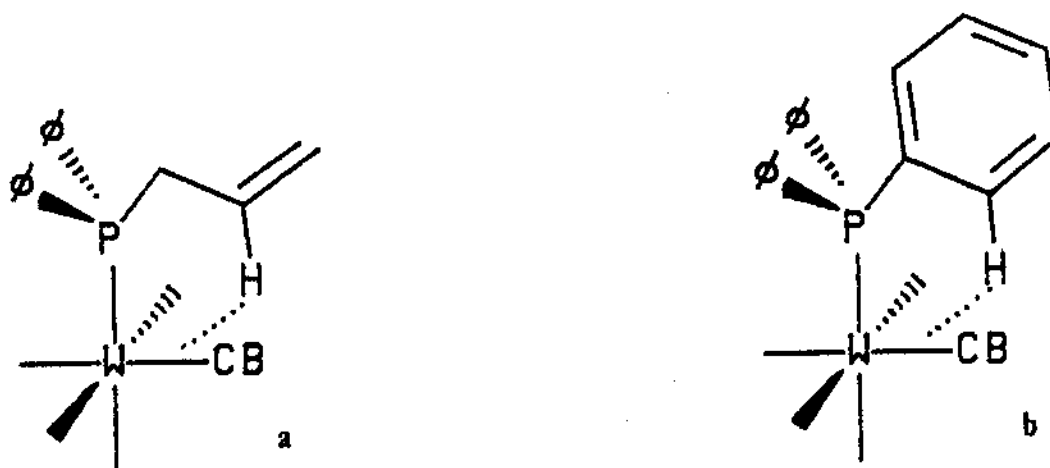
Figure 39. a. The effect of the hydrogen (bonded to sp^2 carbon atom) to CB dissociation in cis-(CB)(η^1-PRDPP)W(CO)$_4$ complex; b. Similar interaction in cis-(CB)(PPh$_3$)W(CO)$_4$ complex.

> PDPP as are shown in Table XXXVIII, which indicate the importance of the chelate bond formation. However, examination of the activation parameters also indicate these ring closure processes are basically dissociative interchange mechanisms (I_d). Therefore, the same factor(s) which influence the CB dissociation (k_1, vide supra) will presumably also influence the W-CB bond breaking in the I_d process. To compare the relative importance of bond formation to afford the chelate ring, it might be better to compare the ratio:

$$R = \frac{k_3}{k_1 k_2 / (k_{-1}[CB]_o)} \tag{57}$$

Since k_2/k_{-1} ratios are almost the same for all the complexes (vide supra), the relative R values actually represent relative k_3/k_1 ratios among different complexes. From these R values (Table XXXVIII), the order of stabilities for various chelate rings is as following:

BDPP(7.8) > PRDPP(3.5) > HDPP(1.1) $\geq$ PDPP(1.0)
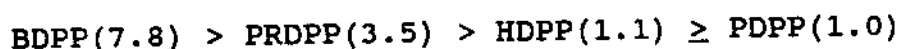
The "five-membered" ring formed from BDPP is the most stable.

The contributions ($C_{inter}\%$) of the interchange pathways to the rates of the overall ring-closure processes in neat CB solutions were also calculated (Table XXXVIII). The order of these values is also a manifestation of the relative importance of the chelate ring-size to the rate of an interchange pathway. The enthalpies of activation ($\Delta H^{\ddagger}_{rc}$; cf Eq. 48) for the overall ring-closure reactions in pip/CB solutions, determined previously by Wang,[87] Wermer, and Dobson,[150] are also listed in Table XXXVIII for comparison. According to Eq. 56, values of $\Delta H^{\ddagger}_3$ as well as ($\Delta H^{\ddagger}_1$ + $\Delta H^{\ddagger}_2$ - $\Delta H^{\ddagger}_{-1}$) will contribute to the values of $\Delta H^{\ddagger}_{rc}$. In fact, a rough calculation based on values of $C_{inter}\%$, $\Delta H^{\ddagger}_3$ and ($\Delta H^{\ddagger}_1$ + $\Delta H^{\ddagger}_2$ - $\Delta H^{\ddagger}_{-1}$) according to Eq. 58 afforded $\Delta H^{\ddagger}_{rc}$ = 13.1(7), 14.8(4), 12.1(7), and 12.1(5) kcal/mol for the HDPP, PDPP, BDPP, and PRDPP complexes respectively, which are in fairly good agreement with the previously reported values.

$$\Delta H^{\dagger}_{rc} = C_{inter}\% \; \Delta H^{\dagger}_{3} \; + \; (1 - C_{inter}\%)(\Delta H^{\dagger}_{1} + \Delta H^{\dagger}_{2} - \Delta H^{\dagger}_{-1})$$

$$(58)$$

The activation enthalpies for interchange pathways (k_3) show slightly lower value for BDPP and PRDPP indicating more bond formation in the corresponding transition states of reactions. The small entropies of activation ($\Delta S^{\dagger}_{3}$) and volumes of activation ($\Delta V^{\dagger}_{3}$) are consistent with the dissociative interchange mechanisms (I_d).

$\Delta V^{\dagger}_{3}$ for BDPP complex was estimated from the slope of plot of k_{obsd} vs P in neat CB at various pressures, since the predominant contribution to k_{obsd} is k_3 (Table XXXVIII); $\Delta V^{\dagger}_{1} + \Delta V^{\dagger}_{2} - \Delta V^{\dagger}_{-1}$ value for PDPP complex was estimated also from the plot of k_{obsd} vs P in neat CB at various pressures, but for predominant contribution to k_{obsd}, in this case is $k_1 k_2 / k_{-1}$.

Recalling the small difference values of $\Delta A^{\dagger}_{2} - \Delta A^{\dagger}_{-1}$ (A = H, S, V) from the reaction of cis-[(Ph$_2$PMe)W(CO)$_4$] with 1-hexene and CB (section B), values of $\Delta A^{\dagger}_{1} + \Delta A^{\dagger}_{2} - \Delta A^{\dagger}_{-1}$ can be considered to be very close to $\Delta A^{\dagger}_{1}$. Thus these positive entropies and volumes of activation are consistent with the dissociative pathway. The CB-W bond strengths, which can be estimated from ($\Delta H^{\dagger}_{1} + \Delta H^{\dagger}_{2} - \Delta H^{\dagger}_{-1}$), are very close to one another in these complexes (13-15 kcal/mol).

Chapter Summary

Studies of intermolecular solvent displacement by hex from $(BZ)W(CO)_5$ and cis-$(CB)(Ph_2PMe)W(CO)_4$ by employing flash photolysis of $W(CO)_6$ and cis-$(pip)(Ph_2PMe)W(CO)_4$ in hex/solv mixtures have suggested the dissociative mechanisms. These results also suggested a stronger solvent-metal bond strength (kcal/mol) in $(BZ)W(CO)_5$ (< 14.9) than in cis-$(CB)(PPh_2Me)W(CO)_4$ (< 12.1), $(BZ)Cr(CO)_5$ (< 9.4) and $(CB)Cr(CO)_5$ (< 14.0). On the basis of activation parameters, it seemed that there are three different bonding "modes" in these solvated species, e.g. $(BZ)-W(CO)_5$ bonding involves the whole benzene ring, $(CB)-Cr(CO)_5$ involves the Cl atom, while $(BZ)-Cr(CO)_5$ and $(CB)-W(CO)_4(PPh_2Me)$ bonding involve η^2- "isolated" double bonds. These differences were mainly considered to have arisen from the steric environments around coordinating metal centers.

The intramolecular CB displacements from cis-$(CB)(\eta^1-P-ol)W(CO)_4$ (P-ol = $Ph_2P(CH_2)_nCH=CH_2$, n = 1-4) to form $(\eta^3-P-ol)W(CO)_4$ were found to take place via competitive interchange and dissociative pathways based on studies of reaction rate laws and the activation parameters $\Delta A^\dagger$ (A = H, S, V). The relative rates (in parentheses) via the interchange pathway varying in the order of the length of $-(CH_2)-$ chelate ring backbone, n, 3 (1) $<$ 4 (1.5) $<$ 2 (5.9) $<$

1 (12.8). The ratios of rate constants of the interchange and dissociative pathway varied with n in the order 3 (0.77) ≈ 4 (0.82) < 1 (2.69) < 2 (5.99). These results indicate the sensitivity of reaction mechanism to chelate ring sizes.

REFERENCE LIST

(1) Parshall, G.W. <u>Homogeneous Catalysis</u>, Wiley: New York, **1980**.

(2) Moggi, L.; Juris, A.; Sandrini, D.; Manfrin, M.F. <u>Rev. Chem. Intermed.</u> **1981**, <u>4</u>, 171.

(3) Wrighton, M.S.; Graff, J.; Kaslauskas, R.J.; Mitchener, J.C.; Reichel, C.J. <u>Pure Appl. Chem.</u> **1982**, <u>54</u>, 161.

(4) Collman, J.P. <u>Acc. Chem. Res.</u> **1968**, <u>1</u>, 136.

(5) Hoffmann, R. <u>Angew. Chem. Intl. Ed.</u> **1982**, <u>21</u>, 711.

(6) Dobson, G.R. <u>Acc. Chem. Res.</u> **1976**, <u>9</u>, 300.

(7) (a) Werner, H. <u>J. Organomet. Chem.</u> **1975**, <u>94</u>, 285. (b) Werner, H. <u>Angew. Chem., Int. Ed. Engl.,</u> **1968**, <u>7</u>, 930.

(8) Rubezhov, A.Z.; Gubin, S.P. <u>Adv. Organomet. Chem.</u> **1972**. <u>10</u>, 347.

(9) Angelici, R.J. <u>Organomet. Chem. Rev.</u> **1968**, <u>3</u>, 173.

(10) (a) Basolo, F.; Pearson, R.G. <u>Mechanisms of Inorganic Reactions</u>, 2nd ed., Wiley: New York, **1967**; (b) Basolo, F. <u>Inorg. Chim. Acta,</u> **1981**, <u>50</u>, 65.

(11) Darensbourg, D.J. <u>Adv. Organomet. Chem.</u> **1982**, <u>21</u>, 113.

(12) Langford, C.H; Gray, H.B. <u>Ligand Substitution Processes</u>, 2nd ed., Benjamin, W.A., Reading, MA, **1974**.

(13) Howell, J.A.S.; Burkinshaw, P.M. <u>Chem. Rev.</u> **1983**, <u>83</u>, 557.

(14) Parshall, G.W. Acc. Chem. Res. 1975, 8, 113.

(15) (a) Shilov, A.E.; Shteinman, A.A. Coord. Chem. Rev. 1977, 24, 97; (b) Shilov, A.E. Activation of Saturated Hydrocarbons by Transition Metal Complexes, D. Riedel: Dordrecht, 1984.

(16) (a) Janowicz, A.H.; Bergman, R.G. J. Am. Chem. Soc. 1982, 104, 352; (b) Janowicz, A.H.; Bergman, R.G. J. Am. Chem. Soc. 1983, 105, 3929; (c) Janowicz, A.H.; Periana, R.A.; Buchanan, J.M.; Kovac, C.A.; Stryker, J.M.; Wax, M.J.; Bergman, R.G. Pure Appl. Chem. 1984, 56, 13; (d) Buchanan, J.M.; Stryker, J.M.; Bergman, R.G. J. Am. Chem. Soc. 1986, 108, 1537.

(17) Hoyano, J.K.; Graham, W.A.G. J. Am. Chem. Soc. 1982, 104, 3723.

(18) (a) Brookhart, M.; Green, M.L.H. J. Organomet. Chem. 1983, 250, 395. (b) Green, M.L.H. Pure Appl. Chem. 1984, 56, 47.

(19) (a) Crabtree, R.H. Chem. Rev. 1985, 85, 245; (b) Crabtree, R.H.; Holt, E.M.; Lavin, M.; Morehouse, S.M. Inorg. Chem. 1985, 24, 1986.

(20) Saillard, J.Y.; Hoffmann, R.J. J. Am. Chem. Soc. 1984, 106, 2006.

(21) Jones, W.D.; Feher, F.J. J. Am. Chem. Soc. 1982, 104, 4240.

(22) Jones, W.D.; Feher, F.J. Organometallics 1983, 2, 562.

(23) Jones, W.D.; Feher, F.J. J. Am. Chem. Soc. 1984, 106, 1650.

(24) Jones, W.D.; Feher, F.J. J. Am. Chem. Soc. 1986, 108, 4814.

(25) Stoutland, P.O.; Bergman, R.G. J. Am. Chem. Soc. 1985, 107, 4581.

(26) Stoutland, P.O.; Bergman, R.G. J. Am. Chem. Soc. 1988, 110, 5732.

(27) Browning, J.; Green, M.; Penfold, B.R.; Spencer, J.L.; Stone, F.G.A. J. Chem. Soc., Chem. Comm. 1973, 31.

(28) Browning, J.; Green, M.; Penfold, B.R. J. Cryst. Mol. Str. 1974, 4, 335.

(29) Cobbledick, R.E.; Einstein, F.W.B. Acta Cryst. 1978, B34, 1894.

(30) Sweet, J.R.; Graham, W.A.G. J. Am. Chem. Soc. 1983, 105, 305.

(31) van der Heijden, H.; Orpen, A.G.; Pasman, P. J. Chem. Soc., Chem. Comm. 1985, 1576.

(32) Belt, S.T.; Duckett, S.B.; Perutz, R.N. J. Chem. Soc., Chem. Comm. 1989, 928.

(33) Jones, W.D.; Dong, L. J. Am. Chem. Soc. 1989, 111, 8722.

(34) Harman, W.D.; Sekine, M.; Taude, H. J. Am. Chem. Soc. 1988, 110, 5725.

(35) van Eldik, R. Ed., Inorganic High Pressure Chemistry:

Kinetics and Mechanism; Elsevier: Amsterdam **1986**.

(36) (a) Turner, J.J.; Poliakoff, M. Inoganic Chemistry: Toward the 21st Centrury (M.H. Chisholm, ed.), ACS Symposium Series, 211, p. 35 **1983**. (b) Burdett, J.K.; Poliakoff, M.; Turner, J.J; Dubost, H. Advance in Infrared and Raman Spectroscopy (R.J.H. Clark and R.E. Hester, eds.) 2, p.1. Heyden, London, **1976**.

(37) Norrish, R.G.W.; Porter, G. Nature (London) **1949**, 164, 658.

(38) Braterman, P.S. Metal Carnonyl Spectra, Academic: New York, **1975**.

(39) Braterman, P.S. Structure and Bonding **1976**, 26, 1.

(40) Hester, R.E. Spex Speaker **1982**, 27, 1.

(41) Bradley, P.G.; Kress, N.; Homberger, B.A.; Dallinger, R.F.; Woodruff, W.H. J. Am. Chem. Soc. **1981**, 103, 7441.

(42) Forster, M.; Hester, R.E. Chem. Phys. Lett. **1981**, 81, 42.

(43) Forster, M.; Hester, R.E. Chem. Phys. Lett. **1982**, 85, 287.

(44) Smothers, W.K; Wrighton, M.S. J. Am. Chem. Soc. **1983**, 105, 1067.

(45) Orman, L.K; Hopkins, J.B. Chem. Phys. Lett. **1988**, 149, 375.

(46) Bell, S.E.J.; Gordon, K.C.; McGarvey, J.J. J. Am. Chem. Soc. **1988**, 110, 3107.

(47) Poliakoff, M.; Weitz, E. Adv. Organometal. Chem. 1986, 25, 277.

(48) Weitz, E. J. Phys. Chem. 1987, 91, 3945.

(49) Hermann, H.; Grevels, F.-W.; Henne, A.; Schaffner, K. J. Phys. Chem. 1982, 86, 5151.

(50) Church, S.P; Hermann, H. Gravels, F.-W.; Schaffner, K. J. Chem. Soc., Chem. Commun. 1984, 785.

(51) Moore, B.D.; Simpson, M.B; Poliakoff, M.; Turner, J.J. J. Chem. Soc., Chem. Commun. 1984, 972.

(52) Dixon, A.J.; Healy, N.A.; Hodges, P.M.; Moore, B.D.; Poliakoff, M.; Simpson, M.B.; Turner, J.J.; West, M.A. J. Chem. Soc., Faraday Trans.2 1986, 82, 2083.

(53) Creaven, B.S.; Dixon, A.J.; Kelly, J.M.; Long, C.; Poliakoff, M. Organometallics 1987, 6, 2600.

(54) Ouderkirk, A.J.; Wermer, P.; Schultz, N.L.; Weitz, E. J. Am. Chem. Soc. 1983, 105, 3354.

(55) Fletcher T.R.; Rosenfeld, R.N. J. Am. Chem. Soc. 1983, 105, 6358.

(56) Sonobe, B.I.; Fletcher T.R.; Rosenfeld, R.N. J. Am. Chem. Soc. 1984, 106, 4352.

(57) Fletcher T.R.; Rosenfeld, R.N. J. Am. Chem. Soc. 1985, 107, 2203.

(58) Fletcher T.R.; Rosenfeld, R.N. J. Am. Chem. Soc. 1988, 110, 2097.

(59) Wasserman, E.P.; Bergman, R.G.; Moore, C.B. J. Am.

Chem. Soc. **1988**, 110, 6076.

(60) Dobson, G.R.; Hodges, P.M.; Healy, M.A.; Poliakoff, M.; Turner, J.J.; Firth, S.; Asali, K. J. Am. Chem. Soc. **1987**, 109, 4218.

(61) Petek, H.; Nesbitt, D.J.; Ogllby, P.R.; Moore, C.B. J. Phys. Chem. **1983**, 87, 5367.

(62) Wang, L.; Zhu, X.; Spears, K.G. J. Am. Chem. Soc. **1988**, 110, 8695.

(63) Wang, L.; Zhu, X.; Spears, K. J. Phys. Chem. **1989**, 93, 2.

(64) A.W. Adamson A.W.; Cimolino, M.C J. Phys. Chem. **1984**, 88, 488.

(65) Butler, J.F.; Linden, K.J. Opt. Eng. **1980**, 19, 945;

(66) Moore, J.N.; Hansen, P.A.; Hochstrasser, R.M. Chem. Phys. Lett. **1987**, 138, 110.

(67) Ansari, A.; Berendzen, J.; Braunstein, D.; Coven, B.R.; Frauenfelder, H.; Hong, M.K.; Iben, I.E.T.; Johnson, J.B.; Ormos, P.; Sauke, T.B.; Scholl, R.; Schutte, A.; Steinbach, P.J.; Vittitow, J.; Young, R.D. Biophys. Chem. **1987**, 26, 337.

(68) Wermer, P.; Dobson, G.R. Inorg. Chim. Acta **1988**, 142, 91.

(69) Geoffroy, G.L.; Wrighton, M.S. Organometallic Photochemistry, Academic Press: New York, **1979**.

(70) Wrighton, M.S. Chem. Rev. **1974**, 74, 401.

(71) Simon, J.D.; Peters, K.S. Chem. Phys. Lett. 1983, 98, 53.

(72) Simon, J.D.; Xie, X. J. Phys. Chem. 1986, 90, 6751.

(73) Kelly, J.M.; Long, C.; Bonneau, R. J. Phys. Chem. 1983, 87, 3344.

(74) Joly, A.G.; Nelson, K.A. J. Phys. Chem. 1989, 93, 2876;

(75) Lee, M.; Harris, C.B. J. Am. Chem. Soc. 1989, 111, 8963.

(76) Wink, D.; Ford, P.C. J. Am. Chem. Soc. 1985, 107, 1794.

(77) Wrighton, M.; Hammond, G.S.; Gray, H.B. J. Am. Chem. Soc. 1971, 93, 6048.

(78) Lees, A.J.; Adamson, A.W. Inorg. Chem. 1981, 20, 4381.

(79) Wax, M.J.; Bergman, R.G. J. Am. Chem. Soc. 1981, 103, 7028.

(80) Asali, K.J.; Basson, S.S.; Tucker, J.S.; Hester, B.C.; Cortes, J.E.; Awad, H.H.; Dobson, G.R. J. Am. Chem. Soc. 1987, 109, 5386.

(81) Zhang, S.; Dobson, G.R. Inorg. Chem. 1989, 28, 324.

(82) Yang, G.K.; Peters, K.S.; Vaida, V. Chem. Phys. Lett. 1986, 125, 566.

(83) Yang, G.K.; Vaida, V.; Peters, K.S. Polyhedron. 1988, 7, 1619.

(84) Schwarzenbach, G. Helv. Chim. Acta 1952, 35, 2344.

(85) Bennett, M.A.; Kouwenhoven, H.W.; Lewis, J.; Nyholm, R.S. J. Chem. Soc. 1964, 4570;

(86) (a) Garrou, P.E.; Hartwell, G.E. J. Organomet. Chem. 1973, 55, 331; (b) Clark, P.W.; Curtis, J.L.S.; Garrou, P.E.; Hartwell, G.E. Can. J. Chem. 1974, 52, 1714.

(87) Wang, I-H., Ph.D. Dissertation, University of North Texas, 1989.

(88) Zhang, S. unpublished references manual, Department of Chemistry, University of North Texas, 1990.

(89) Dobson, G.R.; Dobson, C.B.; Mansour, S.E. Inorg. Chem. 1985, 24, 2179.

(90) (a) le Noble, W.J.; Schlott, R. Rev. Sci. Instrum. 1976, 47, 770; (b) Spitzer, M.; Gartig, F.; Van Eldik, R. Rev. Sci. Instrum. 1988, 59, 2092.

(91) Awad, H.H.; Dobson, G.R.; van Eldik, R. J. Chem. Soc., Chem. Comm. 1987, 1839.

(92) Awad, H.H., Ph.D. Dissertation, University of North Texas, 1989.

(93) This chapter is partly transferred from manuscripts submitted for publications. (a) Dobson, G.R; Zhang, S. J. Coord. Chem., in press; (b) Zhang, S.; Dobson, G.R.; Zang, V.; Bajaj, H.C.; van Eldik, R. Inorg. Chem., manuscript submitted. Dr. Dobson's contribution for writing the manuscripts and participation in high pressure experiments by other authors are gratefully acknowledged.

(94) (a) Oishi, S. Organometallics, 1988, 7, 1237; (b) Kalyanasundaram, K. J. Phys. Chem. 1988, 92, 2219.

(95) (a) Mitteilung, K. Z. Phys. Chem. (Frankfurt am Main) 1961, 27, 439; (b) Perutz, R.N.; Turner, J.J. J. Am. Chem. Soc. 1975, 97, 4791; (c) Burdett, J.K.; Grzybowski, J.M.; Perutz, R.N.; Poliakoff, M.; Turner, J.J.; Turner, R.F. Inorg. Chem. 1978, 17, 147.

(96) Dennenberg, R.J.; Darensbourg, D.J. Inorg. Chem. 1972, 11, 72.

(97) van Eldik, R.; Asano, T.; Le Noble, W.J. Chem. Rev. 1989, 89, 549, and references cited therein.

(98) Stolz, I.W.; Haas, H.; Sheline, R.K. J. Am. Chem. Soc. 1965, 87, 715.

(99) Oishi, S. J. Organomet. Chem. 1987, 335, 207.

(100) Crabtree, R.H.; Hamilton, D.G. Adv. Organomet. Chem. 1988, 28, 299.

(101) Leusink, A.J.; Budding, H.A.; Drenth, W. J. Organomet. Chem. 1967, 9, 295.

(102) Creemers, H.M.J.C.; Verbeek, F.; Noltes, J.G. J. Organomet. Chem. 1967, 8, 469.

(103) Bigeleisen, J. Pure Appl. Chem. 1964, 8, 217.

(104) Melander, L. Acta. Chem. Scand. 1971, 25, 3821.

(105) Parkin, G.; Bercaw, J.E. Organometallics 1989, 8, 1172.

(106) Strausz, O.P.; Safarik, I.; O'Callaghan, W.B.; Gunning, H.E. J. Am. Chem. Soc. 1972, 94, 1828.

(107) Streitwieser, A. Jr; Jagow, R.H.; Fahey, R.C.; Suzuki,

S. *J. Am. Chem. Soc.* **1958**, 80, 2326.

(108) Morse, J.; Parker, G.; Burkey, T.J. *Organometallics* **1989**, 8, 2471.

(109) This section is partly transferred from manuscript submitted for publication. Zhang, S.; Zang, V.; Bajaj, H.C.; Dobson, G.R.; van Eldik, R. *J. Organomet. Chem.*, manuscript submitted. Dr. Dobson's contribution for writing the manuscript and participation in high pressure experiments by other authors are gratefully acknowledged.

(110) Lawson, D.N.; Osborn J.A.; Wilkinson, G. *J. Chem. Soc., A.* **1966**, 1733.

(111) Beck, W.; Schloter, K. *Z. Naturf.* **1978**, 33b, 1214.

(112) Crabtree, R.H.; Faller, J.W.; Mellea, M.F.; Quirk, J.M. *Organometallics* **1982**, 1, 1361.

(113) Uson, R.; Fornies, J.; M. Tomas, M.; Cotton, F.A.; Falvello, L.R. *J. Am. Chem. Soc.* **1984**, 106, 2482.

(114) Crabtree, R.H.; Mellea, M.F.; Quirk, J.M. *J. Am. Chem. Soc.* **1984**, 106, 3913.

(115) Burk, M.J.; Crabtree, R.H.; Holt, E.M. *Organometallics* **1984**, 3, 638.

(116) Barcello, F.L.; Lahuerta, P.; Ubeda, M.A.; Foces-Foces, C.; Cano, F.H.; Martinez-Ripoll, M. *J. Chem. Soc., Chem. Comm.* **1985**, 43.

(117) Solans, X.; Font-Altaba, M.; Aguilo, M.; Miratvilles, C.; Besteiro, J.; Lahuerta, P. *Cryst. Struct. Comm.* **1985**,

c41, 841.

(118) Cotton, F.A.; Lahuerta, P.; Sanau, M.; Schwotzer, W.;

Solana, I. Inorg. Chemi. 1986, 25, 3526.

(119) Barcelo, F.L.; Cotton, F.A.; Lahuerta, P.; Llusar, R.;

Sanau, M.; Schwotzer, W.; Ubeda, M. Organometallics, 1985,

5, 808.

(120) Burk, M.J.; Seegmuller, B.; Crabtree, R.H.

Organometallics 1986, 3, 2241.

(121) Liotta, F.J.; van Duyne, G.; Carpenter, B.K.

Organometallics 1987, 6, 1010.

(122) Barcelo, F.L.; Cotton, F.A.; Lahuerta, P.; Sanau, M.;

Schwotzer, W.; Ubeda, M. Organometallics, 1987, 6, 1105.

(123) Kulawwiec, R.J.; Holt, E.M.; Lavin, M.; Crabtree, R.H.

Inorg. Chem 1987, 26, 2559.

(124) Catala, R.M.; Cruz-Garritz, D.; Hills, A.; Hughes,

D.L.; Richards, R.L.; Soss, P.; Torrens, H. J. Chem. Soc.,

Chem. Comm. 1987, 261.

(125) Winter, C.H.; Arif, A.; Gladysz, J.A. J. Am. Chem.

Soc. 1987, 109, 7560.

(126) Barcello, F.L.; Lahuerta, P.; Ubeda, M.A.; Foces-

Foces, C.; Cano, F.H.; Martinez-Ripoll, M. Organometallics

1988, 7, 584.

(127) Kulawiec, J.; Crabtree, R.H. Organometallics, 1988, 7,

1891.

(128) Awad, H.H.; Dobson, C.B.; Dobson, G.R.; Leipoldt,

J.G.; Schneider, K.; van Eldik, R.; Wood, H.E. Inorg. Chem. 1989, 26, 1654.

(129) Graham, J.R.; Angelici, R.J. Inorg. Chem. 1967, 6, 992.

(130) Graham, J.R.; Angelici, R.J. Inorg. Chem. 1967, 6, 2082.

(131) Dobson, G.R.; Spradling, M.D. Inorg. Chem. in press.

(132) Periana, R.A.; Bergman, R.G. J. Am. Chem. Soc. 1986, 108, 7332.

(133) Buchanan, J.M.; Stryker, J.M.; Bergman, R.G. J. Am. Chem. Soc. 1986, 108, 1537.

(134) Janowicz, A.H.; Periana, R.A.; Buchanan, J.M.; Kovac, C.A.; Stryker, J.M.; Wax, M.J.; Bergman, R.G. Pure Appl. Chem. 1984, 56, 13.

(135) Espenson, J.H. Chemical Kinetics and Reaction Mechanisms, McGraw-Hill: New York, 1981, p193.

(136) Jaffe, H.H. Chem. Rev. 1953, 53, 191.

(137) Taft, R.W. in Steric Effects in Organic Chemistry, Newman, M.S. Ed., Wiley: New York, 1956, p556.

(138) Brown, H.C.; Okamoto, Y. J. Am. Chem. Soc. 1958, 80, 4979.

(139) Wells, P.R. Linear Free Energy Relationships, Academic Press: London, 1968.

(140) Chapman, N.B.; Shorter, J., Ed. Advances in Linear Free Energy Relationships, Plenum Press: Ney York, 1972.

(141) Tolman, C.A. _Chem. Rev._ **1977**, _77_, 313, and references cited therein.

(142) Dahlinger, K.; Falcone, F.; Poe, A.J. _Inorg. Chem._ **1986**, _25_, 2654.

(143) Hansch, C.; Leo, A.; Unger, S.H.; Kim, K.H.; Nikaitani, D.; Lien, E.J. _J. Med. Chem._ **1973**, _16_, 1207.

(144) Vogel, A.I. _J. Chem. Soc._ **1948**, 1833.

(145) This section is partly transferred from manuscript submitted for publication. Zhang, S.; Dobson, G.R. _Inorg. Chim Acta_ **1989**, _165_, 11. Dr. Dobson's contribution for writing the manuscript is gratefully acknowledged.

(146) Wermer, P.H.; Dobson, G.R. _J. Coord. Chem._ **1989**, _20_, 125.

(147) (a) Connor, J.A.; Day, J.P.; Jones, E.M.; McEwen, G.K. _J. Chem. Soc., Dalton Trans._ **1973**, 347; (b) Connor, J.A.; Hudson, G.A. _J. Organomet. Chem._ **1974**, _73_, 351; (c) Connor, J.A.; Riley, P.I. _J. Organomet. Chem._ **1975**, _94_, 55; (d) Connor, J.A.; Hudson, G.A. _J. Chem. Soc., Dalton Trans._ **1975**, 1025.

(148) (a) Schadt, M.J.; Lees, A.J. _J. Chem. Soc., Chem. Comm._ **1984**, 506; (b) Schadt, M.J.; Lees, A.J. _Inorg. Chem._ **1985**, _24_, 2942; (c) Schadt, M.J.; Lees, A.J. _Inorg. Chem._ **1986**, _25_, 672; (d) Chan, L.; Lees, A.J. _Inorg. Chim. Acta_ **1986**, _113_, L3.

(149) Kazlauskas, R.L.; Wrighton, M.S. _J. Am. Chem. Soc._

1982, <u>104</u>, 5784.

(150) Wermer, P.H.; Dobson, C.B.; Dobson, G.R. <u>J. Organomet.</u> <u>Chem.</u> **1986**, <u>311</u>, C47.

(151) Dobson, G.R.; Bernal, I.; Reisner, G.M.; Dobson, C.B.; Mansour, S.E. <u>J. Am. Chem. Soc.</u> **1985**, <u>107</u>, 525.

(152) Mansour, S.E., Ph.D. Dissertation, University of North Texas, **1986**.